ACTIVE TRANSPORT AND CNS DELIVERY OF NOVEL TYROSINE KINASE INHIBITORS

A DISSERTATION

SUBMITTED TO THE FACULTY OF THE GRADUATE SCHOOL

OF THE UNIVERSITY OF MINNESOTA

BY

Ying Chen

IN PARTIAL FULFILLMENT OF THE REQUIREMENTS

FOR THE DEGREE OF

DOCTOR OF PHILOSOPHY

Dr. William Elmquist

March 2009

Acknowledgements

I would like to express my greatest gratitude to Dr. William Elmquist, my advisor, for his guidance, knowledge, and support that he offered throughout the course of my graduate study. Dr. Elmquist is an inspiring teacher and I feel very fortunate to have had him as my advisor. He always encouraged me to discover and explore my own research interests. My research skills have developed significantly under his mentorship. Dr. Elmquist was always supportive, encouraging, and helpful. For this I am deeply indebted. I believe what I learned from Dr. Elmquist, both scientific and non-scientific, will be beneficial to me throughout my life.

I would like to express my sincerest appreciation to my thesis committee members, Dr. Ronald Sawchuk, Dr. Tim Tracy and Dr. Carolyn Fairbanks for graciously serving on my thesis committee and guiding me through my graduate life.

I would like to thank all the Elmquist lab members, Haiqing Dai, Naveed Shaik, Nagdeep Giri, Guoyu Pan, Li Li, Tianli Wang and Sagar Agarwal, for their friendship, support and encouragement throughout good times and bad times.

There are many other people who have been part of this study indirectly. I wish to thank my faculty members, staff and colleagues in the Department of Pharmaceutics for their kindly support.

I would especially like to thank my parents for their constant encouragement and support during my graduate study.

Finally, my utmost gratitude and love are extended to my husband, Xin Ye, and my children, Jonathan Chunkai Ye and Alina Yikai Chen. They have always been my source of energy, motivation, and confidence throughout my graduate study. Without their patience, understanding and sacrifice, this academic achievement would have been impossible.

Abstract

Word count: 346

Tyrosine kinase inhibitors (TKIs) are promising agents for specific inhibition of malignant cell growth and metastasis formation. They directly interfere with TK enzymes that are activated in tumor cells and are critical to tumor growth. The success of the first generation TKI, imatinib, in the treatment of CML has led to the broader examination of its application in the treatment of other tumors, such as glioma. However, early studies showed imatinib has difficulty penetrating blood-brain barrier (BBB). One component of the BBB that may limit the delivery of imatinib into the CNS is the drug efflux transporters, such as ABCB1 (p-glycoprotein) and ABCG2 (breast cancer resistance protein). Dasatinib is a second-generation TKI developed to overcome the molecular resistance to imatinib and may be very promising in the treatment of brain tumor. Thus far little information is known about the CNS delivery of dasatinib, including the action of relevant BBB transporters in modulating this delivery. The objectives of this work were to assess the influence of various drug efflux transporters, such as ABCB1 and ABCG2, on the specific delivery of imatinib and dasatinib to CNS and the possibility of improving CNS delivery of imatinib and dasatinib by effective pharmacological inhibition. In *in vitro* studies, we demonstrated that imatinib is a substrate of Abcg2 by using cellular accumulation and permeability methods. In *in vivo* studies, we further explored that ABCB1and ABCG2 together play an important role in limiting the CNS delivery of imatinib. Saturation or inhibition of ABCB1 and ABCG2 could effectively improve CNS delivery of imatinib.

In vitro evidence pointed that dasatinib is a substrate of ABCB1 and Abcg2. *In vivo* results revealed that the CNS delivery of dasatinib was low. ABCB1 and ABCG2 could be a factor limiting the CNS delivery of dasatinib. ABCB1 plays a more important role than ABCG2 in effecting the CNS delivery of dasatinib. The use of potent inhibitors for both ABCB1 and ABCG2 can improve dasatinib CNS delivery. These findings provide significant insight into current and new clinical strategies to more effectively use the TKIs for CNS disease treatment and prevention.

Table of Contents

List of Tables

List of Figures

CHAPTER 1

INTRODUCTION

1.1 Introduction

The objective of this thesis is to assess the influence of various drug efflux transporters, such as ABCB1 (p-glycoprotein, p-gp) and ABCG2 (breast cancer resistant protein, bcrp), on the specific delivery of tyrosine kinase inhibitors (TKIs) to central nervous system (CNS). Over the past decade, many efforts have been done in the development of more targeted and specific new treatment modalities that exploit information gained from the molecular biological studies of cancer. Molecularly targeted cancer therapies use drugs that block the growth and spread of cancer by interfering with specific key molecules involved in carcinogenesis and tumor growth. They are designed to be more effective and have fewer side effects. (National Cancer Institute, 2006) The TKIs are designed to directly interfere with TK enzymes that are aberrantly activated in tumor cells and are critical to the growth of the tumor. (Vlahovic and Crawford, 2003) However, the delivery of these inhibitors to the CNS is questionable, and the specific mechanisms that regulate that delivery are unknown. There are several issues of the CNS delivery of chemotherapy agents such as the barriers of the CNS, drug efflux transporters in the CNS, and the relative resistance of many of these tumors to chemotherapy. The efflux transport systems are increasingly recognized as important determinants of drug distribution to the CNS. The phenomenon of "multidrug resistance" is a major hurdle when it comes to the delivery of therapeutics to the brain.(Begley, 2004a) Therefore, this thesis focuses on the role of important drug efflux transporters on the active transport and CNS delivery of the novel TKIs.

1.1.1 Tyrosine kinase inhibitors

1.1.1.1 Tyrosine kinases

TKs are enzymes that transfer γ-phosphate groups from ATP to the hydroxyl group of tyrosine residues on signal transduction molecules (Schlessinger, 2000). They are important regulators of intracellular signal-transduction pathways that mediate cellular development and multicellular communications (Alvarez et al., 2006). Phosphorylation of signal transduction molecules is a major activating event that leads to dramatic changes in tumor growth. Approximately 90 TKs have been identified, 58 of which are the transmemberane receptor type and 32 are the cytoplasmic nonreceptor type. However, clinical agents to inhibit the activity of these TKs have been developed for only a few. (Blume-Jensen and Hunter, 2001) These include the transmembrane receptor TKs, epidermal growth factor receptor (EGFR) TK, platelet-derived growth factor receptor (PDGFR) TK and c-kit, and the cytoplasmic nonreceptor TKs, Bcr-Abl and Src family kinases (SFKs) (Blume-Jensen and Hunter, 2001; Baselga, 2006).

PDGFR

PDGF is a family of dimeric isoforms that stimulates cell functions such as growth, chemotaxis and cell shape changes of various connective tissue cell types and certain other cells. The cellular effects of PDGF isoforms are exerted through binding of two structurally related tyrosine kinase receptors denoted the α-receptor and the β-receptor. (Heldin and Westermark, 1999) Ligand binding induces receptor dimerization and autophosphorylation. This enables a number of Src homology 2 (SH2) domain containing signal transduction molecules to bind to the receptors, thereby initiating

various signaling pathways leading to different cellular responses (Ostman and Heldin, 2001). Overactivity of PDGFR has been implicated in certain disorders, including fibrotic conditions, atherosclerosis, and malignancies. In progression of glioblastoma and sarcomas, PDGFR often causes autocrine stimulation of tumor cell growth. In addition, paracrine stimulation of stroma cells by PDGFR made by tumor cells is also important for the balanced growth of different cell types in tumors (Heldin and Westermark, 1999).

Bcr-Abl

Bcr-Abl is a fusion protein product of the distinctive Philadelphia (Ph) chromosome, which is created by the t (9;22) chromosomal translocation that fuses BCR sequences from chromosome 22 upstream of the ABL gene on chromosome 9 (Deininger and Druker, 2003). Ph chromosome has been found in some forms of leukemia, including almost all cases (i.e., 95%) of chronic myelogenous leukemia (CML) and many cases of adult acute lymphoblastic leukemia (ALL) (Blume-Jensen and Hunter, 2001). Bcr-Abl is a constitutively active TK that activates a great number of signal transduction pathways. They appear to target three major cellular functions: increased proliferation, reduced apoptosis and disturbed interaction with the extracellular matrix. These cellular functions drive uncontrolled growth of the Ph^+ cells (Deininger and Druker, 2003). The constitutive tyrosine kinase activity of the chimerical Bcr-Abl protein expressed by leukemia cells is essential for the pathogenesis of the disease.

c-Kit

c-Kit receptor is a transmembrane glycoprotein with a tyrosine kinase activity in the intracellular domain (Yarden et al., 1987). Stem cell factor (SCF), a hematopoetic growth factor, is the natural ligand of c-Kit. Ligand binding activates the receptor dimerization and autophosphorylation at specific tyrosine residues. c-Kit is involved in the signal transduction of several major cellular functions, such as cell survival, proliferation, differentiation, adhesion, and other vital functions in early hematopoietic cells. It also induces apoptosis and enhances the invasive potential activating multiple signal transduction pathways (Edling and Hallberg, 2007; Roussidis et al., 2007). A range of different types of gain-of–function mutations of c-Kit including point mutations, deletions and duplications have been observed. The activating mutations of c-Kit confer constitutive tyrosine kinase activity and downstream activation independent of ligand binding. These c-Kit mutations expose a strong oncogenic potential. Abnormal c-Kit expression has been reported in different types of mast cell neoplasms, gastrointestinal stromal tumors (GISTS), germ cell tumors, malignant melonomas, neuroblastoma and some leukemia. Additionally, aberrant expression of c-Kit has been found in tumors such as small cell lung carcinomas, ovarian carcinomas and breast carcinoma (Miettinen et al., 2005; Ali, 2007).

Src Family Kinases

Src family is the largest family of nonreceptor tyrosine kinases. SFK members include Src, Fyn, Lyn, Hck, Fgr, Blk, Yrk, Lck and Yes (Fizazi, 2007; Finn, 2008). The SFKs have similar structural features. They comprise at least 9 proteins (all approximately 60

kD in molecular weight) and their domain structures have considerable homology (Alvarez et al., 2006). SFKs are responsible for signal transduction during many cellular activities, including differentiation, adhesion, migration, division, motility, angiogenesis and survival (Summy and Gallick, 2003; Fizazi, 2007). Recent studies revealed that SFKs are involved in signal transduction from many receptor tyrosine kinases (RTK), such as PDGFR, EGFR and stem cell factor receptor. SFKs are able to promote signaling from growth factor receptors in a number of ways including: 1) initiating the signaling pathways required for DNA synthesis, 2) modulating RTKs, and 3) controlling receptor turnover and actin cytoskeleton rearrangements (Alvarez et al., 2006). A number of studies have shown that SFKs are upregulated in multiple types of human tumors and are typically associated with advanced malignancies and/or metastatic spread, with Src activity increasing proportionally to the progressive stages of the disease (Playford et al., 2004; Park et al., 2008). Among all family members, Src is implicated most often in cancer. Several studies suggest that Src is involved closely in the genesis and progression of multiple human cancer types, including carcinomas of the breast, gastrointestinal tract, pancreas, lung, ovary and brain, and myeloproliferative disorders (Irby and Yeatman, 2000; Lombardo et al., 2004). Aberrantly activation of SFKs is very common in colorectal and breast cancers. Further, the extent of increased SFK activity often correlates with malignant potential and patient survival. The activation of SFKs is frequently a critical event in tumor progression (Summy and Gallick, 2003).

1.1.1.2 Tyrosine Kinase Inhibitors

Tyrosine kinase inhibitors (TKIs) are developed based on the understanding of the molecular events driving tumor growth and development. TKIs are drugs that work by targeting one or more specific tyrosine kinases that are involved in malignant transformation and tumor progression. This thesis focuses on two TKIs: imatinib and dasatinib (for structures, see fig. 1.1). They are low molecular –weight compounds that inhibit TK phosphorylation by interacting with ATP and/or competing for binding with the enzyme-binding site (Baselga and Hammond, 2002).

Imatinib

Imatinib (Gleevec®, STI-571), a 2-phenylaminopyrimidine compound, is a small molecule TKI used primarily for the treatment of CML (Mauro and Druker, 2001). It was the milestone of molecularly-targeted therapy. Imatinib was discovered by Druker and colleagues in 1996 (Lydon et al., 2004). It blocks the binding of ATP to the Bcr-Abl tyrosine kinase (fig. 1.2), thus inhibiting kinase activity, inducing apoptosis and blocking the growth of Bcr-Abl transformed leukemic cells (Druker, 2003). The Ki for inhibiting Bcr-Abl is 85 nM (Deininger and Druker, 2003). Pharmacokinetic studies demonstrate that imatinib is rapidly absorbed and it has a high systemic bioavailability (98%) (Nikolova et al., 2004; Peng et al., 2004). Imatinib is also a potent inhibitor of c-Kit and PDGFR. Activating mutations of c-Kit are found in the majority of patients with gastrointestinal stromal tumors (GISTs), a neoplasm that is practically unresponsive to conventional cytotoxic drugs (Blanke et al., 2001). GIST patients with c-Kit mutations respond dramatically to imatinib (Joensuu et al., 2001). PDGF was

reported to be involved in the phenotype of malignant gliomas (Rich and Bigner, 2004). Imatinib is undergoing phase I/II investigation for the treatment of glioma(Rich and Bigner, 2004; Raymond et al., 2008).

Netzer et al reported in 2003 that imatinib potently reduced Amyloid-beta (Abeta) production in the N2a cell-free system and in intact N2a cells. It also reduced Abeta production in rat primary neuronal cultures and in vivo in guinea pig brain. Abeta peptides are believed to be major pathological determinants of Alzheimer's disease (Netzer et al., 2003). In 2005, another group showed that imatinib inhibits γ-secretase cleavage of Abeta-protein precursor (APP) without affecting Notch processing (Fraering et al., 2005). The efficacy of imatinib in reducing Abeta production without affecting Notch-1 cleavage may prove useful as a basis for developing novel therapies for Alzheimer's disease.

A very recently published study from Su et al. reported that imatinib treatment reduced cerebrovascular permeability and stroke lesion volume as well as hemorrhagic complications associated with late thrombolysis (Su et al., 2008). These data suggest the potential new strategy of using imatinib with thrombolytic tPA for stroke treatment.

Dasatinib

It has been observed that resistance mutations occur in the kinase domains of BCR-ABL, Kit and PDGFR in the tumor cells of patients treated with imatinib (Baselga,

2006). To overcome this new challenge, the second-generation TKIs are rapidly being developed.

Dasatinib (Sprycel™, BMS-354825), a second-generation TKI, has already been approved for patients with CML with resistance or intolerance to imatinib by the U.S. Food and Drug Administration (Shah, 2007). Dasatinib is a ATP-competitive inhibitor of Src and ABL tyrosine kinase, with measured *K*i values of 16 ± 1.0 pM and 30 ± 22 pM, respectively, approximately 300-fold more potent than imatinib (Lombardo et al., 2004). It differs from imatinib in that it can bind to both the active and inactive conformations of the ABL kinase domain. In addition, it binds ABL with less stringent conformational requirement than imatinib (Baselga, 2006; Schittenhelm et al., 2006; Talpaz et al., 2006). It effectively inhibits the proliferation of cells that express nearly all imatinib-resistant isoforms(Kantarjian et al., 2006). Dasatinib was also found to potently inhibit other Src-family members, such as Lck and Yes. And this compound demonstrated significant activity against c-kit and PDGFRβ (Lombardo et al., 2004). A recent study shows dasatinib also potently inhibits the kinase activity of wild-type, juxtamembrane, and activation loop mutant KIT isoforms associated with human malignancies (Schittenhelm et al., 2006). Clinical studies have reported that dasatinib is active in Philadelphia chromosome–positive CML after failure of imatinib and nilotinib (AMN107) therapy (Quintas-Cardama et al., 2007).

1.1.2 Brain tumor

Brain tumors represent a heterogeneous group of central nervous system (CNS) neoplasms. The World Health Organization (WHO) recognizes approximately 100 different types of brain tumors classified according to pathological diagnosis (Lesniak and Brem, 2004). In general, however, these tumors can be classified into either primary or secondary tumors, depending on whether they originate in the brain or simply spread to the central nervous system from elsewhere (Lesniak and Brem, 2004). Abnormalities in receptor tyrosine kinase pathways and loss of tumor suppressor genes are critical in the transformation and growth of malignant gliomas(Tremont-Lukats and Gilbert, 2003).

1.1.2.1 Primary Brain Tumor

The term 'glioma' encompasses a group of cancers that includes astrocytomas, oligodendrogliomas, oligoastrocytomas, ependymomas and choroid plexus tumors (Rich and Bigner, 2004). Approximately half of all primary brain tumors are glial-cell neoplasms, and more than three quarters of all glial tumors are astrocytomas. Astrocytomas differ in their pathological and clinical behaviors: some astrocytomas are classified as low-grade tumors, meaning they are slow growing, whereas others, such as glioblastoma multiforme (GBM), represent the most aggressive type of tumor known to occur within the CNS (Fig. 1.3) (Lesniak and Brem, 2004). GBM is also the most frequent glioma. Its aggressive and infiltrative growth renders it extremely difficult to treat. Currently, median survival after diagnosis is only 12–14 months (Johansson Swartling and Johansson Swartling, 2008). In standard glioma treatment protocols,

tumor resection and radiation therapy are followed by chemotherapy with drugs causing DNA alkylation, such as nitrosoureas. Standard chemotherapy treatment is a combination of procarbazine, lomustine and vincristine or carmustine or temozolomide alone (Gaya et al., 2002).

Autocrine and paracrine growth-factor loops are frequently present in malignant gliomas; that is, the presence of both growth-factor ligands and their cognate receptors in target tissues. Several growth-factor pathways are involved in the phenotype of malignant gliomas, such as EGF and PDGF (Rich and Bigner, 2004). Overexpression in the EGFR is common in GBM (up to 70% of specimens) and is a hallmark of primary glioblastomas (Tremont-Lukats and Gilbert, 2003).

Imatinib inhibited the growth of U343 and U87 GBM (which contains a PDGF/PDGFR autocrine loop) cell lines both in vitro and in vivo when implanted into the brains of nude mice (Kilic et al., 2000). Recently, more studies have showed the TKIs such as erlotinib and gefitinib are promising in the treatment of brain tumors (Heimberger et al., 2002; Efferth et al., 2004).

1.1.2.2 Secondary brain tumors

As systemic therapy of cancer improves, CNS involvement is becoming a more widespread problem. CNS metastases account for the majority of malignant brain tumors, and may appear either within the brain parenchyma or along the leptomeninges (Lin et al., 2004). The American Cancer Society estimates that 170,000 cancer patients

develop cerebral metastases each year in the United States (Biswas et al., 2006). Patients with lung cancer and breast cancer have greater risk to develop brain metastases compared to other cancer patients.

Patients with locally advanced lung cancer (non-small cell lung cancer or small cell lung cancer) are threatened by concurrent risks of local, regional, and distant treatment failure. By improving locoregional and systemic control within multimodality protocols, brain emerges as one of the major relapse sites. Importantly, the incidence of brain metastases secondary to small cell lung cancer (SCLC) is about 35% (Bach et al., 1996; Pottgen et al., 2004).

Breast cancer is the second most common cause of CNS metastases, and 10-15% of patients develop clinically overt central nervous system disease. Progressive neurologic disability often results and the prognosis is generally poor (Fenner and Possinger, 2002; Lin et al., 2004).

The CNS is also a sanctuary for leukemic cells. CNS relapses have been observed in both animal and CML patients even though they have shown a systemic complete hematological response to imatinib (Takayama et al., 2002; Abruzzese et al., 2003; Pfeifer et al., 2003; Wolff et al., 2003). The fact that adequate treatment of systemic disease with subsequent failure in the CNS may indicate that the CNS delivery of the TKIs is inadequate. Therefore, prevention of brain relapse has become a primary focus of attention.

1.1.3 Issues in Delivery of Anti-tumor drugs to the CNS

The role of drug delivery in the treatment of CNS neoplasms is a crucial consideration in the development of any agent designed to be used in treating brain tumor. Several mechanisms may limit the delivery of antitumor agents to the brain. Many of these delivery problems are related to blood-brain barrier and blood-CSF barriers.

1.1.4 Barriers of the CNS

The CNS contains important cellular barriers that maintain homeostasis by regulating the passage of nutrients and protecting the brain from circulating toxins (Sun et al., 2003). The barriers that limit the concentration of toxins and xenobiotics in the interstitial fluids of the CNS are the blood–brain barrier (BBB) and the blood–cerebrospinal fluid barrier (BCSFB).

The BBB is composed of a system of tissue sites, including the brain capillary endothelium, choroids plexus epithelium, and arachnoid membrane. An important component of the BBB is the brain microvessel endothelial cell. These cells are characterized by the presence of tight junctions between the cells and the absence of fenestration and reduced pinocytotic activity. These tissue sites work together to restrict and regulate the flux of hydrophilic ions, proteins, and nonelectrolytes from blood to brain extracellular fluid and cerebrospinal fluid (Pardridge et al., 1986; Smith, 1996). The BCSFB is formed by a single continuous layer of epithelial cells that line the endothelial cells of the choroid plexus. BCSFB differs from BBB in that it is the tight junctions between the epithelial cells, not the endothelial cells, that are involved in the

functional role of the barrier (Motl et al., 2006). The important functional characteristic of both the BBB and BCSFB is that compounds in the blood have to be transported transcellularly across the brain endothelial cells and choroid plexus epithelial cells. Because of the physical nature of the BBB and BCSFB, molecules can cross the barrier only if they are transported by the selective transport proteins or if they are small enough and lipiphylic enough to pass through the lipid bilayer. (Miller, 2002; Sun et al., 2003). Given the nature of these barriers, it is likely that a molecule with high molecular weight and/or is hydrophilic, will have limited permeability across the BBB due to limited passive diffusion. On the other hand, if a molecule has moderate passive diffusion but is a substrate for an efflux transport system (carrier-mediated transport from the brain to the blood), the distribution to the brain would also be limited by the functional activity of the CNS barriers.

1.1.5 Drug Efflux Transporters

Molecular identification and functional analysis of drug efflux transport proteins at the BBB and BCSFB have been undertaken recently, and several transport protein families have been recognized, such as the product of the multidrug resistance gene, MDR1 (p-glycoprotein, ABCB1), breast cancer resistance protein (BCRP, ABCG2), the multidrug resistance-associated protein family (MRPs, ABCCs), the organic anion transport proteins (Oatps), and the organic anion transporter (OATs) (Sun et al., 2003; Fricker and Miller, 2004).These efflux transporters efflux toxic metabolites and xenobiotics out of the brain and also keep out many therapeutic agents. The importance of drug efflux

transporters in disease processes and treatment has become increasingly recognized in recent years (Schinkel et al., 2003).

1.1.5.1 ABCB1

ABCB1 (P-gp), the product of the multidrug resistance gene (MDR), is the most extensively studied membrane-bound ATP binding cassette (ABC) transporter. It was first recognized in 1970s as a prototypic transporter involved in the multidrug resistance (MDR) during the treatment of tumors with anticancer regimens containing several drugs (Juliano and Ling, 1976; Begley, 2004a). ABCB1 is a 170 k Da phosphorylated glycoprotein that is produced by the ABCB1 (MDR1) gene (Loscher and Potschka, 2005). It is believed to be one of the most important ABC transporters for drug disposition in humans, which functions to exclude substrates from cells in the brain and a number of other normal tissues (Golden and Pollack, 2003b). It has been found at the luminal surface of the brain microvascular endothelium (Cordon-Cardo et al., 1989) and in isolated brain capillary endothelial cells (Tsuji et al., 1992; Beaulieu et al., 1997). Furthermore, the finding of ABCB1 on isolated human astrocyte foot processes and cultured rat astrocytes and at the choroid plexus indicates that the function of ABCB1 as the ‘‘brain gatekeeper’’ may extend past the BBB to multiple sites in the CNS (Golden and Pollack, 2003b). ABCB1 has a broad range of substrates. It is able to recognize and transport a plethora of diverse substrates that differ considerably in chemical structure and pharmacological action, including many clinically important agents (Hennessy and Spiers, 2007). Studies using recently developed gene knockout animal models have provided compelling evidence that supports a role for ABCB1 at the BBB. For instance,

it has been observed that a wide range of drugs have enhanced BBB penetration in mdr1a knockout mice. These include cyclosporine, morphine, vinblastine, digoxin, quinolone antibacterial agents, indinavir, saquinavir and nelfinavir (Taylor, 2002).

1.1.5.2 ABCG2

ABCG2 (BCRP) is a recently discovered half-molecule ABC transporter (Young et al., 2003). ABCG2 was first discovered in a chemotherapy resistant breast cancer cell line, but there is no indication that its expression is specific for breast cancer cells (Schinkel and Jonker, 2003). It has been reported to confer resistance to a variety of chemotherapeutic agents such as mitoxantrone, the camptothecins topotecan and SN-38, doxorubicin, and flavopiridol (Robey et al., 2003). ABCB1 was found to be physiologically expressed in the canalicular membrane of the liver, in the epithelia of small intestine, placental trophoblasts, colon, lung, kidney, adrenal and sweat glands, as well as in the endothelia of veins and capillaries (Allen et al., 2002a; Sarkadi et al., 2004). Its expression in brain microvessels is high compare to other tissues (Doyle and Ross, 2003). The presence of BCRP in the luminal surface of the endothelium of human brain microvessels was recently demonstrated by immunofluorescence confocal microscopy (Cooray et al., 2002a). It appears to be expressed in the luminal membrane of the cerebral endothelial cells in a manner that is similar to ABCB1. Therefore, it is also considered to be an important component of the efflux activity of the BBB.(Begley, 2004b)

1.1.5.3 Pharmacologic modulators

Efflux mediated multidrug resistance is believed to play a major role in the clinical resistance of numerous human tumors against chemotheapeutic agents, which has stimulated an intense search for inhibitors of drug efflux transporters. LY335979, Ko143 and GF120918 are three commonly used pharmacologic modulators of drug efflux transporters (structures see fig. 1.4).

LY335979 (zosuquidar)

LY335979 (zosuquidar, (*R*)-4-((1a*R*, 6R, 10bS)-1,2-difluoro-1, 1a, 6,10b-tetrahydrodibenzo-(*a*, *e*) cyclopropa(*c*) cycloheptan-6-yl)-α- ((5-quinoloyloxy) methyl)-1-piperazineethanol, trihydrochloride) is a second-generation modulator of ABCB1. It is an excellent pharmacologic modulator of ABCB1 that possesses features of an "ideal modulateor" (Starling et al., 1997). LY335979 is a selective ABCB1 inhibitor that does not interact with ABCC1, ABCC2 or ABCG2 and has a significantly lower affinity for CYP3A than for ABCB1 (Dantzig et al., 1999; Dantzig et al., 2001; Shepard et al., 2003). LY335979 is very potent. It was able to fully restore sensitivity to vinblastine, doxorubicin, etoposide, and taxol in CEM/VLB_{100} cells at the concentration of 0.1μM (Dantzig et al., 1996). Both cytotoxicity data and cellular uptake data showed that LY335979 is not a substrate for ABCB1-mediated efflux. Another characteristic of LY335979 is that it lacks pharmacokinetic interactions with coadministered agents. It increased the brain penetration of taxol, doxorubicin or etoposide in mice without altering their pharmacokinetics (Starling et al., 1997). In several phase I/II clinical trials, when LY335979 was administered p.o. or i.v. alone or in combination with

doxorubicin, it did not significantly affect the pharmacokinetics of doxorubicin (Rubin et al., 2002; Sandler et al., 2004; Morschhauser et al., 2007). More clinical trials are undergoing to investigate the safety and tolerability of LY335979.

Ko143

Ko143 (3-(6-isobutyl-9-methoxy-1, 4-dioxo-1, 2, 3, 4, 6, 7, 12,12a-octahydropyrazino [1', 2': 1, 6] pyrido [3, 4-*b*] indol-3-yl)-propionic acid *tert*-butyl ester) is a recently designed ABCG2 inhibitor. It was first described by John Allen and colleagues (Allen et al., 2002a). Ko143 is an analogue of fungal toxin fumitremorgin C (FTC). Ko143 is a selective ABCG2 inhibitor. It was at least 200-fold less active against ABCB1 than ABCG2, and it had little effect on the activity of ABCCs 1-5. Ko143 is the most potent ABCG2 inhibitor known thus far. The EC_{90} of Ko143 for reversal of ABCG2-mediated resistance to mitoxantrone and topotecan was ~25nM. No noticeable toxicity of Ko143 was observed *in vitro* or in mice at doses effective for inhibition of ABCG2 activity (Allen et al., 2002a).

GF120918 (elacridar)

GF120918 (elacridar, N- [4-[2-(6, 7-Dimethoxy-3, 4-dihydro-1H-isoquinolin-2-yl) ethyl]-5-methoxy-9-oxo-10H-acridine-4-carboxamide) originally was selected from a chemical program aimed at identifying an optimized inhibitor of ABCB1. It fully reversed the ABCB1-mediated resistance of doxorubicin and vincristine in CH^RC5, OV1/DXR and MCF7/ADR cells at 0.05 to 0.1μM (Hyafil et al., 1993). In 1999, de Bruin and coworkers reported that GF120918 was able to sensitize S1-B1-20, a subline

expressing ABCB1, and S1-M1-80, a subline expressing ABCG2 at a concentration of 1 μM in cytotoxicity assays. GF120918 (250 nM) completely inhibited rhodamine 123 efflux in S1-B1-20 cells while complete inhibition of rhodamine efflux in ABCG2-resistant S1-M1-80 cells required 10 μM (de Bruin et al., 1999). GF120918 had no significant effect on ABCC1 (Germann et al., 1997; de Bruin et al., 1999; Evers et al., 2000). So GF120918 is potent dual pharmacologic modulator that inhibits both ABCB1 and ABCG2. Preclinical and clinical studies showed that GF120918 is well tolerated in animals (Malingre et al., 2001) and human (Planting et al., 2005). In mice, GF120918 increased the oral bioavailability of paclitaxel from 8.5 to 40.2% at 25 mg/kg p.o. (Bardelmeijer et al., 2000). Another study reported that GF120918 increased the distribution of unbound amprenavir to CNS in rats (Edwards et al., 2002). In a phase I clinical trial, coadministration of 100 mg GF120918 with oral topotecan results in complete apparent bioavailability of topotecan (Kuppens et al., 2007). Since the substrate spectrum of ABCB1 and ABCG2 overlaps (Xia et al., 2007c), GF120918 could be very beneficial for chemotherapy agents that are substrates of ABCB1 and ABCG2 and have poor oral bioavailability or brain penetration due to the efflux function of ABCB1 and ABCG2.

1.2 Statement of the problem

CNS delivery has always been an issue for chemotherapy, even for the recently designed molecular-targeted tyrosine kinase inhibitors. The inadequate concentrations of therapeutic agents in CNS caused by poor CNS delivery make it a sanctuary for

tumor cells. CNS relapses or CNS metastases have been observed in patients who had systemic response to therapeutic agents. Efflux transporter systems in the BBB is an important factor, other than the tight junctions, that restricts the entry of xenobiotics and toxic metabolites from systemic blood to CNS. However, many desirable therapeutic agents are also kept out of CNS because of efflux transporters. Efflux transporters may play a role in limiting the CNS delivery of TKIs, and the inhibition of efflux transporters could possibly result in enhanced TKI- CNS delivery.

1.3 Objective of thesis project

The objective of this research was to assess the influence of various drug efflux transporters, such as ABCB1 and ABCG2, on the specific delivery of TKIs to CNS. Our hypothesis was that various drug efflux transporters, such as ABCB1 and ABCG2, can influence the targeted bioavailability (i.e., specific delivery) of TKIs (imatinib and dasatinib), to the CNS and therefore, effective pharmacological inhibition of these transporters will lead to improved CNS delivery.

1.4 Specific aims

1. The first aim was to identify and characterize the interaction of TKIs with various active transport systems by using an *in vitro* cell culture model. The kinetics of cellular accumulation and permeability of TKIs was tested in drug efflux transporter protein (ABCB1 and ABCG2) transfected epithelial cell monolayers. The effects of various

pharmacological modulators (LY335979, KO143 and GF120918) on the interaction of TKIs and transporters were examined.

2. The second aim was to examine the influence of selected transporters (ABCB1 and ABCG2) on the targeted delivery of TKIs to CNS by using *in vivo* mouse models. First, we measured the total brain to blood area-under-the-curve (AUC) ratios of TKIs following intravenous or oral administration of TKIs alone and with an inhibitor, LY335979, Ko143 or GF-120918, in the Abcb1a/b-Abcg2 intact (wild type) *in vivo* mouse model. Then we compared the results to the Abcb1 gene deficient (*Mdr1a/b (-/-)* knockout) mice, Abcg2 gene deficient (*Bcrp1* knockout) mice and Abcb1a/b-Abcg2 gene deficient (Mdr1a/b-Bcrp1 knockout) mice.

The completion of these aims provides information on the affinity of these efflux transporters for TKIs and the potential influence of these selected transporters on targeted delivery of TKIs to CNS.

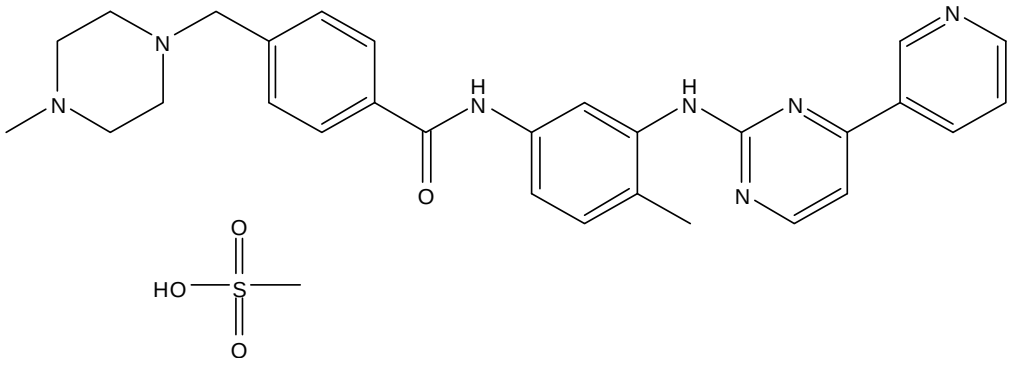

Imatinib (mesylate salt form)

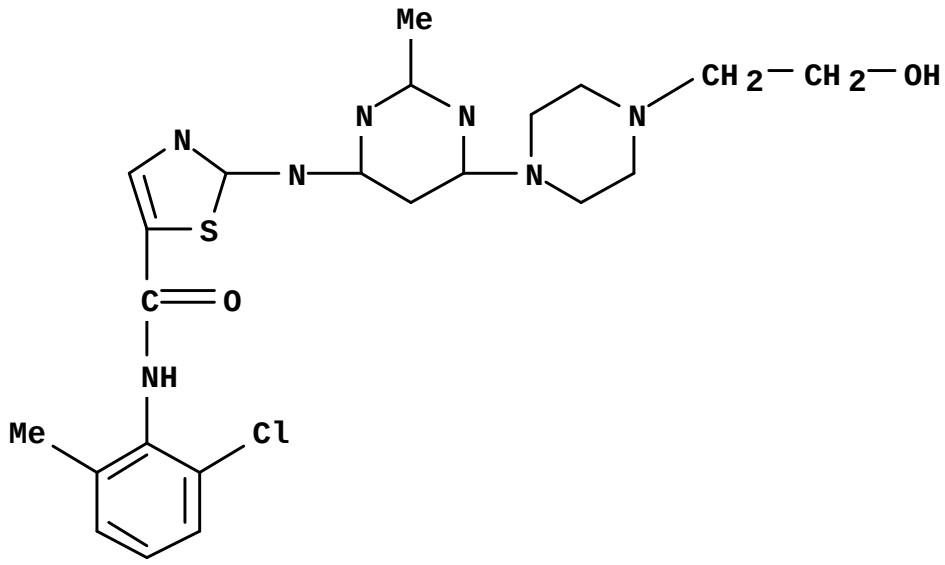

Dasatinib

Figure 1.1. Chemical structures of imatinib and dastinib.

Figure 1.2. Schematic figure of the mechanism of action of imatinib.

Imatinib blocks the binding of ATP to the Bcr-Abl tyrosine kinase, thus inhibiting kinase activity, blocking the downstream signal transduction pathway leading to the growth of leukemia cells and inducing apoptosis (Hernandez-Boluda et al., 2002)

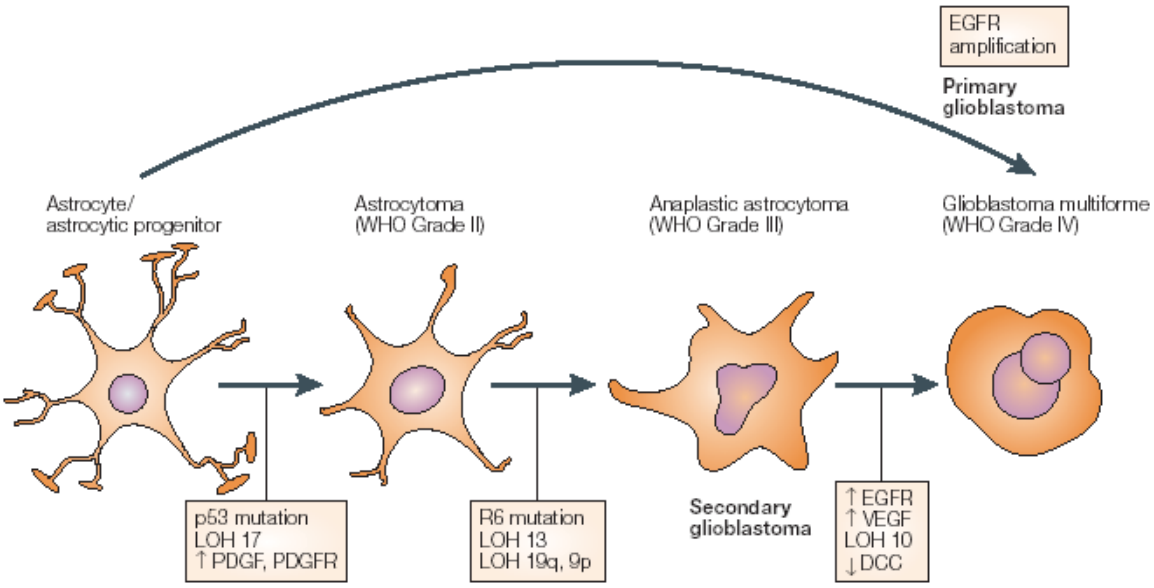

Figure 1.3. Development and progression of astrocytic brain tumours.

Malignant brain tumors can arise in one of two ways. On the one hand, astrocytes undergo genetic changes accompanied by upregulation of certain receptors, such as the platelet-derived growth factor (PDGF), endothelial growth factor receptor (EGFR) or vascular endothelial growth factor (VEGF). These progressive changes culminate in the formation of a glioblastoma. On the other hand, most primary glioblastomas arise de novo, without the need for gradual progression from an astrocytoma to a high-grade astrocytoma to a glioblastoma multiforme (Lesniak and Brem, 2004).

GF120918

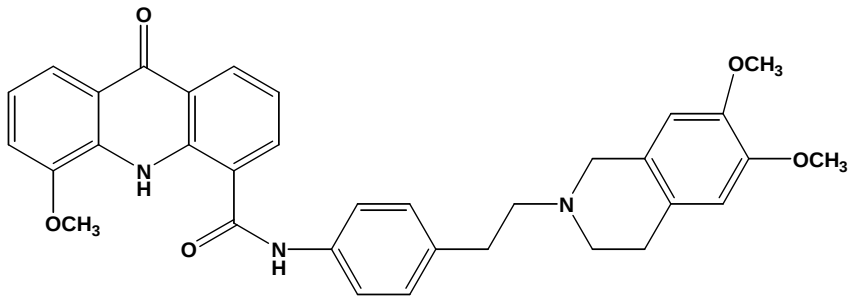

Ko143

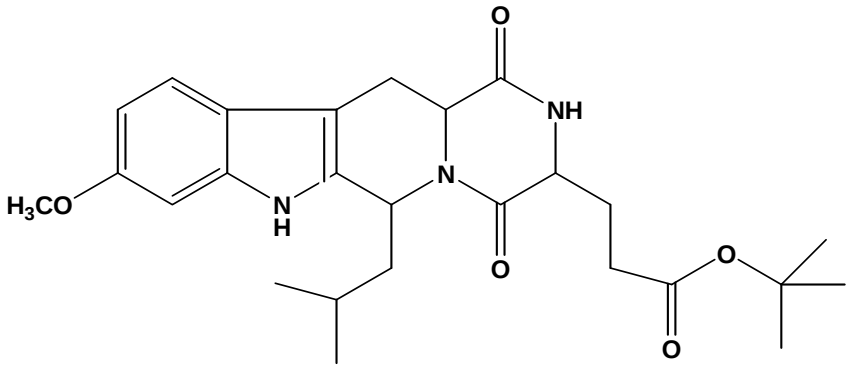

LY335979

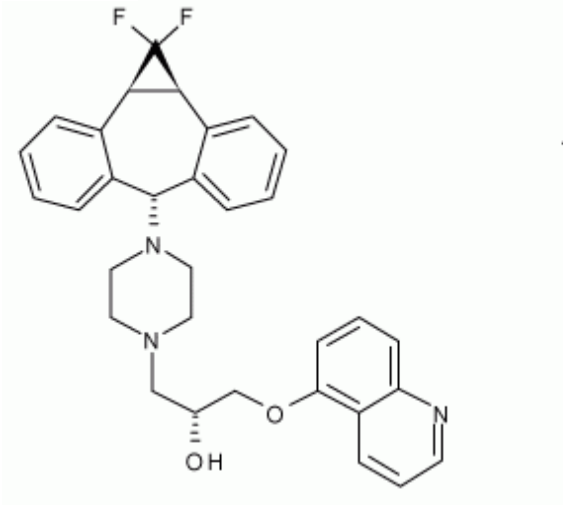

Figure 1.4. chemical structures of LY335979, Ko143 and GF120918

CHAPTER 2

IN VITRO INTERACTION BETWEEN IMATINIB AND Abcg2

2.1 Abstract and introduction

2.1.1 Abstract

The objective of this study was to identify the interaction between imatinib and the ABC drug transporter Abcg2 (Bcrp1). The kinetics of cellular accumulation and permeability of imatinib were studied in MDCKII epithelial cell monolayers, both parental and Abcg2-transfected. The intracellular accumulation after 3 hours incubation and the apical-to-basolateral (A-to-B) and basolateral-to-apical (B-to-A) permeability at various time points up to 3 hours were measured using radiolabeled imatinib. The effect of Abcg2 inhibiters (GF120918 and Ko143) on the accumulation and permeability was also determined using MDCKII-Abcg2 cell monolayers. The intracellular accumulation of imatinib in the parental monolayers was 8-fold greater than that in the transfected cells. Abcg2 inhibiter GF120918 abolished this difference in the intracellular accumulation. The B-to-A flux permeability of imatinib was 63-fold greater than the A-to-B flux permeability in the transfected cells. This difference in directional flux permeability was decreased by Abcg2 inhibiter GF120918 and abolished by a specific Abcg2 inhibiter Ko143. The estimated Km value for the interaction between imatinib and ABCG2 was 3.89 ± 0.44 μM. These data show that imatinib is an Abcg2 substrate.

The effect of inhibitors LY335979 and GF120918 on the cellular accumulation of imatinib in mouse glioma cells was examined. The cross reactivity of PSC833 and CSA on imatinib accumulation in Abcg2-transfected MDCKII cells was also assessed. LY335979 and GF120918 significantly increased imatinib accumulation in mouse

glioma cells. Both PSC833 and CsA showed mild inhibitory effect on Abcg2-mediated cell efflux of imatinib.

2.1.2 Introduction

The success of imatinib in treating CML has led to broader examination of its application in the treatment of other tumors, such as glioma. A study has shown that imatinib inhibited the growth of U343 and U87 GBM (which contains a PDGF/PDGFR autocrine loop) cell lines in vitro and when implanted into the brains of nude mice (Kilic et al., 2000). However, early studies showed imatinib has difficulty in penetrating the blood-brain-barrier (BBB). The CSF concentration of imatinib was only a small fraction of its plasma concentration, thus the CSF imatinib levels are below the threshold that is necessary for the Bcr-Abl inhibition and cell death *in vitro*. CNS relapses have been observed in CML patients even though they have shown a complete hematological response to imatinib (Takayama et al., 2002; Abruzzese et al., 2003; Pfeifer et al., 2003; Bornhauser et al., 2004; Bujassoum et al., 2004; Leis et al., 2004; Neville et al., 2004; Rajappa et al., 2004).

Several mechanisms may limit the delivery of antitumor agents to the brain. Many of these CNS delivery problems are related to BBB and blood-CSF barriers. Besides the tight junctions, various efflux transporters expressed at the BBB, such as ABCB1 and ABCG2. (Sun et al., 2003). Both ABCB1 and ABCB2 are ABC transporters. They are expressed in brain and a number of other tissues including gut wall, liver canaliculi and kidney proximal tubule (Schinkel et al., 2003) In brain, they are located at the luminal

surface of the brain microvascular endothelium and function to keep their diverse rang of substrates out the brain (Cordon-Cardo et al., 1989; Cooray et al., 2002a). Therefore, an emerging question is the possible interaction of imatinib with the drug efflux transporters. The understanding of the interaction of imatinib with the drug efflux transporters will provide useful information for new approaches to enhance the targeted bioavailability of imatinib in the CNS, thus prevent the CNS relapse of CML, and might make it possible to treat PDGFR-related primary and secondary brain cancer with imatinib.

Lately, several studies showed that imatinib is a substrate of ABCB1. Early study in our lab reported the basolateral-to-apical flux of imatinib was 39-fold greater than the apical-to-basolateral flux in the MDR1-transfected cells and 8-fold greater in the parental cell monolayers. This difference in directional flux was significantly reduced by the specific P-glycoprotein inhibitor LY335979 (Dai et al., 2003). Chen et al. also reported K562-n/VCR cell line expressing bcr-abl and mdr1 positive was resistant to imatinib, and could be reversed by 5.18, 1.82 and 1.67-fold respectively when treated with CsA, TAM, and IFN-alpha (Chen et al., 2003). These data indicate that imatinib is a substrate of ABCB1, and that the inhibition of ABCB1 affects the transport of imatinib. *In Vivo* studies strongly supported that imatinib is a substrate of ABCB1. In the wild-type mice, the brain-to-plasma imatinib concentration ratio at all time points was low (1-3%); however, there was an 11-fold greater brain partitioning of STI-571 at 1 h postdose in the mdr1a/b (-/-) mice compared with the wild-type mice. When 12.5 mg/kg STI-571 was given intravenously, the brain-to-plasma ratio of STI-571 in the

mdr1a/b (-/-) mice was approximately 7-fold greater than that of wild-type mice up to 120 min postdose (Dai et al., 2003).

In addition, some new studies have shown that imatinib might interact with the ABCG2 transporter. However, the information regarding the substrate statue of imatinib to ABCG2 has been the subject of controversy (Burger et al., 2004; Houghton et al., 2004a; Ozvegy-Laczka et al., 2004). In this study, we conducted cellular accumulation and cellular permeability studies in parental and Abcg2-transfected MDCKII cells to identify and characterize the interaction between imatinib and Abcg2.

The ability to clone specific transporters has led to the possibility of studying characteristics of transporter function in transfected cells. Transporters that have been transfected include isoforms of MRP, isoforms of P-gp and isoforms of BCRP (Rabindran et al., 2000; Golden and Pollack, 2003a; Breedveld et al., 2004; Pavek et al., 2005). With the expression of the cloned transporter, experiments can now be conducted to address a variety of relevant questions, such as substrate specificity, structure–transport relationships, and drug–drug interaction. The most significant advantage of this technique is that transfected cells allow unambiguous determination of the interaction between a substrate and a specific transporter. However, this system has a weakness that the regulation and activity of cloned transporters in transfected cells are unlikely to be quantitatively equivalent to in vivo BBB transporters (Golden and Pollack, 2003a).

The transporter-transfected cell line used in this study is the Madin Darby canine kidney (MDCKII) cell line. It is a dog renal epithelia derived cell line. MDCKII cells differentiate into columnar epithelium and form tight junctions in a short period of time (~3 days) when grown onto Transwell® inserts (Agarwal et al., 2007). In 1989, Pastan et al. first transfected human ABCB1 into polarized MDCKII cells. Since then, MDCKII–ABCB1 cell line has been extensively selected as a model to study ABCB1-mediated drug efflux, such as identify and characterize the substrate and inhibitors of ABCB1 and predict the permeability of ABCB1 substrates across BBB (Wang et al., 2005; Xia et al., 2007c). In 2000, Jonker and coworkers transfected murine Abcg2 into MDCKII cells to study the role of Abcg2 in the bioavailability and fetal penetration of topotecan (Jonker et al., 2000). Now this useful cell model has been widely used to study Abcg2-mediated drug efflux (Marchetti et al., 2007; Pan et al., 2007).

The objective of this study was to identify and characterize the interaction between imatinib and the ABC drug transporter Abcg2 (Bcrp1) by using cellular accumulation and directional flux methods.

2.2 Material and methods

2.2.1 Chemicals and cell lines

2.2.1.1 Chemicals

Imatinib and ^{14}C-imatinib were kindly provided by Novartis Pharma (East Hanover, NJ). GF120918 (N-[4-[2-(6, 7-Dimethoxy-3, 4-dihydro-1H-isoquinolin-2-yl) ethyl]-5-

methoxy-9-oxo-10H-acridine-4-carboxamide) was generously given by GlaxoSmithKline (Research Triangle, NC). Ko143 was kindly provided by Dr. Alfred Schinkel (Netherlands Cancer Institute, Amsterdam, Netherlands). LY335979 ((*R*)-4-((1a*R*, 6R, 10bS)-1,2-difluoro-1, 1a, 6,10b-tetrahydrodibenzo-(*a*,*e*)cyclopropa(*c*)cycloheptan-6-yl)-α-((5-quinoloyloxy)methyl)-1-piperazineethanol, trihydrochloride) was a gift from Eli Lilly and Co. (Indianapolis, IN). PSC833 and cyclosporine A (CsA) were generously given by Novartis Pharma, (East Hanover, NJ). All other chemicals used were HPLC or reagent grade.

2.2.1.2 Cell lines

Wild-type (WT) and Abcg2-transfected epithelial Madin-Darby canine kidney (MDCKII) cells were a gift from Dr. Schinkle (Netherlands Cancer Institute, Amsterdam, Netherlands). Cells were cultured in Dulbecco's modified Eagle's medium (Mediatech, Inc., Herndon, VA) fortified with 10% heat-deactivated fetal bovine serum (SeraCare Life Sciences, Inc., Oceanside, CA), 100 U/ml penicillin G, 100 µg/ml streptomycin and 250 ng/mL amphotericin B (Sigma-Aldrich, St. Louis, MO) at 37°C under humidity and 5% CO_2 tension. Cells used in all experiments were between passages 5 and 15.

Mouse glioma cells M7 were kindly provided by Dr. John Olhfest (University of Minnesota, Minneapolis, MN). The brain tumor specimen was delivered on ice in a tube containing Neurobasal (NB) media (Invitrogen, Carlsbad, CA). Upon arrival to the lab tumor tissue was transferred to NB supplemented with 50 ng/mL bFGF, 50 ng/mL EGF,

5 μg/mL gentamicin, and 0.9 μg/mL Fungizone under serum free conditions. The tissue was transferred to a petri dish and minced using scalpels until the tissue particles were of a size that can be drawn in and out of a 10 ml pipette. The cell suspension was strained to remove any connective tissue. The cells were washed in PBS and once in Red Blood Cell Lysis solution. Cultures were grown in a cell culture incubator at 37° C, 5% CO_2, and 90% relative humidity in culture media consisting of: DMEM/F12 w/ L-glutamine and sodium bicarbonate (Invitrogen, Carlsbad, CA), B27 supplement (0.5X) (Invitrogen, Carlsbad, CA), N2 supplement (0.5X) (Invitrogen, Carlsbad, CA), 20 ng/ml human EGF (Peppro Tech, Princeton, NJ), 20 ng/ml human FGF (Peppro Tech, Princeton, NJ), 1X non-essential amino acids (Gibco), 1% penn/strep (Gibco) and 10 mM Hepes (Gibco). Fresh EGF and FGF were added to the cells every 2-3 days regardless of whether the cells were passaged (20 ng/nl final concentration for both).

2.2.2 Cellular accumulation studies in MDCKII cell

For the accumulation experiments, cells were seeded in clear polystyrene 12-well plates (TPP cell culture plate; Sigma-Aldrich, St. Louis, MO) at a seeding density of 2×10^5 cells/well. The medium was changed every other day and the cells formed confluent monolayers in 3-4 days. On the day of the experiment, the medium was aspirated and the confluent monolayer was washed twice with 1 mL prewarmed (37°C) assay buffer (122 mM NaCl, 25 mM $NaHCO_3$, 10 mM glucose, 10 mM HEPES, 3 mM KCl, 1.2 mM $MgSO_4 \cdot 7H_2O$, 1.4 mM $CaCl_2 \cdot H_2O$, 0.4 mM K_2HPO_4, pH 7.4). The cells were preincubated with 1 ml of assay buffer for 30 min, after which the buffer was aspirated and the experiment was initiated by adding 1 ml tracer solution of radiolabeled drug

(0.22 μg ^{14}C-imatinib) in assay buffer into each well. The plates were continuously agitated at 60 rpm in an orbital shaker at 37°C. After a 3-h accumulation period, the supernatant was aspirated and the cells were first washed three times with 2 ml of ice-cold phosphate-buffered saline and then solubilized using 1 ml of mammalian protein extraction reagent (M-PER®, Pierce Biotechnology, Inc., Rockford, IL). A 200μl sample of solubilized cell fractions was drawn from each well in triplicate, and 4 ml of scintillation fluid (ScintiSafe Econo cocktail; Fisher Scientific Co., Pittsburgh, PA) was added to each sample and counted using liquid scintillation counting (LS-6500; Beckman Coulter, Inc., Fullerton, CA) to determine the radioactivity associated with the cell fractions. The protein concentration was determined using the BCA protein assay (Pierce Biotechnology, Inc., Rockford, IL) to normalize the radioactivity in each well. For inhibition studies, the cells were treated with the inhibitor (5 μM GF120918) during both the preincubation and the accumulation periods. Drug accumulation in cells was expressed as a percentage of the accumulated radioactivity measured in the wild-type control cells (dpm) per microgram of protein. The stock solutions for all the inhibitors used were prepared in dimethyl sulfoxide (DMSO) and diluted using assay buffer to obtain working solutions, so that the final concentration of DMSO was less than 0.1%.

2.2.3 Cellular permeability studies in MDCKII cell

The methods used for directional flux were similar to that previously described by Dai et al. (Dai et al., 2003). In brief, cells were seeded at a density of 2×10^5 cells/well on polyester semipermeable membrane supports of the inserts in six-well Transwells (Corning Inc., Corning, NY). The medium was changed every day and the cells formed

confluent polarized epithelial monolayers in 3-4 days. The representative transepithelial electrical resistance was 300 ± 8 ohm·cm^2 (n=6) in the WT MDCKII monolayers and 248± 27 ohm·cm^2 (n=6) in the Abcg2-transfected MDCKII monolayers. Mannitol flux across the monolayer was also measured to confirm the existence of tight junctions with approximately 1% per hour flux (P_{eff}= 9 × 10^{-8} cm/s). The monolayers were washed with 2 mL prewarmed (37°C) assay buffer, and after a 30-min preincubation, the experiment was initiated by adding a tracer solution of radiolabeled drug in assay buffer to the donor side (apical side, 1.5 ml; basolateral side, 2.6 ml). Fresh assay buffer was added to the receiver side and 200 µl was sampled from the receiver compartment at 0, 15, 30, 60, 90, 120 and 180 min. The volume sampled was immediately replaced with fresh assay buffer. Additional samples were drawn at 0 and 180 min from the donor compartment. The amount of radioactivity in the samples was determined using liquid scintillation counting as described previously. The apical-to-basolateral (A-to-B) flux was determined by addition of radiolabeled drug solution to the apical compartment and sampling the basolateral compartment, whereas for basolateral-to-apical (B-to-A) flux, the donor was the basolateral compartment and the apical compartment was the receiver compartment. When an inhibitor was used in the flux study, the cell monolayers were preincubated with the inhibitor (5 µM GF120918 and 200 nM Ko143) for 30 min, followed by the inhibitor being present in both compartments throughout the course of the experiment.

Permeability Calculation

The effective permeability (*P*eff) was calculated by the following equation,

$$P_{eff} = \frac{\left(\frac{dQ}{dt}\right)}{A * C_0} \qquad (1)$$

where Q is the amount of radiolabled drug transported though the cell monolayer, t is the time, dQ/dt is the mass transport rate, A is the effective area of the cell monolayer ($4.67cm^2$) and C_0 is the initial concentration of radiolabled drug in the donor compartment. To make sure the two assumptions, 1) sink condition and2) linear condition are satisfied, only data generated between 0 and 90 min was used to calculate P_{eff}. Efflux ratio is defined as the ratio of *P*eff of the B-to-A flux over the *P*eff of the A-to-B flux.

2.2.4 Estimation of apparent Km

WT and Abcg2 transfected MDCKII cells were seeded at a density of 2×10^5 cells/well on polyester semipermeable membrane supports of the inserts in six-well Transwells. The medium was changed every day and the cells formed confluent polarized epithelial monolayers in 3-4 days. The monolayers were washed twice with 2 mL prewarmed (37°C) assay buffer, and then incubated with assay buffer with or without various concentrations of non-radiolabled imatinib (2, 5, 10, 20 and 50 μM imatinib) for 30 min, and the preincubation media was then aspirated. Assay buffer with or without various concentrations of non-radiolabled imatinib was added into the receiver compartment (apical side, 1.5 ml; basolateral side, 2.6 ml). Assay buffer with or without various concentrations of non-radiolabled imatinib added with tracer ^{14}C-imatinib was applied into the donor compartment to start the experiment. 200 μl was sampled from the receiver compartment at 0, 15, 30, 60, 90, 120 and 180 min and the volume sampled

was immediately replaced with assay buffer with or without various concentrations of non-radiolabled imatinib. Additional samples were drawn at 0 and 180 min from the donor compartment. The amount of radioactivity in the samples was determined using liquid scintillation counting as described previously. The apical-to-basolateral (A-to-B) flux and basolateral-to-apical (B-to-A) flux were determined as previously described in section 2.2.3.. The effective permeabilities of the B-to-A flux and the A-to-B flux of ^{14}C-imatinib with and without the presence of different concentrations of non-radiolabled imatinib were calculated based on equation (1). Then the efflux ratio corresponding to the presence of each concentration of non-radiolabled imatinib was determined. Apparent Km (EC50) was estimated by fitting the inhibitory effect Emax model to the efflux ratio data. The equation of the inhibitory effect Emax model is listed below:

$$E=Emax- (Emax-E0)*(C/(C+EC50)) \quad (2)$$

Where E is effect (efflux ratio), Emax is the maximum effect at C=0, E0 is the effect at C=0, C is the concentration of non-radiolabled imatinib and EC50 is the concentration of non-radiolabled imatinib when the inhibitory effect reaches the 50% of the maximum inhibitory effect (Emax-E0).

2.2.5 Cellular accumulation studies in mice glioma cells

M7 cells (mouse glioma cells) were spun down and lysed by HyQtase and counted. Lysed cells were diluted with assay buffer to reach a final density of 2×10^6 cells/mL. Cell suspension was added to 12-well plates (TPP cell culture plate; Sigma-Aldrich, St. Louis, MO), 500 µL per well. Plates were preincubated in an orbital shaker at 37°C for

30 min. Experiment was initiated by adding 500 µL tracer solution of ^{14}C-imatinib into each well. Plates were continuously agitated at 60 rpm in an orbital shaker at 37°C for 3 hr, and all the material in each well was removed to a corresponding 15 mL conical tube. Reaction was stopped by adding 9mL ice-cold PBS into each tube. Cell suspension was centrifuged at 2500 rpm for 5 min. The supernatant was aspirated. The cell pellet was washed one more time with 5 mL ice-cold PBS and centrifuged at 2500 rpm for 5 min. The remained cell pellet was solubilized using 600 µl of M-PER® (Pierce Biotechnology, Inc., Rockford, IL). A 100 µl sample of solubilized cell fractions was drawn from each tube in triplicate, and 4 ml of scintillation fluid (ScintiSafe Econo cocktail; Fisher Scientific Co., Pittsburgh, PA) was added to each sample and counted using liquid scintillation counting (LS-6500; Beckman Coulter, Inc., Fullerton, CA) to determine the radioactivity associated with the cell fractions. The protein concentration was determined using the BCA protein assay (Pierce Biotechnology, Inc., Rockford, IL) to normalize the radioactivity in each well. For inhibition studies, the cells were treated with the inhibitor (1 µM LY335979 or 5 µM GF120918) during both the preincubation and the accumulation periods. Drug accumulation in cells was expressed as dpm per microgram of protein. The stock solutions for all the inhibitors used were prepared in dimethyl sulfoxide (DMSO) and diluted using assay buffer to obtain working solutions, so that the final concentration of DMSO was less than 0.1%.

2.2.6 Inhibitors cross reactivity

Cellular accumulation method was used to study inhibitor cross reactivity. WT and Abcg2-trasfected cells were seeded in clear polystyrene 24-well plates (SARSTEDT,

Newton, NC) at a seeding density of 1×10^5 cells/well. The medium was changed every other day and the cells formed confluent monolayers in 3-4 days. On the day of the experiment, the medium was aspirated and the confluent monolayer was washed twice with 1mL prewarmed (37°C) assay buffer. The cells were preincubated with 1 ml of assay buffer with and without different concentrations of inhibitors (5, 10, 15 and 30 μM PSC833; 5, 10,15 and 30 μM CsA) for 30 min, after which the buffer was aspirated and the experiment was initiated by adding 1 ml tracer solution of radiolabeled drug (0.22 μg ^{14}C-imatinib) in assay buffer with and without different concentrations of inhibitors into each well. The plates were continuously agitated at 60 rpm in an orbital shaker at 37°C. After a 3-h accumulation period, the supernatant was aspirated and the cells were first washed three times with 2 ml of ice-cold phosphate-buffered saline and then solubilized using 1 ml of mammalian protein extraction reagent M-PER. The amount of radioactivity in the samples and the protein concentration of each sample was determined as previously described in section 2.2.2.

2.2.7 Statistical and data analysis

Statistical analysis was conducted using SigmaStat, version 3.1(Systat Software, Inc., Point Richmond, CA). Statistical comparisons between two groups were made by using two-sample t-test at $p < 0.01$ significance level. If groups failed the normality test, then the nonparametric alternative of two-sample *t* test, the Mann-Whitney rank sum test, was used. Groups were compared by one-way analysis of variance with the Holm-Sidak post-hoc test for multiple comparisons at a significance level of $p < 0.01$. When groups

failed the normality or equal variance test, analysis of variance on ranks with the Tukey post-hoc test was used for multiple comparisons.

2.3 Results

2.3.1 Imatinib accumulation in WT and Abcg2-transfected MDCKIIcells

^{3}H-mitoxantrone was used as a positive control (Doyle et al., 1998) to verify the Abcg2 protein function in the Abcg2-transfected MDCKII cell. The cellular accumulation of ^{3}H-mitoxantrone was significantly lower ($p < 0.01$) in the Abcg2-transfected cells than that in the wild-type cells. Mitoxantrone accumulation in the Abcg2 cells was only 19% of that in WT MDCKII cells (figure 2.1).). ^{14}C-imatinib had a significant lower accumulation (~5% of WT control, $p < 0.01$) in the Abcg2-transfected cells than the wild-type cells. When the Abcg2 inhibitor GF120918 was applied, it was able to increase the imatinib net accumulation in Abcg2-transfected cell to a similar level as wild-type cells (figure 2.2)

2.3.2 Imatinib flux in WT and Abcg2-transfected MDCKII cells

The B-to-A flux of imatinib in Abcg2-transfected MDCKII cells was greater than that in WT cells, while the A-to-B flux was lower in Abcg2-transgected cells compared to that in WT cells (figure 2.3). The B-to-A flux effective permeability of imatinib in the transfected cells was (1.81E-05±8.76E-07 cm/s), which was 63-fold greater ($p<0.01$) than the A-to-B flux apparent permeability (2.87E-07±4.86E-08 cm/s) (figure 2.4). When Abcg2 inhibitor GF120918 was applied, it was able to decrease the difference

between the B-to-A flux and A-to-B flux of imatinib in Abcg2-transfected cells (figure 2.5). The efflux ratio of imatinib in Abcg2-transfected cells was decreased to 8.55 by GF120918 (figure 2.6). In the case when the potent Abcg2 selective inhibitor Ko143 was used, Ko143 eliminated the difference between the B-to-A flux and A-to-B flux of imatinib in Abcg2-transfected cells (figure 2.7). Ko143 minimized the efflux ratio of imatinib in Abcg2-transfected cells to 2.22 (figure 2.8).

2.3.3 Estimated apparent Km for interaction between imatinib and Abcg2

The efflux ratio of imatinib in Abcg2-transfected cells without the presence of non-radiolabeled imatinib, i.e., the maximum observed efflux ratio (Emax) was 63. The observed efflux ratio of imatinib at the highest presented concentration of non-radiolabeled imatinib was 2.75. The estimated apparent Km (EC50) value of imatinib for Abcg2 was 3.89 ± 0.44 μM (figure 2.9).

2.3.4 Imatinib accumulation in mouse glioma cells

Imatinib accumulation in M7 cells was 102.50 ± 21.52 DPM/μg protein. ABCB1 selective inhibitor LY335979 significantly increased the cellular accumulation of imatinib in M7 cells ($p<0.01$). GF120918, the ABCB1 and Abcg2 dual inhibitor, also increased imatinib accumulation in M7 cells significantly ($p<0.01$). There was no significant difference between the effect of LY335979 and GF120918 on the cellular accumulation of imatinib in M7 cells (figure 2.10).

2.3.5 Inhibitors cross reactivity

ABCB1 inhibitor PSC833 did not show an inhibitory effect on Abcg2 mediated transport of imatinib at concentrations lower than 15 μM. At concentrations higher than 15 μM, PSC833 showed mild inhibitory effect that significantly increased imatinib accumulation in Abcg2-transfected MDCKII cells (figure 2.11). Another ABCB1 inhibitor, CsA, showed significant inhibitory effect on Abcg2 mediated transport of imatinib at concentration as low as 5 μM. However, this effect did not increase significantly as the concentration of CsA increased to 30 μM (figure 2.12).

2.4 Discussion

Imatinib was the milestone of molecularly-targeted therapy for cancer treatment. However, it has difficulty to penetrate CNS. Previous study showed imatinib is an ABCB1 substrate and its CNS distribution is limited by ABCB1. ABCG2 is another important efflux transporter that attracts increasing interest. Recent studies reported that imatinib might also be a substrate of ABCG2/Abcg2 (Burger et al., 2004; Ozvegy-Laczka et al., 2004). We carried out cellular accumulation and permeability studies to identify and characterize the interaction between imatinib and Abcg2.

The cellular accumulation studies showed that ^{14}C-imatinib accumulation in Abcg2-transfected MDCKII cells was just 5% of that in wild-type control cells (figure 2.2). This difference was statistically significant. It was even greater than the difference of mitoxantrone accumulation between Abcg2-transfected and WT MDCKII cells, while

mitoxantrone is a well-known excellent Abcg2 substrate (Doyle et al., 2003). Abcg2 inhibitor GF120918 abolished the difference of ^{14}C-imatinib accumulation between Abcg2-transfected and WT MDCKII cells. In cellular permeability studies, the efflux ratio of imatinib in Abcg2-transfected MDCKII cells was 63 while the efflux ratio in WT cells was 1.77. Ko143, the selective Abcg2 inhibitor (Allen et al., 2002b), decreased the efflux ratio of imatinib in Abcg2-transfected MDCKII cells to 2.22. GF120918 was also able to reduce the efflux ratio of imatinib in Abcg2-transfected MDCKII cell, from 63.03 to 8.55. It is quite interesting that the inhibitory effect of GF120918 in the cellular permeability study was not as great as that in the cellular accumulation studies. In accumulation study, 5 μM GF120918 completely inhibited Abcg2-mediate efflux of imatinib. However, in permeability study, the efflux ratio of imatinib in Abcg2-transfected cell with the presence of 5 μM GF120918 was still different from that in WT cells. Further studies are needed to reveal the underlying mechnism.

Houghton et al. reported that imatinib increased topotecan and SN-38 accumulation in ABCG2 expressing Saos2 cells. In the same study, the parental and ABCG2 expressing Saos2 cells had similar sensitivity to imatinib. So they concluded that imatinib is a inhibitor of ABCG2 but is not a substrate for it (Houghton et al., 2004b). Almost at the same time, Ozvegy-Laczka and colleagues discovered that imatinib interacts with ABCG2 with high affinity in ATPase assays and fluorescent dye uptake experiments (Ozvegy-Laczka et al., 2004). Later on, Burger et al. showed in their study that ^{14}C-imatinib accumulation in ABCG2 expressing MCF7 cells was significantly lower than

that in the parental MCF7 cell after 2-hr incubation and declared that imatinib is a substrate of ABCG2 (Burger et al., 2004). Our results of cellular accumulation studies and cellular permeability studies strongly indicated that imatinib is an Abcg2 substrate.

To further study the interaction between imatinib and Abcg2, the apparent Km of Abcg2 for its interaction with imatinib was estimated by dose dependence study. As the concentration of non-radiolabeled imatinib increased, the effective permeability (*P*eff) of ^{14}C-imatinib in A-to-B direction increased and the *P*eff in B-to-A direction decreased. The efflux ratio, which is defined as the raio of *P*eff of the B-to-A flux over the *P*eff of the A-to-B flux, decreased with the increase of non-radiolabeled imatinib. Since efflux ratio takes both *P*eff in A-to-B direction and *P*eff in B-to-A direction into account, it was taken as effect (Muenster et al., 2008). The inhibitory effect Emax model was used to fit the data because ideally the efflux ratio will be approaching 1. The estimated EC50 value of imatinib, the same as the apparent Km value of imatinib, was 3.89 ± 0.44 μM. Apparent Km is important information that tells the affinity between imatinib and Abcg2. This result suggested again imatinib is a significant Abcg2 substrate that interacts with Abcg2 at low micro molar range. One thing should be pointed out is that the efflux ratio did not reach plateau at the highest concentration we examined. However, cellular permeability study with higher concentration of non-radiolabeled imatinib was failed due to cell death at the end of the experiments. It is very likely caused by the cytotoxicity effect of imatinib at high concentration (eg. 100 μM).

With the conclusion that imatinib is a substrate of both ABCB1 and Abcg2, the cellular accumulation of imatinib in mouse glioma cells was studied. The multidrug resistance in tumor cells also plays an important role in the brain tumor treatment besides the resistance in BBB (Nies and Nies, 2007). Both ABCB1 selective inhibitor LY335979 and ABCB1, ABCG2 dual inhibitor GF120918 significantly increased imatinib accumulation in mouse glioma cells. Nevertheless, there was no significant difference between the effect of LY335979 and GF120918. So the inhibition of Abcg1 increased imatinib uptake in mice giloma cells. The reason that no dual effect of GF120918 was seen in this study could be that Abcg2 is present in the brain tumor capillaries, but not in these brain tumor cells (Cooray et al., 2002b). This experiment provided information that the inhibition of efflux transporter(s) in glioma cells could result in increased cellular accumulation and might further lead to improved treatment.

ABCB1 and ABCG2 are two major ATP-binding cassette (ABC) membrane efflux transporters that confer drug resistance in cancer (Merino et al., 2004). The two have a partly overlapped substrate spectrum (Xia et al., 2007c). So it is possible for some ABCB1 modulators to interact with ABCG2, such as GF120918. Recently, Xia et al. revealed that CsA, one of the first-generation ABCB1 modulators, is an inhibitor but not a substrate of ABCG2 (Xia et al., 2007a). Since PSC833 is the nonimmunosuppressive analog of CsA (Friche et al., 1992), we highly suspect that it might also have inhibitory effect on ABCG2. The cellular accumulation of ^{14}C-imatinib in Abcg2-transfected MDCKII cells with the presence of PSC833 in different concentrations indicated that PSC833 inhibits the Abcg2-mediated imatinib transport at

concentrations above 15 μM (figure 2.11). On the other hand, CsA showed inhibitory effect on Abcg2 at the lowest concentration (5μM) we tested, though the effect remained the same as CsA concentration increased from 5 μM to 30 μM (figure 2.12). These are important transporter modulator cross activity information that can be useful in choosing modulators and data interpretation.

2.5 Conclusion

In summary, this study used both cellular accumulation and cellular permeability methods to identify the substrate status of imatinib to efflux transporter Abcg2. In cellular accumulation studies, the accumulation of ^{14}C-imatinb in WT MDCKII cells was significantly greater than that in Abcg2-transfected cells. This difference was abolished by GF120918. The efflux ratio of imatinib in Abcg2-transfected MDCKII cells was about 36 fold greater than the imatinib efflux ratio in WT cells. GF120918 decreased and Ko143 abolished the difference of imatinib efflux ratios between Abcg2-transfected and WT MDCKII cells. The estimated Km for the interaction between imatinib and Abcg2 was 3.89 ± 0.44 μM. LY335979 and GF120918 significantly increased imatinib accumulation in mouse glioma cells. Both PSC833 and CsA showed mild inhibitory effect on Abcg2-mediated cell efflux of imatinib. In conclusion, imatinib is an Abcg2 substrate, and that the inhibition of Abcg2 will dramatically affect the *in vitro* intracellular accumulation of imatinib in MDCKII monolayers and the transport of imatinib across MDCKII monolayers.

2.6 Acknowledgement

We would like to thank Novartis Pharma for kindly providing us imatinib, ^{14}C-imatinib, CsA and PSC833. We thank Dr. Schinkle from Netherlands Cancer Institute for generously providing us WT and Abcg2-transfected MDCKII cells and Ko143. We thank Eli Lilly and Co. for kindly providing us LY335979. We thank GlaxoSmithKline for kindly providing us GF120918.

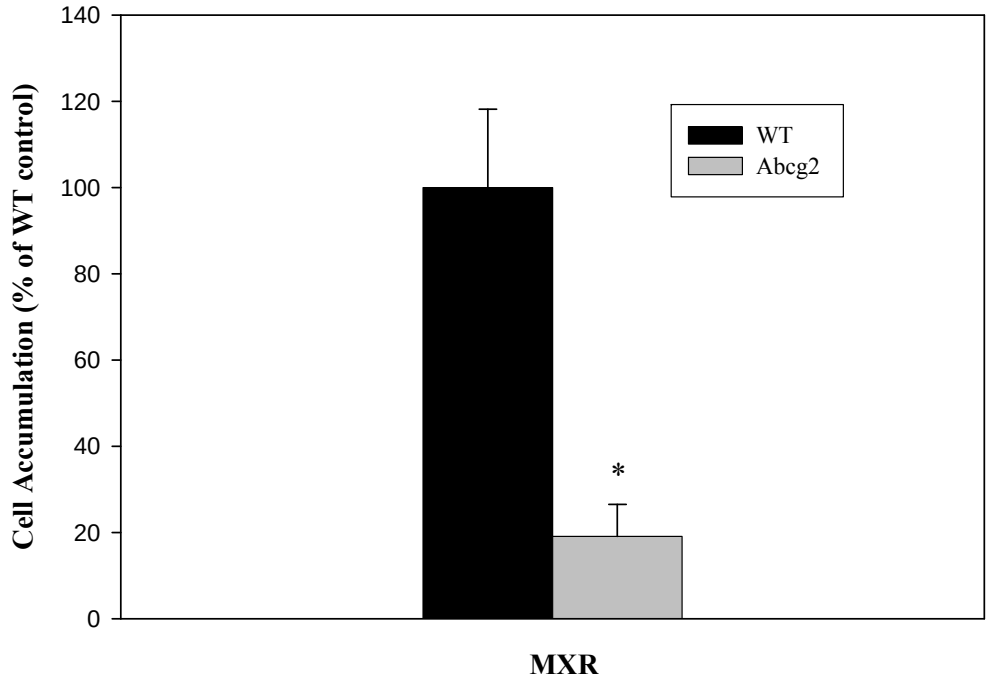

Figure 2.1. Accumulation of 3H-mitoxantrone in WT (black bar) and Abcg2-transfected (gray bar) MDCKII cells.

Results are presented as mean ±S.D., (as percentage of wild-type control), n = 12. Mitoxantrone accumulation in Abcg2-transfected cells was significantly lower than in the wild-type cells, $p < 0.01$.

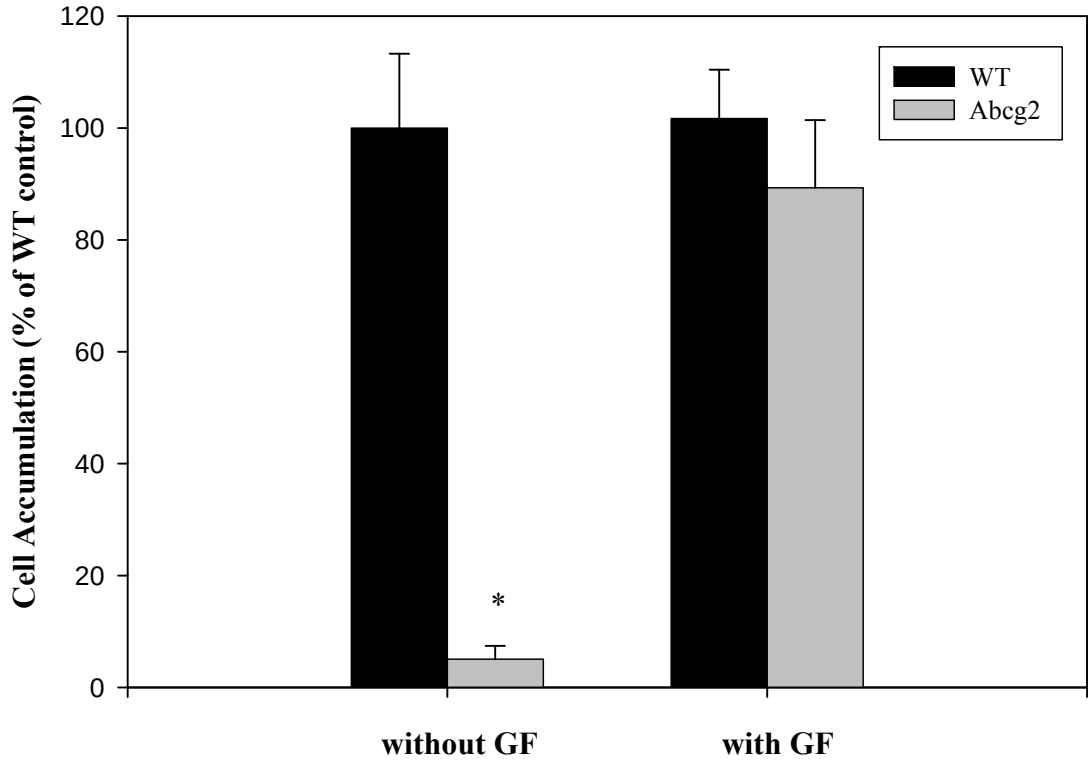

Figure 2.2. Accumulation of ^{14}C-imatinib in WT (black bar) and Abcg2-transfected (gray bar) MDCKII cells with and without GF120918 (5 μM).

Results are presented as mean ±S.D., (as percentage of wild-type control), n = 12. Imatinib accumulation in Abcg2-transfected cells was significantly lower than in the wild-type cells, $p < 0.01$. Abcg2 inhibitor GF120918 abolished the difference between the imatinib accumulation in Abcg2-transfected and WT cells.

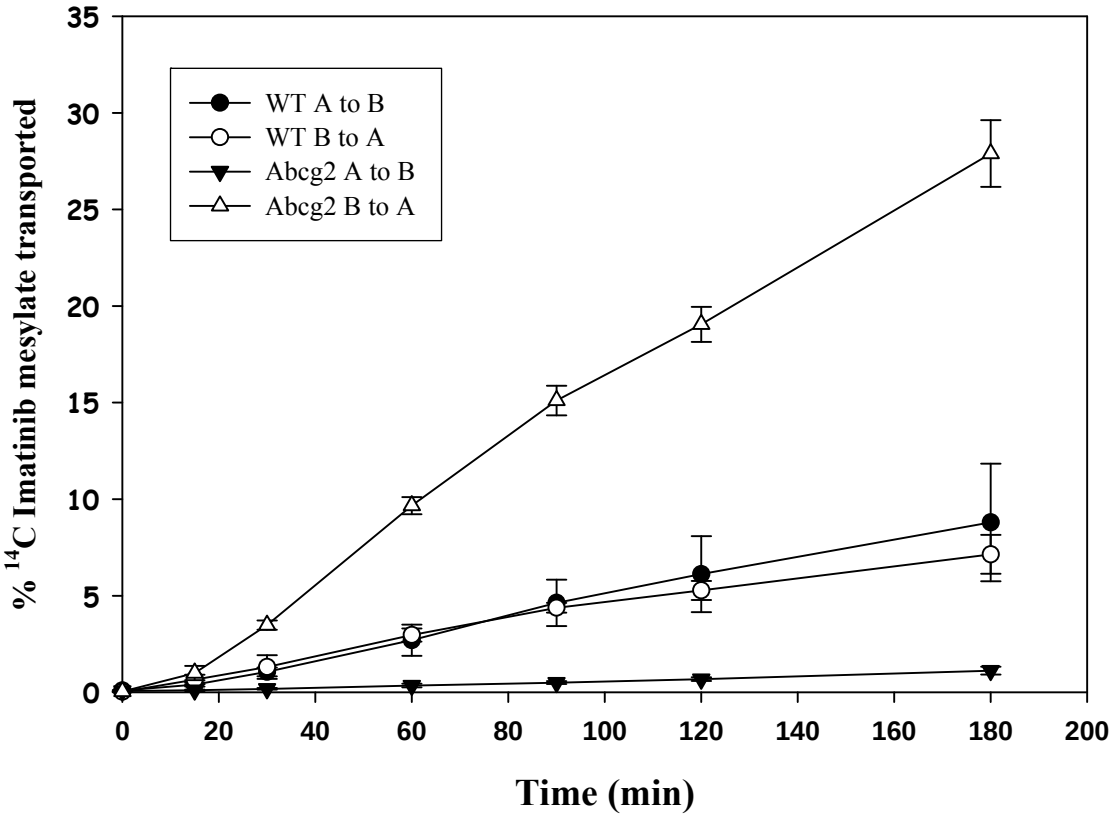

Figure 2.3. Directional flux of ^{14}C-imatinib across the MDCKII monolayers in wild-type (●, A-to-B direction; ○, B-to-A direction) and Abcg2-transfected cells (▼, A-to-B direction; △, B-to-A direction).

Results are expressed as mean ±S.D., n=9. The difference between the B-to-A flux and A-to-B flux of imatinib in Abcg2-transfected cells was greater than that in wild-type cells.

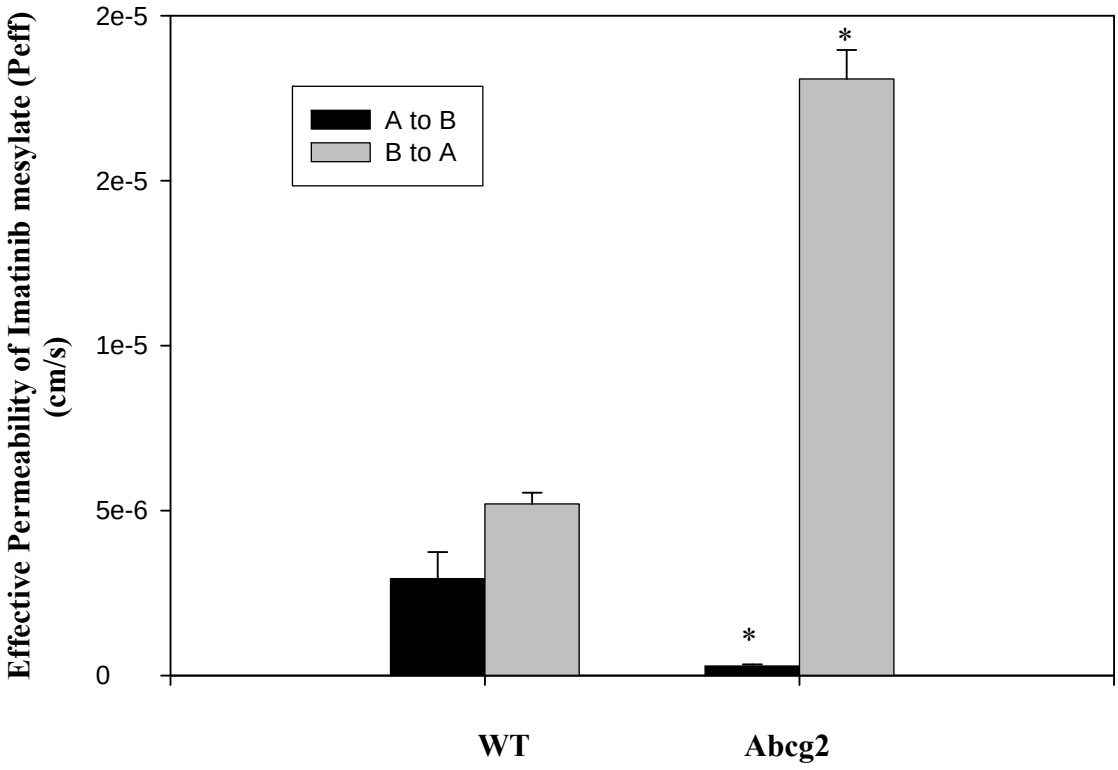

Figure 2.4. The A-to-B direction effective permeability (black bar) and B-to-A direction effective permeability (gray bar) of imatinib (cm/s) across the WT and Abcg2-transfected MDCKII cell monolayers.

Results are expressed as mean ±S.D., n=9 (*, $p < 0.01$). The efflux ratio of imatinib in Abcg2-transfected cells was 63 while that in WT cells was 1.8.

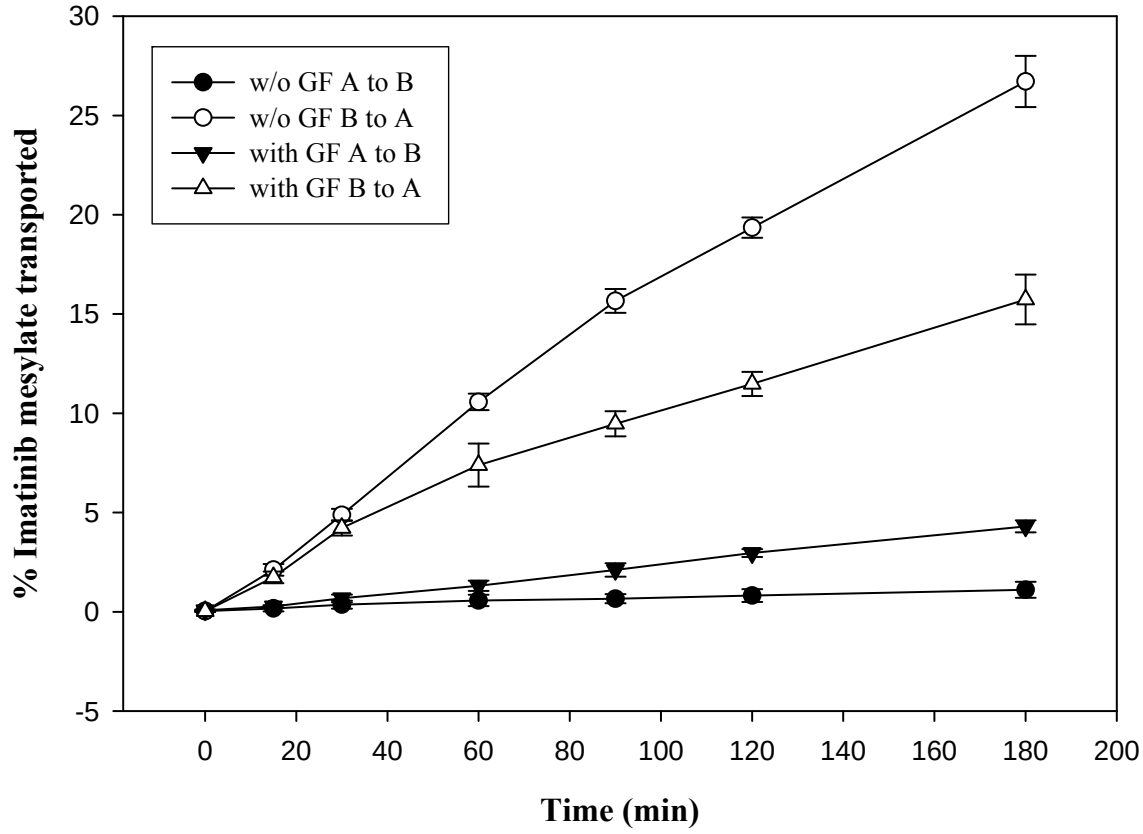

Figure 2.5. Directional flux of 14C-imatinib across the Abcg2-transfected MDCKII cells monolayers with (▼, A-to-B direction; △, B-to-A direction) and without inhibitor GF120918 (5 μM) (●, A-to-B direction; ○, B-to-A direction).

Results are expressed as mean ±S.D., n=9. The difference between the B-to-A flux and A-to-B flux of imatinib in Abcg2-transfected cells was decreased by GF120918.

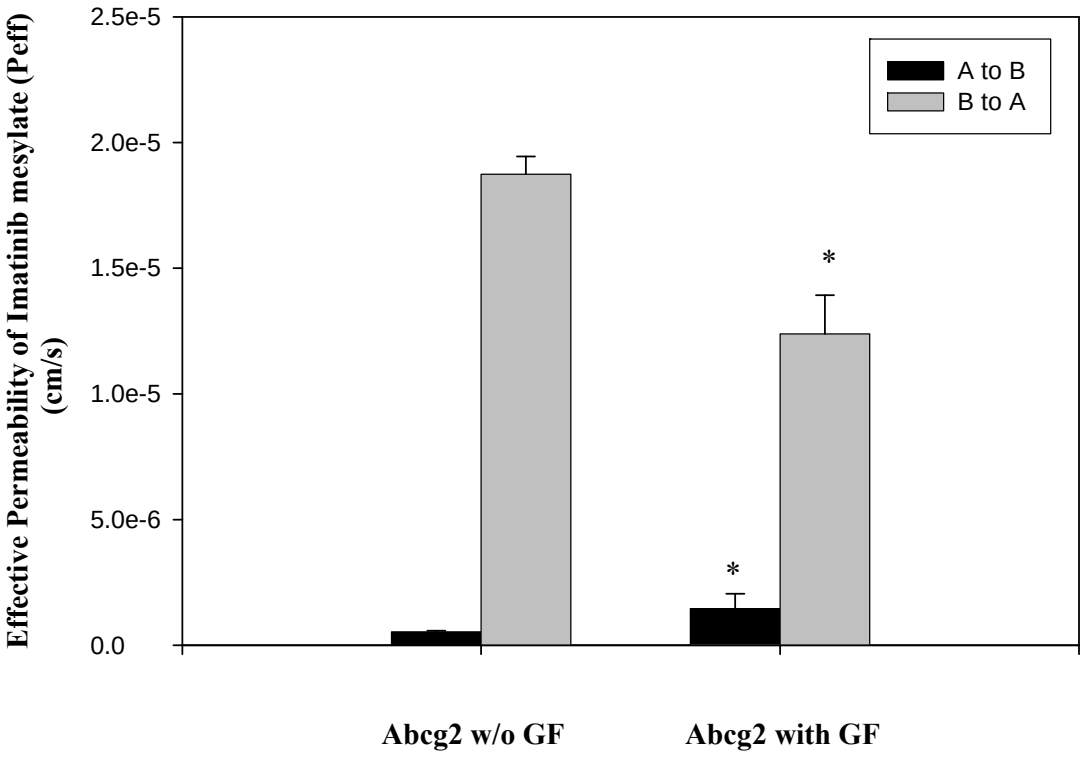

Figure 2.6. The A-to-B direction effective permeability (black bar) and B-to-A direction effective permeability (gray bar) of imatinib (cm/s) across the Abcg2-transfected MDCKII cell monolayers with and without GF120918 (5 μM).

Results are expressed as mean ±S.D., n=9 (*, $p < 0.01$). The efflux ratio of imatinib in Abcg2-transfected cells was decreased by GF120918 from 63 to 8.55.

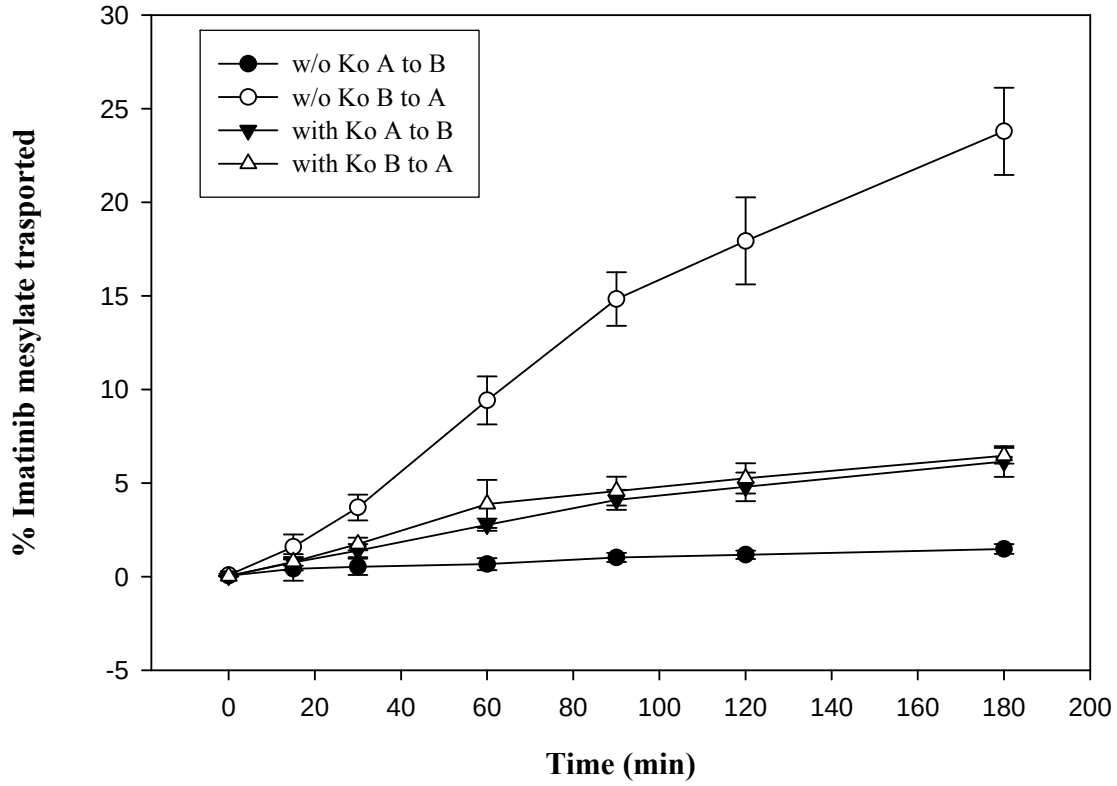

Figure 2.7. Directional flux of 14C-imatinib across the Abcg2-transfected MDCKII cells monolayers with (▼, A-to-B direction; △, B-to-A direction) and without potent and selective Abcg2 inhibitor Ko143 (200 nM) (●, A-to-B direction; ○, B-to-A direction).

Results are expressed as mean ±S.D., n=9. Ko143 eliminated the difference between the B-to-A flux and A-to-B flux of imatinib in Abcg2-transfected cells.

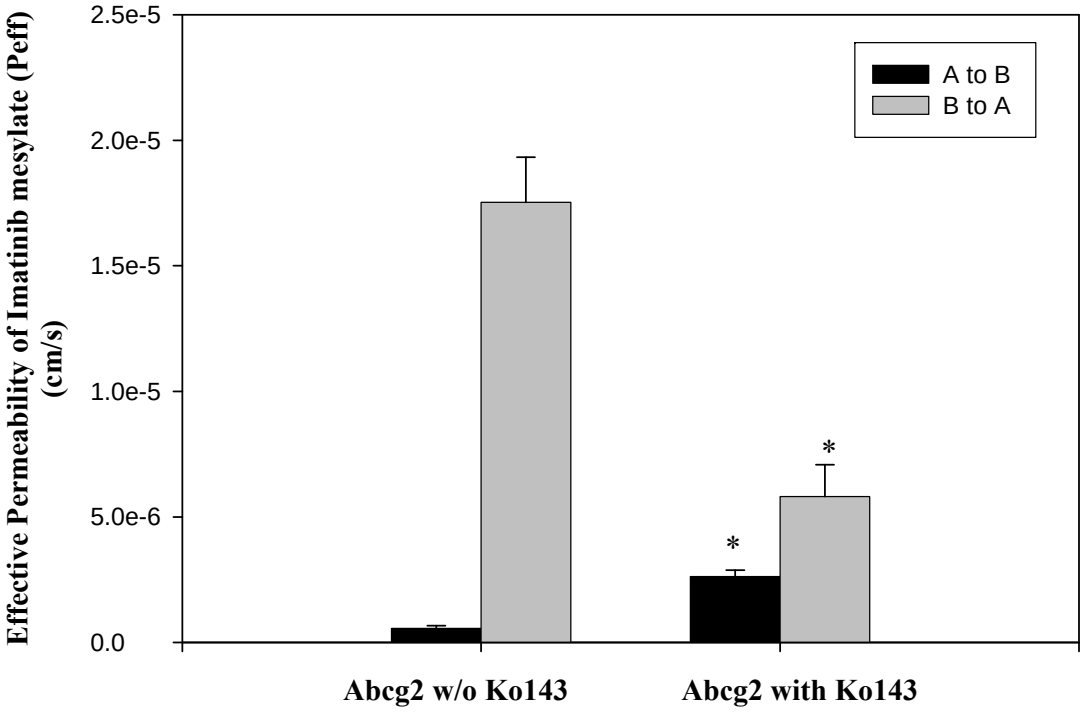

Figure 2.8. The A-to-B direction effective permeability (black bar) and B-to-A direction effective permeability (gray bar) of imatinib (cm/s) across the Abcg2-transfected MDCKII cell monolayers with and without Ko143 (200 nM).

Results are expressed as mean ±S.D., n=9 (*, $p < 0.01$). Ko143 decreased the efflux ratio of imatinib in Abcg2-transfected cells to the same level as that in WT cells.

Table 2-1. Effective permeability of 14C-imatinib in Abcg2-transfected and WT MDCKII cells with and without the presence of inhibitors (GF120918 5 µM, Ko143 200 nM).

Results are expressed as mean ±S.D., n=9.

	WT cells w/o inhibitor (cm/s)	Abcg2 cells w/o inhibitor (cm/s)	Abcg2 cells with GF120918 (cm/s)	Abcg2 cells with Ko143 (cm/s)
A-to-B (n=9)	2.94E-06 ± 8.04E-07	2.87E-07 ± 4.86E-08	1.45E-06 ± 6.00E-07	2.62E-06 ± 2.56E-07
B-to-A (n=9)	5.21E-06 ± 3.35E-07	1.81E-05 ± 8.76E-07	1.24E-05 ± 1.54E-06	5.81E-06 ± 1.26E-06
Efflux ratio	1.77	63.03	8.55	2.22

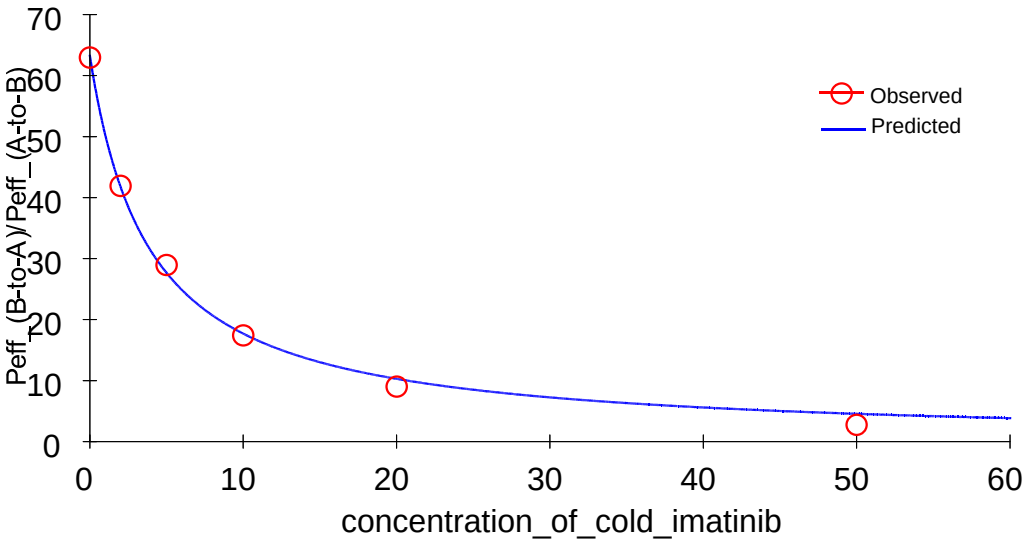

Figure 2.9. Plot of efflux ratios of 14C-imatinib in Abcg2-transfected MDCKII cells with increasing concentrations of non-radiolabeled imatinib (0, 2, 5, 10, 20 and 50 µM).

The inhibitory effect Emax model was fitted to data to obtain estimate of Km (EC50). Error bars are not avalible since each point represents a ratio of two average values.

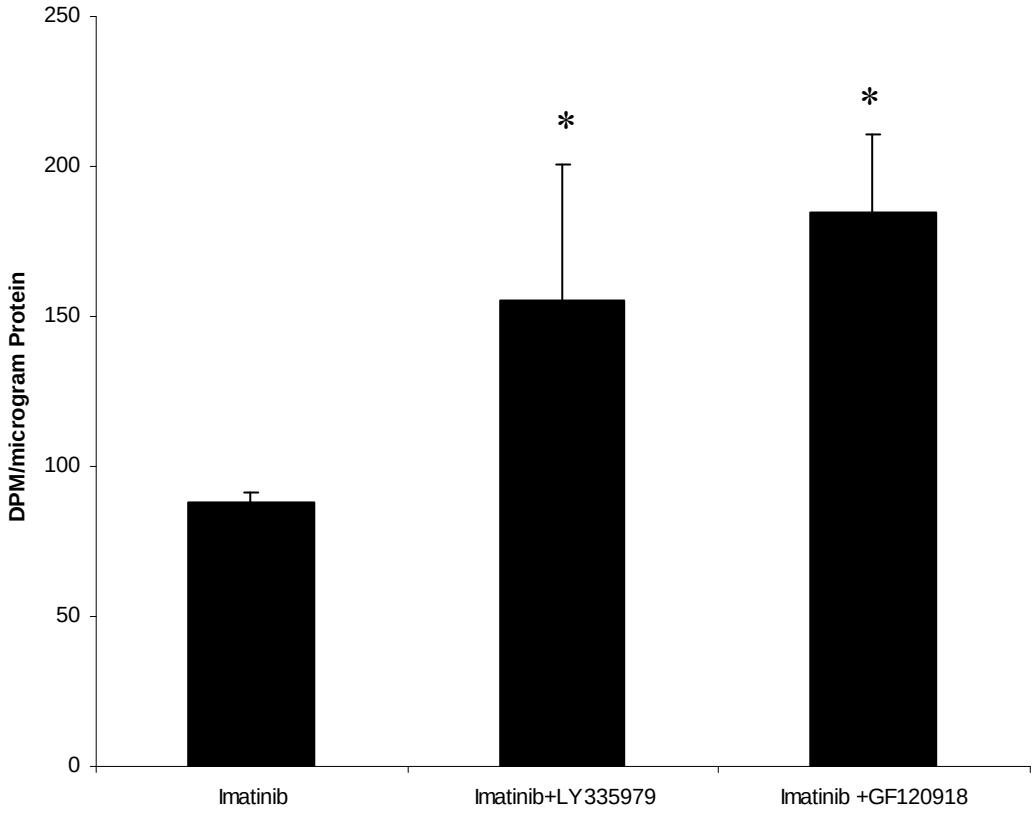

Figure 2.10. Accumulation of ^{14}C-imatinib in mouse glioma M7 cells with and without inhibitors (LY335979 1 μM, GF120918 5 μM).

Results are presented as mean ±S.D., n = 4. Imatinib accumulation in M7 cells was significantly increased with the presence of inhibitors LY335979 and GF120918, p <0.05.

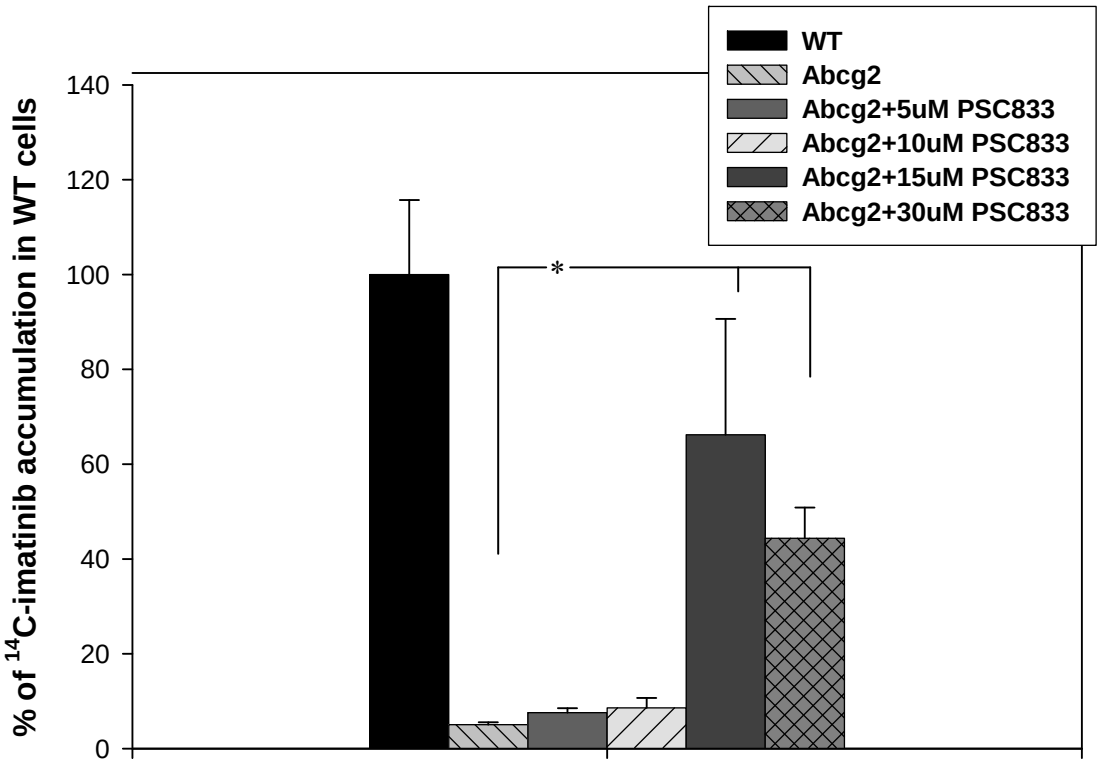

Figure 2.11. Accumulation of ^{14}C-imatinib in WT and Abcg2-transfected MDCKII cells with increasing concentrations of PSC833 (0, 5, 10, 15 and 30 μM).

Results are presented as mean ±S.D. (as percentage of wild-type control), $n = 6$. PSC833 was able to increase imatinib accumulation in Abcg2-transfected cells at the concentration of 30 μM significantly, $p < 0.01$.

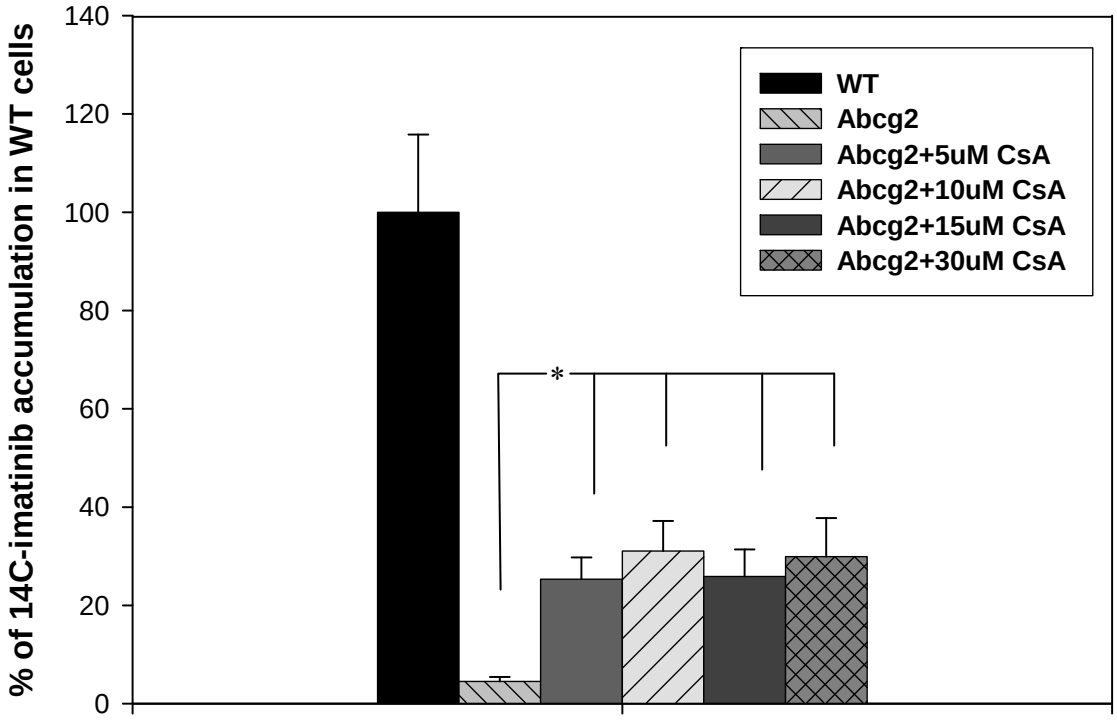

Figure 2.12. Accumulation of 14C-imatinib in WT and Abcg2-transfected MDCKII cells with increasing concentrations of CsA (0, 5, 10, 15 and 30 μM). Results are presented as mean ±S.D. (as percentage of wild-type control), n = 6. CsA has inhibitory effect on the Abcg2-mediated transport of imatinib at concentrations higher than 30 μM, $p < 0.01$.

CHAPTER 3

IN VIVO EFFECT OF EFFLUX TRANSPORTERS ON THE CNS DELIVERY OF IMATINIB

3.1 Abstract and introduction

3.1.1 Abstract

The objective of this study was to examine the influence of selected transporters (Abcb1 and Abcg2) on targeted delivery of imatinib to CNS. Wild type FVB mice received 12.5mg/kg or 50mg/kg imatinib as a single bolus with and without coadministration of 10mg/kg GF120918. Plasma and brain were sampled at different times postdose (10, 30, 60, 90, and 120 min). The concentration of imatinib in plasma and brain were determined by LC_MS. The average area-under-the curves (AUCs) from zero to infinity were calculated for plasma and brain for each group. The Drug Targeting Index (DTI= $[(AUC_{brain} / AUC_{plasma})_{groupA}]/ [(AUC_{brain} / AUC_{plasma})_{groupB}$) was determined. The plasma protein binding of imatinib was examined at different concentrations (100 ng/mL, 1000 ng/mL, and 7500 ng/mL). The DTI value between the high dose group and the low dose group was 2.74. The DTI value between the low dose with coadministration of GF120918 group and the control low dose group was 7.05. There was no difference among the free fractions of imatinib in plasma at three different concentrations. The results indicated that Abcb1 and Abcg2 play a role in limiting the CNS delivery of imatinib.

3.1.2 Introduction

Active transporters play important roles in drug absorption, distribution, metabolism and elimination (ADME) by governing drug substance in and out of different tissue and cells. Over time, more evidence has been accumulated indicating that active transporters are critical factors in the distribution of anticancer agents to the CNS. One example is

doxorubicin. Doxorubicin is a substrate of ABCB1 (Toffoli et al., 1996). *In vitro* evidence has showed that it has anti-tumor effects in glioblastoma cell lines. However, no clinical benefit has been observed from the use of doxorubicin in the treatment of primary CNS malignancies. The lack of *in vivo* effect might be due to the efflux by ABCB1 in the CNS (Motl et al., 2006). Vinblastine is another example. Vinblastine was originally thought to be effective in CNS tumors based on its lipophilicity. Nevertheless, preclinical studies showed that vinblastine has limited CNS penetration. Schinkel and group reported that ABCB1 knockout (mdr1a (-/-)) mice displayed an increased sensitivity to vinblastine (3-fold) compared to the wild type mice. So the poor CNS penetration of vinblastine might also be caused by the efflux by ABCB1 in the CNS (Schinkel et al., 1994; Motl et al., 2006).

Imatinib (Gleevec, STI571) is a first generation tyrosine kinase inhibitor (TKI). It has shown remarkable results in the treatment of chronic myelogenous leukemia (CML) and gastrointestinal stromal tumors (GISTS) (Druker, 2003). However, CNS relapses have been observed in CML patients even though they have shown a complete hematological response to imatinib mesylate (Takayama et al., 2002; Abruzzese et al., 2003; Pfeifer et al., 2003; Bornhauser et al., 2004; Bujassoum et al., 2004; Leis et al., 2004; Neville et al., 2004; Rajappa et al., 2004). Preclinical studies have shown that imatinib inhibited the growth of U343 and U87 glioblastoma multiforme (GBM) cell lines in vitro and when implanted into the brains of nude mice (Kilic et al., 2000). But in clinical studies, imatinib had limited antitumor activity in patients with recurrent gliomas in the dose range of 600 to 1,000 mg/d (Raymond et al., 2008). When imatinib CSF concentrations

were measured in patients treated with imatinib, they were less than 3 percent of plasma concentration. The lower than effective threshold concentration of imatinib in CNS led to CNS relapse in CML patients even though they had good systemic response to imatinib and limited the effect of imatinib in the treatment of brain tumor.

Recently, studies from other groups and our group showed that imatinib is a substrate of efflux transporters ABCB1 and ABCG2 (Dai et al., 2003; Mahon et al., 2003; Burger et al., 2004; Ozvegy-Laczka et al., 2004). In addition, a previous study in our lab showed that ABCB1 plays an important role in the CNS delivery of imatinib (Dai et al., 2003).However, the effect of ABCB1 and ABCG2 on the CNS delivery of imatinib needs to be further addressed. In this study the effect of Abcb1 and Abcg2 on the CNS delivery of imatinib was studied by the direct sampling method in an *in vivo* mouse model.

Direct sampling of brain tissue is the most straightforward technique for examining CNS uptake. In this approach, the study compound is administered systemically [typically by intravenous (iv) or oral (po) routes] to the animal. Later the animal is sacrificed at a specified time postdose in order to collect brain tissue and blood. One way to identify the presence of efflux transport at the BBB is to compare the brain: blood distribution ratio in animals with and without the presence of a specific transport inhibitor. An increase in brain: blood partitioning in the presence of the inhibitor indicates the effect of efflux transport. The strength of this approach is the capability of retaining the physical integrity of the BBB and the dynamic nature of the barrier

(normal blood flow and protein concentration). However, the brain tissue samples are contaminated by residual blood, which is a limitation shared by all techniques based on direct tissue sampling. Corrections can be made for estimates of residual blood volume either by using the data from literature or by performing capillary depletion of the sample prior to quantitating tissue concentration (Golden and Pollack, 2003a).

The objective of this chapter was to examine the influence of Abcb1 and Abccg2 on the targeted delivery of imatinib to the CNS by using an *in vivo* mouse model.

3.2 Material and methods

3.2.1 Chemicals and Animals

3.2.1.1 Chemicals

Imatinib was generously given by Novartis Pharma (East Hanover, N J). GF120918 (N-[4-[2-(6, 7-Dimethoxy-3, 4-dihydro-1H-isoquinolin-2-yl) ethyl]-5-methoxy-9-oxo-10H-acridine-4-carboxamide) was kindly provided by GlaxoSmithKline (Research Triangle, NC). Heparin was purchased from Baxter Healthcare Corporation (Deerfield, IL). All other chemicals used were HPLC or reagent grade.

3.2.1.2 Animals

Wild-type FVB mice were purchased from Taconic Farms. Inc. (Germantown, NY) All mice were male and between 8 to 10 weeks old. Animals were maintained under temperature-controlled conditions with a 12-h light/dark cycle and unlimited access to

food and water. All studies were approved by the Institutional Animal Care and Use Committee of the University of Minnesota

3.2.2 CNS distribution of imatinib in wild-type FVB mice

Due to the inability to obtain concentrations at multiple time points from a single mouse, destructive sampling was used. 80 wild-type (WT) FVB mice were randomly separated into 4 groups. Group 1 received 12.5-mg/kg imatinib via tail vein injection as the control group. Group 2 received 50 mg/kg imatinib via tail vein injection. Group 3 received 10 mg/kg GF120918 (DMSO: TWEEN80: propylene glycol: saline = 6.6: 3.95:24.67:64.67) via tail vain injection 30 min before the injection of 12.5 mg/kg imatinib. Group 4 had an injection of 10mg/kg GF120918 (DMSO: TWEEN80: propylene glycol: saline = 6.6: 3.95:24.67:64.67) via tail vein and another injection of 50mg/kg imatinib 30 min later. For each group, mice (n=4) were euthanized at various time points (5, 20, 60, 120, 180 min postdose). Blood was immediately harvested via cardiac puncture and collected in tubes preloaded with heparin. Then whole brain was harvested within 2 min and rinsed with ice-cold saline to remove extraneous blood. At the end of the experiment, plasma was separated from blood by centrifugation at 3000 rpm for 10 min at 4°C. All plasma and whole brain samples were stored at -80°C until analysis by LC-MS.

3.2.3 Plasma protein binding of imatinib

Glass culture tubes were spiked with non-radiolabeled imatinib and tracer ^{14}C-imatinib in methanol (in triplicate) to gain desired concentrations (100 ng/mL, 1000 ng/mL and

7500 ng/mL) in 600 μL plasma. Methanol was removed by drying under nitrogen. Then 600 μL FVB mouse plasma was added into each of the tubes and vortexed on high for 1 min. Tubes were incubated in orbital shaker at 37°C and continuously agitated at 120 rpm. Tubes were taken out and vortexed on high for 1 min during the incubation at 10, 20 and 30 minutes. After 45 min incubation, 150 μL plasma sample (triplicate for each tube) was transferred into individual Microcon® centrifugal filter Device (microcon YM-30, 30kDa MWCO, Millipore Corporation, Bedford, MA) for each concentration. The centrifugal filter devices then were centrifuged in an eppendorf 5417-R centrifuge at 14000 rpm for 15 min. A 100 μl sample of spiked plasma or filtered plasma was drawn, and 4 ml of scintillation fluid (ScintiSafe Econo cocktail; Fisher Scientific Co., Pittsburgh, PA) was added to each sample and counted using liquid scintillation counting (LS-6500; Beckman Coulter, Inc., Fullerton, CA) to determine the radioactivity associated with the plasma sample.

3.2.4 Pharmacokinetic analysis

The areas under the concentration-time curves for plasma (AUCplasma) and brain (AUCbrain) from time 0 to infinity were calculated by using noncompartmental analysis (WinNonlin 5.0.1; Pharsight, Mountain View, CA). The enhancement in brain exposure of imatinib in the treatment group compared with control group was represented by the drug targeting index (DTI), calculated as

DTI = (AUCbrain/AUCplasma) treatment group/ (AUCbrain/AUCplasma)control group.

3.2.5 Statistical analysis

Statistical analysis was conducted using SigmaStat, version 3.1(Systat Software, Inc., Point Richmond, CA). Statistical comparisons between two groups were made by using two-sample t-test at $p < 0.05$ significance level. If groups failed the normality test, then the nonparametric alternative of two-sample *t* test, the Mann-Whitney rank sum test was used. Groups were compared by one-way analysis of variance with the Holm-Sidak post-hoc test for multiple comparisons at a significance level of $p < 0.05$.

3.3 Results

3.3.1 CNS distribution of imatinib in wild-type FVB mice in low dose group

The disadvantage of direct sampling of brain tissue is that the brain tissue samples are contaminated by residual blood. To accurately determine the penetration of drug across the blood-brain barrier, the drug remaining in the brain vascular space needs to be excluded. This is especially important when the drug of interest has a relatively low CNS distribution. Previous study in our lab determined that the volume of brain vascular space in FVB mice accounts for 1.4% of the whole brain volume by using [^{3}H] inulin (Dai et al., 2003). All the brain concentration data in this thesis were corrected by excluding the drug in the 1.4% remaining blood from the drug in the whole brain tissue.

The brain and plasma concentration-time profiles of imatinib in FVB WT mice that received an intravenous dose of 12.5 mg/kg imatinib were determined (Figure 3.1). The brain distribution of imatinib reached equilibrium rapidly within 5min. The imatinib

brain concentrations were significantly lower than those in the plasma at all the measured time points (5, 20, 60, 120, 180 min postdose). The brain-to-plasma concentration ratios (B/P) were less than 0.12 (0.02-0.12). The AUC from time 0 to infinity in plasma and brain was 96885 min·ng/mL and 9561 min·ng/mL, respectively. The ratio of AUCs (AUC_{brain}/AUC_{plasma}) was 0.099 (table 3.1).

3.3.2 CNS distribution of imatinib in wild-type FVB mice in high dose group

The brain and plasma concentrations of imatinib at various time points (5, 20, 60, 120, 180 min postdose) in FVB WT mice following the tail vein injection of 50 mg/kg were measured (Figure 3.2). Both the brain concentrations and the plasma concentrations were increased compared to those in mice received low dose imatinib. When the B/P ratios were determined, they were greater (0.08-0.32) than those in the low dose group (Figure 3.6). The AUC value from time 0 to infinity in plasma and brain was 231792min·ng/mL and 56750 min·ng/mL, respectively. The ratio of AUCs (AUC_{brain}/AUC_{plasma}) was 0.245. The DTI value calculated as [$(AUC_{brain} / AUC_{plasma})_{high\ dose}$]/ [$(AUC_{brain} / AUC_{plasma})_{low\ dose}$] was 2.47 (table 3.1).

3.3.3 CNS distribution of imatinib in wild-type FVB mice in low dose with coadministration of dual inhibitor group

The brain and plasma concentration-time profiles of imatinib in FVB WT mice that received an intravenous dose of 12.5 mg/kg imatinib with the coadministration of 10 mg/kg GF120918 are shown in Figure 3.3. The brain concentrations and the plasma concentrations both increased compared to those in mice received low dose imatinib,

especially the brain concentrations. The B/P ratios in this group were greater (0.26-1.5) than those in the low dose group at the five time points measured (Figure 3.6). The AUC value from time 0 to infinity in plasma and brain was 342872 min·ng/mL and 239289 min·ng/mL, respectively. The ratio of AUCs (AUC_{brain}/AUC_{plasma}) was 0.698. The DTI value calculated as [$(AUC_{brain} / AUC_{plasma})_{\text{low dose with GF}}$]/ [$(AUC_{brain} / AUC_{plasma})_{\text{low dose}}$] was 7.05 (table 3.2).

3.3.4 CNS distribution of imatinib in wild-type FVB mice in high dose with coadministration of dual inhibitor group

The brain and plasma concentration-time profiles of imatinib in FVB WT mice that received an intravenous dose of 50 mg/kg imatinib following the coadministration of 10 mg/kg GF120918 were determined (Figure 3.4). Both the brain concentrations and the plasma concentrations increased compared to the concentrations in the high dose group. The brain concentrations reached the similar level as the plasma concentrations. The B/P ratios in this group were the greatest (0.61-2.14) among the 4 groups (Figure 3.6). However, due to the fluctuation in the brain concentration-time profile, a reliable terminal rate constant could not be estimated. Therefore, the DTI between the high dose groups with and without the coadministration of GF120918 could not be calculated. When the B/P ratios were compared between these two groups, those in group 4 were significantly higher than those in group 3 at 60, 120, 180 min postdose.

3.3.5 Plasma protein binding of imatinib

The free fractions of imatinib in plasma at three different concentrations (100 ng/mL, 1000 ng/mL and 7500 ng/mL) are listed in table 3.1. There was no difference among the three free fractions. The plasma protein binding of imatinib did not change as the plasma concentration of imatinib increased from 100 ng/mL to 7500 ng/mL. There was no sign of plasma protein binding saturation at the highest concentration we tested.

3.4 Discussion

In this chapter we examined the influence of Abcb1 and Abcg2 on the CNS distribution of imatinib by comparing imatinib CNS distribution among 4 wild-type FVB mice groups that received different treatments.

The first treatment group was served as the control group. In this group, mice received a low dose of imatinib only via tail vein injection. The distribution phase of imatinib from plasma to brain was shorter than 5 min. Previous study in our lab observed similar phenomenon. One possible explanation for this is that the concentration-time profile in the brain will quickly reflect changes in the concentration-time profile in the plasma for a drug with a small volume of distribution in the CNS, and a rapid efflux, because the small volume will quickly respond to a change in driving force as long as the drug can exit easily (Dai et al., 2003). The brain AUC over plasma AUC ratio in this control group was just 0.099. The CNS delivery of imatinib is limited.

In the second treatment group, an imatinib dose that was 4 fold greater than the low dose was given to mice via tail vein injection. Both plasma and brain concentrations increased with the administration of the high dose. The brain AUC over plasma AUC ratio in this control group was 0.245. To find out if the increase of imatinb brain concentration was due to enhanced CNS delivery or simply increase of plasma concentration, the DTI value was calculated. An open two-compartment model as shown in figure 3.7 was used to help understanding the meaning of DTI. In the model, plasma and brain were taken as two separate compartments. Cl_{in} stands for the clearance into brain from plasma and Cl_{out} stands for the clearance out brain to plasma. The equations following the model showed that the ratio of AUC from time 0 to infinity in brain to AUC from 0 to infinity in plasma actually represents the ratio of the clearance into brain to the clearance out of brain. Therefore, in this case, a DTI value of 2.45, which is greater than 1, means the ratio of CL_{in}/CL_{out} in brain of the high dose group increased. The clearance into brain from plasma consists of one or two components: passive diffusion and influx (if there is any). Meanwhile, the clearance get out from brain to plasma consists of two components: passive diffusion and efflux. As the plasma concentration increases, CL_{in} either keeps the same or decreases when the influx transporter is saturated. Under both circumstances, CL_{out} must decrease to result in the decrease of $CLin/CL_{out}$. Therefore, the saturation of the efflux transporters in the BBB by the increased plasma concentration resulted inthe increased CNS delivery of imatinb.

Imatinib is highly plasma protein bound. One study showed that approximately 99% of imatinib was found to be protein bound. It binds $\alpha 1$ acid glycoprotein (AGP) with an

affinity of 4.9×10^6 liters/mol and binds albumin with an affinity of 2.3×10^5 liters/mol (Gambacorti-Passerini et al., 2003). Another study reported the unbound fraction of imatinib in human plasma was 3.1% at 1 g/L (Kretz et al., 2004). We suspected that saturation of protein binding and a greater free fraction may be caused by a higher concentration of imatinib, which would lead to a greater driving force for drug in the plasma to enter the brain. The free fractions of imatinib in plasma at three different concentrations (100 ng/mL, 1000 ng/mL and 7500 ng/mL) were measured (table 3.1). Even at 7500 ng/mL, the highest plasma concentration of imatinib in the high dose group, there was no sign of plasma protein binding saturation. These results further indicated that the increased CNS delivery of imatinib in the high dose treatment group was due to the saturation of the efflux transporters in the BBB.

In group 3, an Abcb1 and Abcg2 dual inhibitor GF120918 was given to mice 30 min prior the dosing of low dose imatinib to inhibit the two efflux transporters in different tissues including the brain. With the pharmacological inhibition of Abcb1 and Abcg2, both plasma and brain concentration of imatinib increased. The inhibition of efflux transporters in elimination organs such as liver and kidney decreased the systemic clearance, thus plasma concentration increased. The inhibition of efflux transporters in BBB resulted in a decreased clearance from brain to plasma (CL_{out}), therefore brain concentration increased. The DTI value for the comparison between group 3 and the control group was 7.05. This indicates that the enhanced CNS delivery in group 3 was due to pharmacological inhibition of Abcb1 and Abcg2 in the BBB. It also suggests

that the increased plasma concentration in group 2 was not able to fully saturate the efflux transporters in the BBB.

The B/P ratios in group 3 were also compared to the ratios in control group (figure 3.6). There was an about 10-fold (8.4-12.8) difference between these two groups. In previous studies in our lab, we observed a 6-to-7 fold difference between the B/P ratios of Abcb1 knockout (mdr1a/b (-/-)) FVB mice and wild-type FVB mice (Dai et al., 2003). With the inhibition of both Abcb1 and Abcg2 by GF120918, the increase of imatinib brain penetration was greater than that by the inhibition of only Abcb1. Given all the results, it could be concluded that both Abcb1 and Abcg2 influence the CNS delivery of imatinib.

The brain concentration of imatinib reached the similar level as the plasma concentration in group 4. In this group, mice received GF120918 and high dose imatinib 30 min apart. Because of the fluctuation in the brain concentration-time profile, a reliable terminal rate constant could not be estimated. The B/P ratios in this group were the highest among the four groups at all 5 time points. It would be valuable if we could get the DTI value for the comparison between group 4 and the control group. If it is greater than 7.05, which is the DTI value for the comparison between group 3 and the control group, then it will indicate the GF120918 concentration we use in this study (10 mg/kg) was not high enough to completely inhibit the efflux transporters (Abcb1 and Abcg2) in the BBB. Otherwise, 10 mg/kg GF120918 could fully inhibit Abcb1 and Abcg2 in the BBB in this FVB wild-type mouse model.

Breedveld and colleagues studied the effect of Abcg2 on the *in vivo* brain penetration of imatinib through a different approach. In their studies, the brain penetration of i.v. imatinib was determined by comparing the total radioactivity concentration of ^{14}C-imatinib in brain at 2 hr postdose to plasma AUC (0-2hrs). Their results showed the brain penetration of imatinib increased 2.5-fold, 3.6-fold and 4.2-fold in Abcg2 knockout mice, Abcb1 knockout mice and WT mice treated with GF120918 respectively, compared to WT control mice(Breedveld et al., 2005). Since metabolites accounted for about 60-65% of the total radioactivity in brain and plasma samples (Dai et al., 2003), the use of total radioactivity as measurement can lead to erroneous interpretations. Another study done by Bihorel and coworkers investigated the brain concentration over blood concentration ratio (BB ratio) of imatinib in mice with different treatment at 1 hr postdose (Bihorel et al., 2007b). They reported that GF120918 significantly increased the BB ratio of imatinib in WT mice. The effect of GF120918 was not dose-dependent (3, 10, 30 mg/kg) at this one time point and the average increase was 9.3-fold, which is similar as the effect of 10 mg/kg GF120918 we observed on the CNS delivery of imatinib. However the effect of different doses of GF120918 could be better characterized by the approach we used.

3.5 Conclusion

In summary, this study examined the influence of Abcb1 and Abcg2 on targeted delivery of imatinib to CNS by using an *in vivo* mouse model. The DTI value for the

comparison between the high dose group and the low dose group was 2.74. This indicates that increased imatinib concentration that resulted from increased dose can saturate the efflux transporters (Abcb and Abcg2) in the BBB and lead to increased CNS delivery of imatinib. The DTI value for the comparison between the GF120918 treated low dose group and the low dose group was 7.05, which indicates the inhibition of both Abcb1 and Abcg2 can enhance the CNS delivery of imatinib. The treatment of high dose and coadministration of GF120918 resulted in highest B/P ratios among the 4 groups. There was no change of plasma protein binding of imatinib at the concentrations we tested. In conclusion, Abcb1 and Abcg2 together play an important role in limiting the CNS delivery of imatinib.

3.6 Acknowledgement

We would like to thank Novartis Pharma for kindly providing us imatinib. We thank GlaxoSmithKline for generously providing us GF120918.

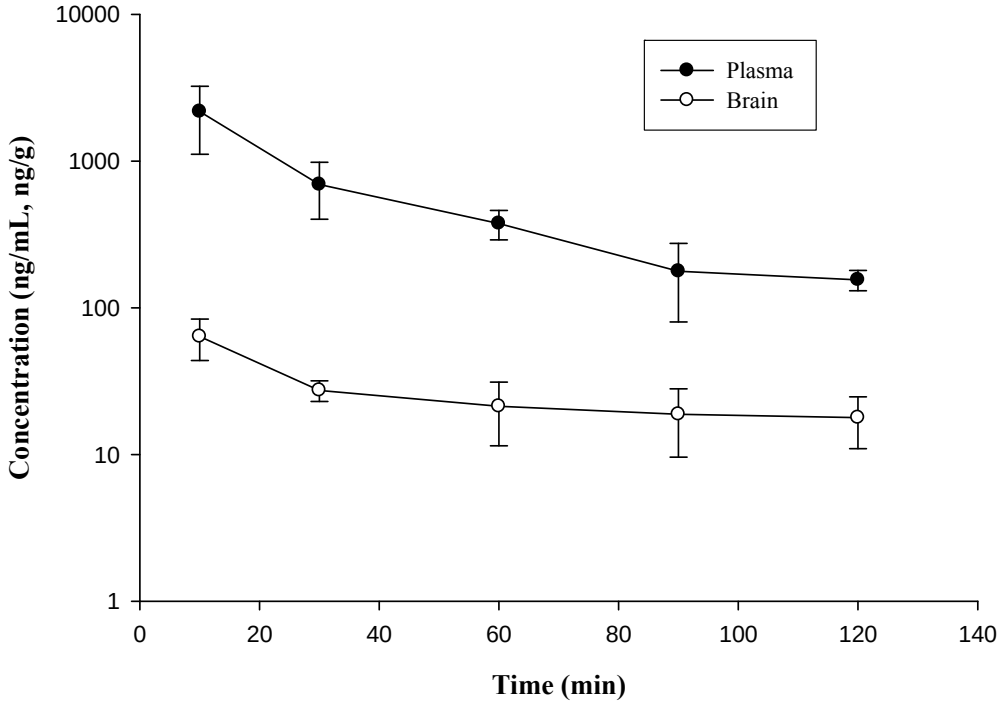

Figure 3.1. Plasma and brain concentration of imatinib versus time in wild-type FVB mice.

Mice received 12.5 mg/kg imatinib via tail vein injection. Plasma and whole brain tissue were collected at different time points (5, 20, 60, 120, 180 min postdose, n=4 at each time point) and analyzed for imatinib using LC-MS. Results are presented as mean ± S.D.

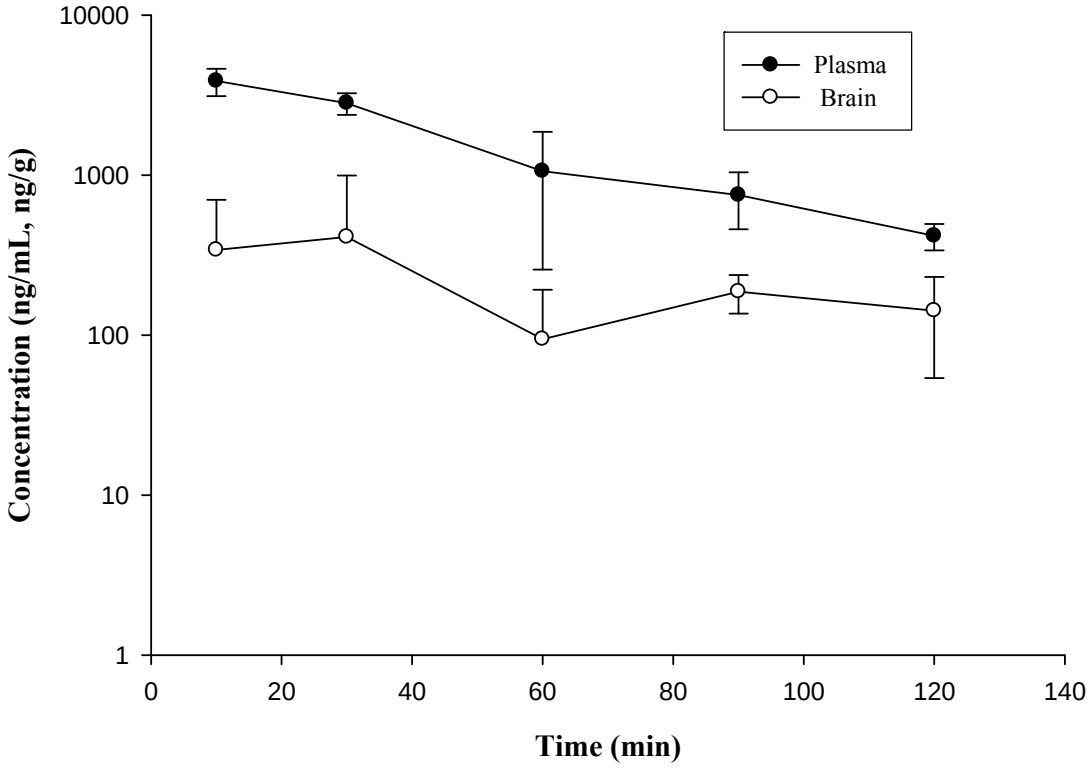

Figure 3.2. Plasma and brain concentration of imatinib versus time in wild-type FVB mice.

Mice received 50 mg/kg imatinib via tail vein injection. Plasma and whole brain tissue were collected at different time points (5, 20, 60, 120, 180 min postdose, n=4 at each time point) and analyzed for imatinib using LC-MS. Results are presented as mean ± S.D.

Table 3-1. Brain and plasma AUCs of imatinib in wild-type FVB mice (low dose group and high dose group).

	AUCINF_obs (min×ng/mL)	
	Low dose group	High dose group
Plasma	96885	231792
Brain	9561	56750
Brain/Plasma	0.099	0.245

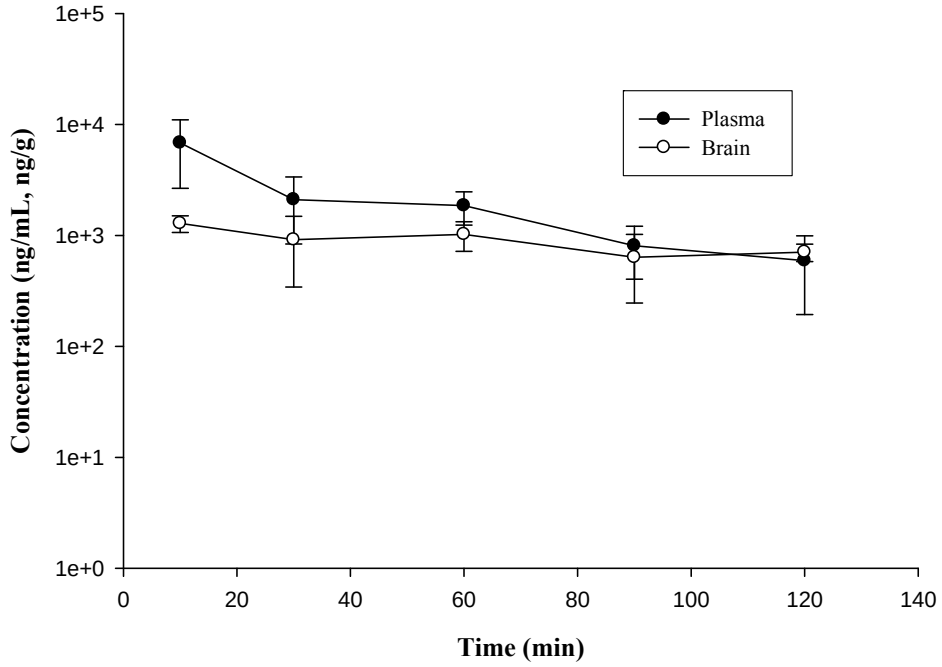

Figure 3.3. Plasma and brain concentration of imatinib versus time in wild-type FVB mice with coadministration of GF120918.

Mice received 10 mg/kg GF120918 via tail vein injection 30 min before the injection of 12.5 mg/kg imatinib. Plasma and whole brain tissue were collected at different time points (5, 20, 60, 120, 180 min postdose, n=4 at each time point) and analyzed for imatinib using LC-MS. Results are presented as mean ± S.D.

Table 3-2. Brain and plasma AUCs of imatinib in wild-type FVB mice (low dose without GF120918 group and low dose with GF120918 group).

	AUCINF_obs (min×ng/mL)	
	Low dose without GF120918	Low dose with GF120918
Plasma	96885	342872
Brain	9561	239289
Brain/Plasma	0.099	0.698

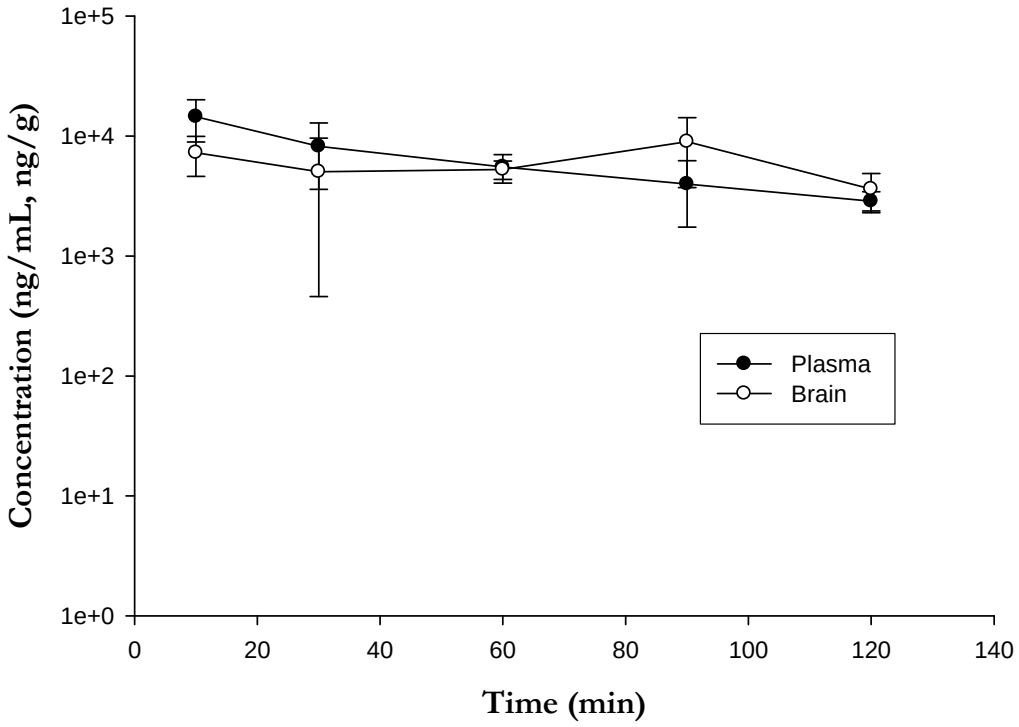

Figure 3.4. Plasma and brain concentration of imatinib versus time in wild-type FVB mice with coadministration of GF120918.

Mice had an injection of 10 mg/kg GF120918 via tail vein and another injection of 50 mg/kg imatinib 30 min later. Plasma and whole brain tissue were collected at different time points (5, 20, 60, 120, 180 min postdose, n=4 at each time point) and analyzed for imatinib using LC-MS. Results are presented as mean ± S.D.

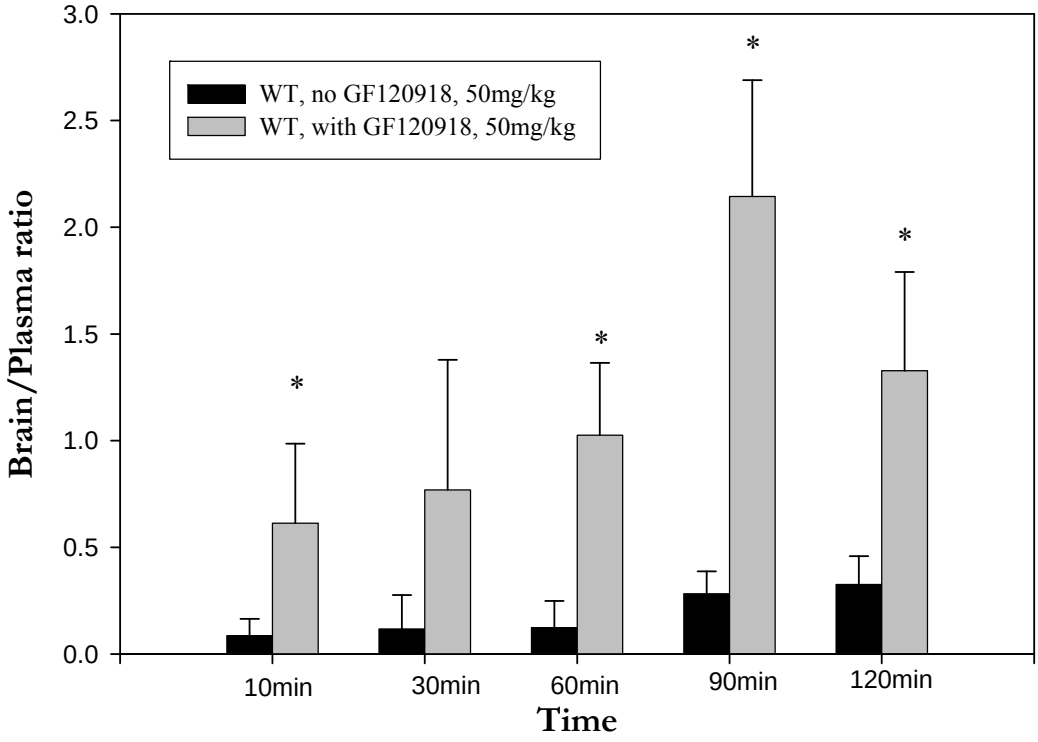

Figure 3.5. The brain-to-plasma ratio of imatinib in wild-type FVB mice with and without coadministration of GF120918.

Mice received 50 mg/kg imatinib via tail vein injection with or without coadministration of 10 mg/kg GF120918. Plasma and whole brain tissue were collected at different time points (5, 20, 60, 120, 180 min postdose, n=4 at each time point) and analyzed for imatinib using LC-MS. (* p <0.05, n=4). Results are presented as mean ± S.D.

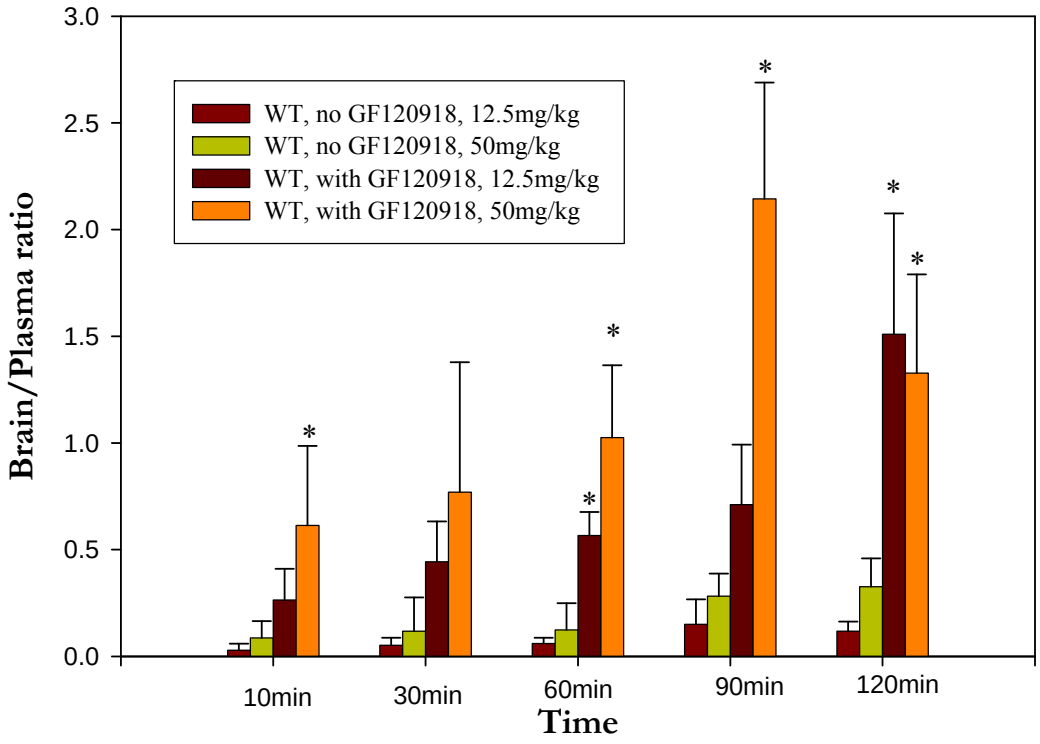

Figure 3.6. The brain-to-plasma ratio of imatinib in 4 wild-type FVB mice groups.

Group 1 received 12.50 mg/kg imatinib via tail vein injection. Group 2 received 50 mg/kg imatinib via tail vein injection. Group 3 received 10 mg/kg GF120918 via tail vein injection 30 min before the injection of 12.5 mg/kg imatinib. Group 4 had an injection of 10 mg/kg GF120918 via tail vein and another injection of 50 mg/kg imatinib 30 min later. Plasma and whole brain tissue were collected at different time points (5, 20, 60, 120, 180 min postdose, n=4 at each time point for each group) and analyzed for imatinib using LC-MS. (* p <0.05, n=4). Results are presented as mean ± S.D.

Table 3-3. Free fraction of imatinib in plasma at different concentrations. Results are presented as mean ± S.D. (n=6)

Concentration	7500ng/mL	1000ng/mL	100ng/mL
Free fraction (fu)	0.062±0.005	0.064±0.005	0.064±0.005

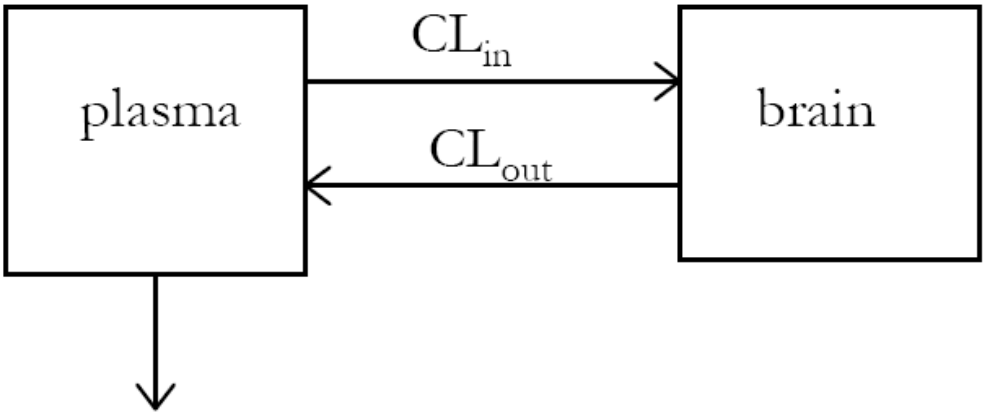

Steady state: $CB \times CLout = CP \times CLin$ (1)

Integrate both sides with regard to time from 0 to infinity

$AUCbrain \times CLout = AUCplasma \times Clin$ (2)

$AUCbrain / AUCplasma = Clin / Clout$ (3)

Figure 3.7. Schematic of an open two-compartment model.

Clin stands for the clearance into brain from plasma and Clout stands for the clearance out brain to plasma.

CHAPTER 4

IN VITRO INTERACTION BETWEEN DASATINIB AND EFFLUX TRANSPORTERS

4.1 Abstract and introduction

4.1.1 Abstract

The objective of this study was to characterize the interaction between the novel tyrosine kinase inhibitor dasatinib and the active efflux transporters, ABCB1 (p-glycoprotein) and ABCG2 (BCRP). The kinetics of cellular accumulation and permeability of dasatinib was studied in wild-type and ABCB1 or Abcg2 transfected MDCKII epithelial cell monolayers, in the presence and absence of selective inhibitors (LY335979 or Ko143). The cellular accumulation of dasatinib in the wild-type MDCKII cells was significantly greater than that in ABCB1-transfected (6-fold) or Abcg2 transfected (30- fold) MDCKII cells ($p<0.01$). The ABCB1 specific inhibitor LY 335979 abolished the difference between wild-type and ABCB1-transfected cells and ABCG2 specific inhibitor Ko143 abolished the difference in Abcg2 cells. The effective permeability of dasatinib in the basolateral-to-apical (B-to-A) direction (1.19E-05±7.46E-07 cm/s, n=9) was 16-fold greater than that in the apical-to-basolateral (A-to-B) direction (7.61E-07±2.83E-07cm/s, n=9) in ABCB1-transfected cells and this difference was significantly decreased by LY335979. In Abcg2-transfected cells, the effective permeability of dasatinib in the B-to-A direction (1.70E-05±1.15E-06 cm/s, n=18) was 45-fold greater than that in the A-to-B direction (3.74E-07±1.08E-07cm/s, n=18) and the difference was decreased by Ko143. OCT-1 inhibitor TEA did not significantly reduce the cellular accumulation of dasatinib in wild-type and Abcg2-trasfected MDCKII cells. Imatinib significantly increased dasatinib accumulation in wild-type and Abcg2-transfected cells and reduced efflux ratio of dasatinib from 45.45 to 9.67.

4.1.2 Introduction

The recently designed molecularly targeted tyrosine kinase inhibitors (TKIs) have been shown to clinically inhibit the action of pathogenic tyrosine kinases (TK), which was one of the most exciting developments in cancer research in the past decade (Baselga, 2006). Imatinib (Gleevec, STI571) is a successful example as the first-generation TKI. It is the first line treatment of chronic myelogenous leukemia (CML) and gastrointestinal stromal tumor (GIST) (Druker, 2003). However, resistance to imatinib has been increasingly encountered (Baccarani et al., 2006; Druker et al., 2006). Mutation could be one of the causes of imatinib resistance. It has been observed that resistance mutations occur in the kinase domains of BCR-ABL, Kit and PDGFR in the tumor cells of patients treated with imatinib (Baselga, 2006). To overcome this new challenge, the second-generation TKIs are rapidly being developed.

Dasatinib (BMS-354825), a second-generation TKI, has already been approved for patients with CML with resistance or intolerance to imatinib by the U.S. Food and Drug Administration (Shah, 2007). Dasatinib is an ATP-competitive inhibitor of SRC and ABL tyrosine kinase. It is another small-molecule that has potency in the low nanomolar range. It binds ABL with a less stringent conformational requirement than imatinib (Schittenhelm et al., 2006). It effectively inhibits the proliferation of cells that express nearly all imatinib-resistant isoforms (Kantarjian et al., 2006).

Another problem associated with imatinib is central nervous system (CNS) relapse. CNS relapses have been observed in CML patients even though they have shown a complete hematological response to imatinib. An inadequate concentration of imatinib in the CNS makes it a sanctuary of chronic myelogenous leukemia (Takayama et al., 2002; Abruzzese et al., 2003; Pfeifer et al., 2003; Bornhauser et al., 2004; Bujassoum et al., 2004; Leis et al., 2004; Neville et al., 2004; Rajappa et al., 2004). Previous studies in our lab and others showed that efflux transporters such as ABCB1 and ABCG2 play a role in limiting the targeted delivery of imatinib to the CNS(Dai et al., 2003; Breedveld et al., 2005; Bihorel et al., 2007b).

Given that dasatinib is designed to overcome molecular resistance, the question arises; can dasatinib also overcome the CNS delivery problem? So far little information is known about the CNS delivery of dasatinib, including the action of relevant BBB transporters. As a promising multiple targeting TKI, dasatinib CNS delivery is important in terms of the treatment of CNS malignancies and the prevention of CNS metastases.

The objective of this study was to identify and characterize the interaction between dasatinib and efflux transporters ABCB1 and ABCG2.

4.2 Materials and Methods

4.2.1 Chemicals and Cell lines

4.2.1.1 Chemicals

Dasatinib and ^{14}C-dasatinib were kindly provided by Bristol-Myers Squibb Company (Princeton, NJ). LY335979 ((*R*)-4-((1a*R*, 6R, 10bS)-1,2-difluoro-1, 1a, 6,10b-tetrahydrodibenzo-(*a*,*e*)cyclopropa(*c*)cycloheptan-6-yl)-α-((5-quinoloyloxy)methyl)-1-piperazineethanol, trihydrochloride) was a gift from Eli Lilly and Co. (Indianapolis, IN). GF120918 (N-[4-[2-(6, 7-Dimethoxy-3, 4-dihydro-1H-isoquinolin-2-yl) ethyl]-5-methoxy-9-oxo-10H-acridine-4-carboxamide) was generously given by GlaxoSmithKline (Research Triangle, NC). Ko143 was kindly provided by Dr. Alfred Schinkel (Netherlands Cancer Institute, Amsterdam, The Netherlands). All other chemicals used were HPLC or reagent grade.

4.2.1.2 Cell lines

Wild-type (WT) and ABCB1-transfected epithelial Madin-Darby canine kidney (MDCKII) cells were a gift from Dr. Piet Borst (Netherlands Cancer Institute). WT and Abcg2-transfected MDCKII cells were kindly provided by Dr. Schinkle (Netherlands Cancer Institute, Amsterdam, The Netherlands). All cell lines were cultured in Dulbecco's modified Eagle's medium (Mediatech, Inc., Herndon, VA) fortified with 10% heat-deactivated fetal bovine serum (SeraCare Life Sciences, Inc., Oceanside, CA), 100 U/ml penicillin G, 100 μg/ml streptomycin and 250 ng/mL amphotericin B (Sigma-Aldrich, St. Louis, MO) at 37°C under humidity and 5% CO_2 tension. The ABCB1-transfected cell growth medium contained 80 ng/ml colchicine in addition to

maintain positive selection pressure for ABCB1 expression. Cells used in all experiments were between passages 5 and 15.

4.2.2 Cellular accumulation studies in MDCKII cells

For the accumulation experiments, cells were seeded in clear polystyrene 12-well plates (TPP cell culture plate; Sigma-Aldrich, St. Louis, MO) at a seeding density of 2×10^5 cells/well. The medium was changed every other day and the cells formed confluent monolayers in 3-4 days. On the day of the experiment, the medium was aspirated and the confluent monolayer was washed twice with 1 mL prewarmed (37°C) assay buffer (122 mM NaCl, 25 mM NaHCO3, 10 mM glucose, 10 mM HEPES, 3 mM KCl, 1.2 mM MgSO4·7H2O, 1.4 mM CaCl2·H2O, 0.4 mM K2HPO4, pH 7.4). The cells were preincubated with 1 ml of assay buffer for 30 min, after which the buffer was aspirated and the experiment was initiated by adding 1 ml tracer solution (1 μg ^{14}C-dasatinib) of radiolabeled drug in assay buffer into each well. The plates were continuously agitated at 60 rpm in an orbital shaker at 37°C. After a 3-h accumulation period, the supernatant was aspirated and the cells were first washed three times with 2 ml of ice-cold phosphate-buffered saline and then solubilized using 1 ml of mammalian protein extraction reagent (M-PER®, Pierce Biotechnology, Inc., Rockford, IL). A 200 μl sample of solubilized cell fractions was drawn from each well in triplicate, and 4 ml of scintillation fluid (ScintiSafe Econo cocktail; Fisher Scientific Co., Pittsburgh, PA) was added to each sample and counted using liquid scintillation counting (LS-6500; Beckman Coulter, Inc., Fullerton, CA) to determine the radioactivity associated with the cell fractions. The protein concentration was determined using the BCA protein assay

(Pierce Biotechnology, Inc., Rockford, IL) to normalize the radioactivity in each well. For inhibition studies, the cells were treated with the inhibitor (1 μM LY335979 for ABCB1; 200 nM Ko143 for Abcg2) during both the preincubation and the accumulation periods. Drug accumulation in cells was expressed as a percentage of the accumulated radioactivity measured in the wild-type control cells (dpm) per microgram of protein. The stock solutions for all the inhibitors used were prepared in dimethyl sulfoxide (DMSO) and diluted using assay buffer to obtain working solutions, so that the final concentration of DMSO was less than 0.1%.

4.2.3 Cellular permeability studies in MDCKII cells

The methods used for directional flux were similar to that previously described by Dai et al. (Dai et al., 2003) In brief, cells were seeded at a density of 2×10^5 cells/well on polyester semipermeable membrane supports of the inserts in six-well Transwells (Corning Inc.,Corning, NY). The medium was changed every day and the cells formed confluent polarized epithelial monolayers in 3-4 days. The representative transepithelial electrical resistance was 300 ± 8 ohm·cm^2 (n=6) in the WT MDCKII monolayers, 275 ± 26 ohm·cm^2 (n=6) in the ABCB1-transfected MDCKII monolayers and 248± 27 ohm·cm^2 (n=6) in the Abcg2-transfected MDCKII monolayers. Mannitol flux across the monolayer was also measured to confirm the existence of tight junctions with approximately 1% per hour flux ($P_{eff} = 9 \times 10^{-8}$ cm/s). The monolayers were washed with 2 mL prewarmed (37°C) assay buffer, and after a 30-min preincubation, the experiment was initiated by adding a tracer solution of radiolabeled drug in assay buffer to the donor side (apical side, 1.5 ml; basolateral side, 2.6 ml). Fresh assay buffer was

added to the receiver side and 200 µl was sampled from the receiver compartment at 0, 10, 20, 30, 45, 60, and 90 min. The volume sampled was immediately replaced with fresh assay buffer. Additional samples were drawn at 0 and 90 min from the donor compartment. The amount of radioactivity in the samples was determined using liquid scintillation counting as described previously. The apical-to-basolateral (A-to-B) flux was determined by addition of radiolabeled drug solution to the apical compartment and sampling the basolateral compartment, whereas for basolateral-to-apical (B-to-A) flux, the donor was the basolateral compartment and the apical compartment was the receiver compartment. When an inhibitor was used in the flux study, the cell monolayers were preincubated with the inhibitor (1 µM LY335979 for ABCB1 and 200 nM Ko143 for Abcg2) for 30 min, followed by the inhibitor being present in both compartments throughout the course of the experiment.

Permeability Calculation

The effective permeability (*P*eff) was calculated based on the following equation,

$$P_{eff} = \frac{\left(\frac{dQ}{dt}\right)}{A * C_0} \qquad 4.1$$

Q is the amount of radiolabled drug transported though the cell monolayer and t is the corresponding time period. dQ/dt is the amount transport rate. A is the effective area of the cell monolayer (4.67 cm^2). C_0 is the initiated concentration of radiolabled drug in the donor compartment. Efflux ratio is defined as the ratio of *P*eff of the B-to-A flux over the *P*eff of the A-to-B flux.

4.2.4 Characterization of the interaction between dasatinib and ABCB1, Abcg2

A cellular accumulation method was used to characterize the interaction between dasatinib and ABCB1and Abcg2. Cells were seeded in clear polystyrene 24-well plates (SARSTEDT Newton, NC) at a seeding density of 2×10^5 cells/well. The medium was changed every other day and the cells formed confluent monolayers in 3-4 days. On the day of the experiment, the medium was aspirated and the confluent monolayer was washed twice with 1mL prewarmed (37°C) assay buffer. The cells were preincubated with 1 ml of assay buffer with or without non-radiolabeled dasatinib (10, 25, 50, 75, 100 μM) for 30 min, after which the buffer was aspirated and the experiment was initiated by adding 1 ml tracer solution (1 μg ^{14}C-dasatinib) of radiolabeled drug in assay buffer with or without non-radiolabeled dasatinib (10, 25, 50, 75, 100 μM) into each well. The plates were continuously agitated at 60 rpm in an orbital shaker at 37°C. After a 3-h accumulation period, the supernatant was aspirated and the cells were first washed three times with 2 ml of ice-cold phosphate-buffered saline and then solubilized using 1 ml of M-PER®. A 200μl sample of solubilized cell fractions was drawn from each well in triplicate. The radioactivity associated with the cell fractions and the protein concentration was determined as previously described in section 4.2.2. Drug accumulation in cells was expressed as a percentage of the accumulated radioactivity measured in the wild-type control cells (dpm per microgram of protein). The stock solution for non-radiolabeled dasatinib was prepared in dimethyl sulfoxide (DMSO) and diluted using assay buffer to obtain working solutions, so that the final concentration of DMSO was less than 0.1%.

4.2.5 Interaction between dasatinib and OCT-1

4.2.5.1 Effect of TEA on dasatinib accumulation

WT and Abcg2 transfected MDCKII cells were seeded in clear polystyrene 12-well plates at a seeding density of 2×10^5 cells/well. The medium was changed every other day and the cells formed confluent monolayers in 3-4 days. On the day of the experiment, the medium was aspirated and the confluent monolayer was washed twice with 1 mL prewarmed (37°C) assay buffer. The cells were preincubated with 1 ml of assay buffer with or without 2 mM tetraethylammonium (TEA) for 30 min, after which the buffer was aspirated and the experiment was initiated by adding 1 ml tracer solution (1 μg ^{14}C-dasatinib) of radiolabeled drug in assay buffer with or without 2 mM TEA into each well. The plates were continuously agitated at 60 rpm in an orbital shaker at 37°C. After a 3-h accumulation period, the supernatant was aspirated and the cells were first washed three times with 2 ml of ice-cold phosphate-buffered saline and then solubilized using 1 ml of M-PER®. A 200μl sample of solubilized cell fractions was drawn from each well in triplicate. The radioactivity associated with the cell fractions and the protein concentration was determined as previously described in section 4.2.2. Drug accumulation in cells was expressed as a percentage of the accumulated radioactivity measured in the wild-type control cells (dpm per microgram of protein). The stock solution for TEA was prepared in dimethyl sulfoxide (DMSO) and diluted using assay buffer to obtain working solutions, so that the final concentration of DMSO was less than 0.1%.

4.2.5.2 Effect of TEA on dose dependence study of dasatinib

WT MDCKII cells were seeded in clear polystyrene 24-well plates at a seeding density of 2×10^5 cells/well. The medium was changed every other day and the cells formed confluent monolayers in 3-4 days. On the day of the experiment, the medium was aspirated and the confluent monolayer was washed twice with 1mL prewarmed (37°C) assay buffer. The cells were preincubated with 1 ml of assay buffer with or without 2 mM Tetraethylammonium (TEA) at the presence of various concentrations of non-radiolabeled dasatinb (10, 25, 50, 75, 100 μM) for 30 min, then the buffer was aspirated and the experiment was initiated by adding 1 ml tracer solution (1 μg ^{14}C-dasatinib) of radiolabeled drug in assay buffer with or without 2 mM TEA into each well at the presence of various concentrations of non-radiolabeled dasatinb (10, 25, 50, 75, 100 μM). The plates were continuously agitated at 60 rpm in an orbital shaker at 37°C. After a 3-h accumulation period, the supernatant was aspirated and the cells were first washed three times with 2 ml of ice-cold phosphate-buffered saline and then solubilized using 1 ml of M-PER®. A 200 μl sample of solubilized cell fractions was drawn from each well in triplicate. The radioactivity associated with the cell fractions and the protein concentration was determined as previously described in section 4.2.2. Drug accumulation in cells was expressed as a percentage of the accumulated radioactivity measured in the wild-type control cells (dpm per microgram of protein). The stock solution for TEA and non-radiolabeled dasatinb was prepared in dimethyl sulfoxide (DMSO) and diluted using assay buffer to obtain working solutions, so that the final concentration of DMSO was less than 0.1%.

4.2.6 Interaction between imatinib and dasatinib

4.2.6.1 Effect of imatinib on the cellular accumulation of dasatinib

WT and Abcg2 transfected MDCKII cells were seeded in clear polystyrene 24-well plates at a seeding density of 2×10^5 cells/well. The medium was changed every other day and the cells formed confluent monolayers in 3-4 days. On the day of the experiment, the medium was aspirated and the confluent monolayer was washed twice with 1 mL prewarmed (37°C) assay buffer. The cells were preincubated with 1 ml of assay buffer with or without imatinib (5, 10, 20, 30, 50, 100 μM) for 30 min, after which the buffer was aspirated and the experiment was initiated by adding 1 ml tracer solution (1μg ^{14}C-dasatinib) of radiolabeled drug in assay buffer with or without imatinib (5, 10, 20, 30, 50, 100 μM) into each well. The plates were continuously agitated at 60 rpm in an orbital shaker at 37°C. After a 3-h accumulation period, the supernatant was aspirated and the cells were first washed three times with 2 ml of ice-cold phosphate-buffered saline and then solubilized using 1 ml of M-PER®. A 200μl sample of solubilized cell fractions was drawn from each well in triplicate. The radioactivity associated with the cell fractions and the protein concentration was determined as previously described in section 4.2.2. Drug accumulation in cells was expressed as a percentage of the accumulated radioactivity measured in the wild-type control cells (dpm per microgram of protein).

4.2.6.2 Effect of imatinib on the cellular permeability of dasatinib

WT and Abcg2-transfected MDCKII cells were seeded at a density of 2×10^5 cells/well on polyester semipermeable membrane supports of the inserts in six-well Transwells.

The medium was changed every day and the cells formed confluent polarized epithelial monolayers in 3-4 days. The monolayers were washed with 2 mL prewarmed (37°C) assay buffer. After a 30-min preincubation in assay buffer with or without 20 μM imatinib, the experiment was initiated by adding a tracer solution of radiolabeled drug in assay buffer to the donor side (apical side, 1.5 ml; basolateral side, 2.6 ml). Fresh assay buffer with or without 20 μM imatinib was added to the receiver side and 200 μl was sampled from the receiver compartment at 0, 10, 20, 30, 45, 60, and 90 min. The volume sampled was immediately replaced with fresh assay buffer with or without 20 μM imatinib. Additional samples were drawn at 0 and 90 min from the donor compartment. The amount of radioactivity in the samples was determined using liquid scintillation counting as described previously. The apical-to-basolateral (A-to-B) flux was determined by addition of radiolabeled drug solution to the apical compartment and sampling the basolateral compartment, whereas for basolateral-to-apical (B-to-A) flux, the donor was the basolateral compartment and the apical compartment was the receiver compartment. The effective permeabilities of dasatinib in A-to-B direction and B-to-A direction with or without 20 μM imatinib were determined by using equation 4.1.

4.2.7 Statistical and data analysis

Statistical analysis was conducted using SigmaStat, version 3.1(Systat Software, Inc., Point Richmond, CA). Statistical comparisons between two groups were made by using two-sample t-test at $p < 0.01$ significance level. If groups failed the normality test, then the nonparametric alternative of two-sample *t* test, the Mann-Whitney rank sum test, was used. Groups were compared by one-way analysis of variance with the Holm-Sidak

post-hoc test for multiple comparisons at a significance level of $p < 0.01$. When groups failed the normality or equal variance test, analysis of variance on ranks with the Tukey post-hoc test was used for multiple comparisons.

4.3 Results

4.3.1 Dasatinib accumulation in WT and ABCB1 or Abcg2 transfected MDCKII cells

^{3}H-Vinblastine was used as a positive control to verify the ABCB1 protein function in the ABCB1-transfected MDCKII cell. ^{3}H-Vinblastine had a significantly lower accumulation (~13% of WT control, $p < 0.01$) in the ABCB1-transfected cells compared with wild-type cells (figure 4.1). To verify the Abcg2 protein function in the Abcg2-transfected MDCKII cells, ^{3}H-mitoxantrone was used as a prototypical substrate of Abcg2. The cellular accumulation of ^{3}H-mitoxantrone was significantly lower (~19% of WT control, $p < 0.01$) in the Abcg2-transfected cells than that in the wild-type cells (figure 4.2). ^{14}C-Dasatinib had a significant lower accumulation (~ 15% of WT control, $p < 0.01$) in the ABCB1-transfected cells than the wild-type cells. When the ABCB1 selective inhibitor LY335979 was applied, it was able to increase the dasatinib accumulation in ABCB1-transfected cells to a similar level as wild-type cells (figure 4.1). The significant increase in the wild-type cells was due to the inhibition of the endogenous expressed ABCB1 (Goh et al., 2002; Dai et al., 2003). The cellular accumulation of dasatinib in Abcg2-transfected cells was significantly lower (~3.5% of WT control, $p < 0.01$) than that in the wild-type cells. ABCG2 selective inhibitor Ko143 abolished the difference between the dasatinib accumulations in Abcg2-transfected and

WT cells (figure 4.2). These in vitro cellular accumulation results indicate that dasatinib is a substrate of active efflux transporters ABCB1 and Abcg2

4.3.2 Dasatinib flux in WT and ABCB1 or Abcg2 transfected MDCKII cells

The directional flux study measured the A-to-B flux and B-to-A flux of ^{14}C-dasatinib in wild-type and transfected cells. Effective permeability, which represents the overall intrinsic permeability of the cell monolayer for dasatinib, was determined. The directional flux of ^{14}C dasatinib across the WT and ABCB1-transfected MDCKII monolayers is shown in figure 4.3. The B-to-A flux of dasatinib in ABCB1-transfected MDCKII cells was greater than that in WT cells, while the A-to-B flux was lower in ABCB1-transfected cells compared to that in WT cells. ABCB1 selective inhibitor LY335979 was able to decrease the difference between B-to-A and A-to-B flux of dasatinib in ABCB1-transfected cells (figure 4.4). Table 4.1 lists the effective permeabilities of dasatinib in B-to-A direction and A-to-B direction in WT and ABCB1-transfected cells with and without the presence of LY335979 (table 4.1). The efflux ratio was 15.61 in ABCB1-transfected cells and 6.37 in wild-type cells, respectively. LY335979 reduced the efflux ratio to 1.2 in ABCB1-transfected cells, which is lower than the efflux ratio in wild-type cells due to the inhibition of endogenous ABCB1. Figure 4.5 showed the directional flux of [^{14}C] dasatinib across the wild-type and Abcg2-transfected MDCKII monolayers. The B-to-A flux of dasatinib in Abcg2-transfected MDCKII cells was greater than that in WT cells. The A-to-B flux of dasatinib was lower in Abcg2-transgected cells compared to that in WT cells. The difference between B-to-A and A-to-B flux of dasatinib in Abcg2-transfected

cells decreased when Abcg2 selective inhibitor Ko143 was applied (figure 4.6). The effective permeabilities of dasatinib in B-to-A direction and A-to-B direction in wild-type and Abcg2-transfected cells are listed in table 4.2. The efflux ratio was 45.45 in Abcg2-transfected cells, which was about 10 fold greater than the efflux ratio in wild-type cells. Ko143 reduced the efflux ratio in the Abcg2-transfected cells to 9.17. These results from in vitro directional flux studies again lead to the conclusion that dasatinib is substrate of both ABCB1 and Abcg2.

4.3.3 Dose dependence study of dasatinib in WT and ABCB1 or Abcg2 transfected MDCKII cells

The effect of increasing concentration of non-radiolabeled dasatinib (0, 10, 25, 50, 75, 100 μM) on ^{14}C-dasatinib cellular accumulations in WT and ABCB1 transfected MDCKII cells were studied to characterize the interaction between dasatinib and ABCB1 (Figure 4.7). ^{14}C-dasatinib accumulations in WT cells increased at the beginning as dasatinib concentration increased. Then the accumulations plateaued out after dasatinib concentration reached 25 μM. However, ^{14}C-dasatinib accumulation in WT cells dropped back to the original level when dasatinib concentrations were higher than 50 μM. ^{14}C-dasatinib accumulations in ABCB1 transfected cells started to increase slowly as dasatinib concentration increased to 50 μM. It did not reach plateau over the dasatinib concentration range we studied.

The dose dependence of ^{14}C-dasatinib on non-radiolabeled dasatinib was studied in WT and Abcg2 transfected MDCKII cells to characterize the interaction between dasatinib

and Abcg2 (Figure 4.8). The results were similar as that in WT and ABCB1 transfected MDCKII cells. ^{14}C-dasatinib accumulations in WT cells increased first, then reached plateau and declined after dasatinib concentration went higher than 25 μM. It reached another plateau with the presence of 75 μM dasatinib. ^{14}C-dasatinib accumulations in Abcg2 transfected cells did not increase until dasatinib concentration increased to 50 μM. It did not reach plateau either over the dasatinib concentration range we studied.

4.3.4 Cellular accumulation study of dasatinib in MDCKII cells with and without OCT-1 inhibitor

Figure 4.9 showed the effect of an OCT-1 inhibitor TEA (2 mM) on the cellular accumulation of ^{14}C-dasatinib in WT and Abcg2 transfected MDCKII cells. 2 mM TEA significantly increased dasatinib accumulation in WT cells but not in the Abcg2 transfected cells. The effect of 2 mM TEA on dose dependence of ^{14}C-dasatinib on increasing non-radiolabeled dasatinib concentration (0, 5, 10, 20, 30, 50, 100 μM) in wild type MDCKII cells was also examined (Figure 4.10). TEA did not change the accumulation-concentration profile of dasatinib in WT cells. ^{14}C-Dasatinib accumulation increased first and then decreased as non-radiolabeled dasatinib concentration increased from 0 to 100 μM in WT cells with and without the presence of TEA.

4.3.5 Interaction between imatinib and dasatinib

The interaction between imatinib and dasatinib was studied by using both cellular accumulation and permeability methods. In wild-type MDCKII cells, ^{14}C-dasatinib

accumulation increased significantly as imatinib concentrations increased from 0 to 10 μM. Then dasatinib accumulation remained steady when imatinib concentration increased from 10 μM to 30 μM. After imatinib concentration went beyond 30 μM, dasatinib accumulation started to fall (Figure 4.11). WT cells peeled off from plates after 3-hr incubation with 100 μM imatinib. ^{14}C-dasatinib accumulation kept increasing in Abcg2 transfected MDCKII cells and then reached the same level as the steady level of dasatinib accumulation in WT cells while imatinib concentration increased from 0 μM to 30 μM. Dasatinib accumulation also dropped when imatinib concentration was higher than 30 μM and kept steady after imatinib concentration reached 50 μM.

The directional flux of ^{14}C-dasatinib across the Abcg2-transfected MDCKII cell monolayers with and without imatinib (20 μM) was determined (Figure 4.12). Imatinib (20 μM) was able to reduce the difference between B-to-A and A-to-B flux of dasatinib in Abcg2-transfected cells. The efflux ration of dasatinib in Abcg2 transfected cells decreased from 45.45 to 9.67 by 20 μM imatinib.

4.4 Discussion

In vitro cellular accumulation experiments revealed that the cellular accumulation of dasatinib in ABCB1 or Abcg2-transfected MDCKII cells was significantly lower than that in wild-type MDCKII cells. ABCB1 selective inhibitor LY335979 brought up dasatinib accumulation in ABCB1 transfected cells to the same level as that in WT cells (figure 4.1). Abcg2 specific inhibitor Ko143 significantly increased dasatinib

accumulation in Abcg2-transfected cell to a level that is even higher than that in WT cells (figure 4.2). A possible explanation for this is that one or more influx transporters, which transport dasatinib, might be upregulated in Abcg2-transfected MDCKII cells due to the overexpression of Abcg2.

The results from cellular permeability studies showed that the efflux ratios of dasatinib in ABCB1 or Abcg2-transfected MDCKII cells were higher than that in wild-type MDCKII cells. LY335979 decreased the efflux ratio of dasatinib in ABCB1-transfected cells. Ko143 decreased efflux ratio of dasatinib in Abcg2-transfected cells. (Table 4.1, 4.2) Interestingly, the effect of Ko143 on the efflux ratio of dasatinib was not as great as on the cellular accumulation of dasatinib. Further studies are needed to reveal the cause of this phenomenon.

Hiwase and group recently found that the cellular accumulation of dasatinib was significantly lower in K562-DOX and VBL-100 (both ABCB1-overexpressing cell lines) than in the respective parental cell lines. Dasatinib cellular accumulation was also significantly lower in Mef-BCRP1 (ABCG2-overexpressing cell line) cell lines compared with parental cell lines (Hiwase et al., 2008). Giannoudis et al. recently reported that dasatinib is transported by ABCB1 by using confluent ABCB1-transfected MDCKII cell monolayers (Giannoudis et al., 2008). In our study, both cellular accumulation and permeability methods to were used to identify that dasatinib is a substrate of both ABCB1 and Abcg2 and characterize the interaction between dasatinib

and ABCB1 or Abcg2. The results were consistent with the previous findings in the literature.

Dose dependence studies were carried out to characterize the interaction between dasatinib and ABCB1 and Abcg2. However, the results were quiet surprising. In both cases, the cellular accumulation of ^{14}C-dasatinib in WT MDCKII cells increased first, then reached plateau and declined as the concentration of non-radiolabeled dasatinib increased from 0 μM to 100 μM (figure 4.7, 4.8). The increase of ^{14}C-dasatinib accumulation at the early stage was very likely due to the saturation of the endogenous expressed ABCB1 in WT MDCKII cells by non-radiolabeled dasatinib (Goh et al., 2002; Dai et al., 2003). As for the decrease of ^{14}C-dasatinib accumulation with the presence of high concentrations of non-radiolabeled dasatinib, we suspected that it could be caused by the saturation of one or more influx transporters by non-radiolabeled dasatinib in high concentrations. The plateau could be explained as that the endogenous ABCB1 transporters were already fully saturated within that concentration range of non-radiolabeled dasatinib, while the influx transporter(s) were not saturated at all. ^{14}C-dasatinib accumulations tended to plateau out again at the end of the dose dependence profiles in WT cells. At this stage, both the efflux transporter and influx transporter(s) were saturated and a steady-state had been reached. In ABCB1 or Abcg2-transfected cells, dasatinib accumulation increased slowly as the concentration of non-radiolabeled dasatinib increased. We were not able get an estimation of the apparent Km (IC50) since the steady-state was not reached.

The organic cation transporters (OCTs) could be the influx transporter(s) that mediate the cell transport of dasatinib. OCTs are in the class of plasma membrane transporters belonging to the SLC22A family. They mediate intracellular uptake of a broad range of structurally diverse organic cations with molecular masses generally lower than 400 Da (Jonker et al., 2004; Wright and Wright, 2005). OCTs are expressed in different tissues including brain (Koepsell et al., 2007). Recent studies discovered that OCT-1 is an important mediator of active imatinib influx (Thomas et al., 2004; White et al., 2006). Primary studies were conducted to identify the interaction between dasatinib and OCT-1.

The cellular accumulation study of dasatinib in WT and Abcg2-tansfected MDCKII cells with the presence of 2 mM TEA, a OCT1 inhibitor (Koepsell et al., 2007) showed that TEA significantly decreased dasatinib accumulation in WT cells but not in Abcg2-transfected cells (figure 4.9). Nevertheless, when the effect of 2 mM TEA on dose dependence of ^{14}C-dasatinib on increasing non-radiolabeled dasatinib concentration in wild type MDCKII cells was studied, the results were controversial. In this experiment, ^{14}C-dasatinib accumulation in WT cells were similar with and without the application of TEA (figure 4.10). If dasatinib were a substrate of OCT1 and TEA can inhibit its OCT1 mediated influx, then ^{14}C-dasatinib accumulation should have increased to certain level and stay constant with the presence of TEA as non-radiolabeled dasatinib concentration increase. This obviously was not the case in this experiment. A recent study reported that OCT-1 inhibitors including prazosin did not significantly reduce dasatinib cellular accumulation in peripheral blood mononuclear cells from newly diagnosed CML

patients (Hiwase et al., 2008). To further explore the interaction between dasatinib and influx transporters, transporter (OCT-1, 2, 3 et al.) transfected cells could be used as a useful *in vitro* model.

The current strategy for the treatment of CML is sequential treatment. Newly diagnosed patients receive imatinib first, followed by dasatinib at time of resistance or intolerance. However, now patients are beginning to experience clinical relapses on dasatinib. Some relapsed are due to mutations that confer resistance to dasatinib but not imatinib (Shah et al., 2007). There are potential hazards of sequential kinase inhibitor therapy and combination therapy might be the future treatment for CML (Giles et al., 2008; Gora-Tybor et al., 2008; Jabbour et al., 2008; Lee et al., 2008). Since imatinib and dasatinib both are substrates of efflux transporters ABCB1 and ABCG2. It is important to understand possible drug-drug interaction between these two TKIs.

In vitro studies revealed that imatinib does interact with dasatinib. In cellular accumulation studies, ^{14}C-dasatinib accumulations in both wild-type and Abcg2-transfedted MDCKII cells increased as the concentration of non-radiolabeled imatinib increased from 0 to 30 μM (figure 4.11). ^{14}C-dasatinib accumulation was maximized out with the presence of 10 μM imatinib and remained maximized until imatinib concentration reached 30 μM. At this imatinib concentration level, ^{14}C-dasatinib accumulation in Abcg2-transfected cells also reached maximum to the same level as that in WT cells. Therefore, 30 μM imatinib was able to completely inhibit the endogenous ABCB1 and overexpressed Abcg2. If figure 4.11was compared with figure

4.8, the ^{14}C-dasatinib accumulation profiles in WT cells were similar in these two experiments. However the ^{14}C-dasatinib accumulation profiles in Abcg2-transfected cells were quite different. The relatively rapid increase of ^{14}C-dasatinib accumulation in Abcg2-transfected cells with the presence of imatinib suggests that imatinib might have a higher affinity to Abcg2 when compared to dasatinib. The decrease in ^{14}C-dasatinib accumulation in both cell types at the presence of high concentration imatinib might due to the inhibition of influx transporters as previously discussed or the cytotoxicity of imatinib, since the WT cells peeled off from plates at the end of 3-hr incubation with the presence of 100 μM imatinib. The effect of imatinib on the directional flux of dasatinib across Abcg2-transfected cells was also examined. 20 μM imatinib decreased the efflux ratio of dasatinib in Abcg2-transfected cells from 45.45 to 9.67. All these data strongly indicated that imatinib and dasatinb interact with each other. Further studies should be focused on the interaction between imatinib and dasatinib in the clinical relevant concentration range.

4.5 Conclusion

In summary, the cellular accumulation of dasatinib in the wild-type MDCKII cells was significantly lower than that in ABCB1-transfected or Abcg2 transfected MDCKII cells ($p<0.01$). The ABCB1 specific inhibitor LY 335979 abolished the difference between wild-type and ABCB1-transfected cells and ABCG2 specific inhibitor Ko143 abolished the difference in Abcg2 cells. The efflux ratio of dasatinib in ABCB1-transfected cells was 15.61 and was decreased by LY335979. In Abcg2-transfected cells, the efflux ratio of dasatinib was 45.45 and was decreased by Ko143. OCT-1 inhibitor TEA did not

significantly reduce the cellular accumulation of dasatinib in wild-type and Abcg2-trasfected MDCKII cells. Imatinib significantly increased dasatinib accumulation in wild-type and Abcg2-transfected cells and reduced efflux ratio of dasatinib from 45.45 to 9.67. In conclusion, dasatinib is a substrate of ABCB1 and Abcg2. OCT-1 does not play a role in the influx of dasatinib, and imatinib and dasatinib can interact with each other.

4.6 Acknowledgement

We would like to thank Bristol-Myers Squibb Company for kindly providing us dasatinib, ^{14}C-dasatinib. We thank Dr. Schinkle from Netherlands Cancer Institute for generously providing us WT and Abcg2-transfected MDCKII cells and Ko143. We thank Dr. Piet Borst from Netherlands Cancer Institute for generously providing us WT and ABCB1-transfected MDCKII cells. We thank Eli Lilly and Co. for kindly providing us LY335979.

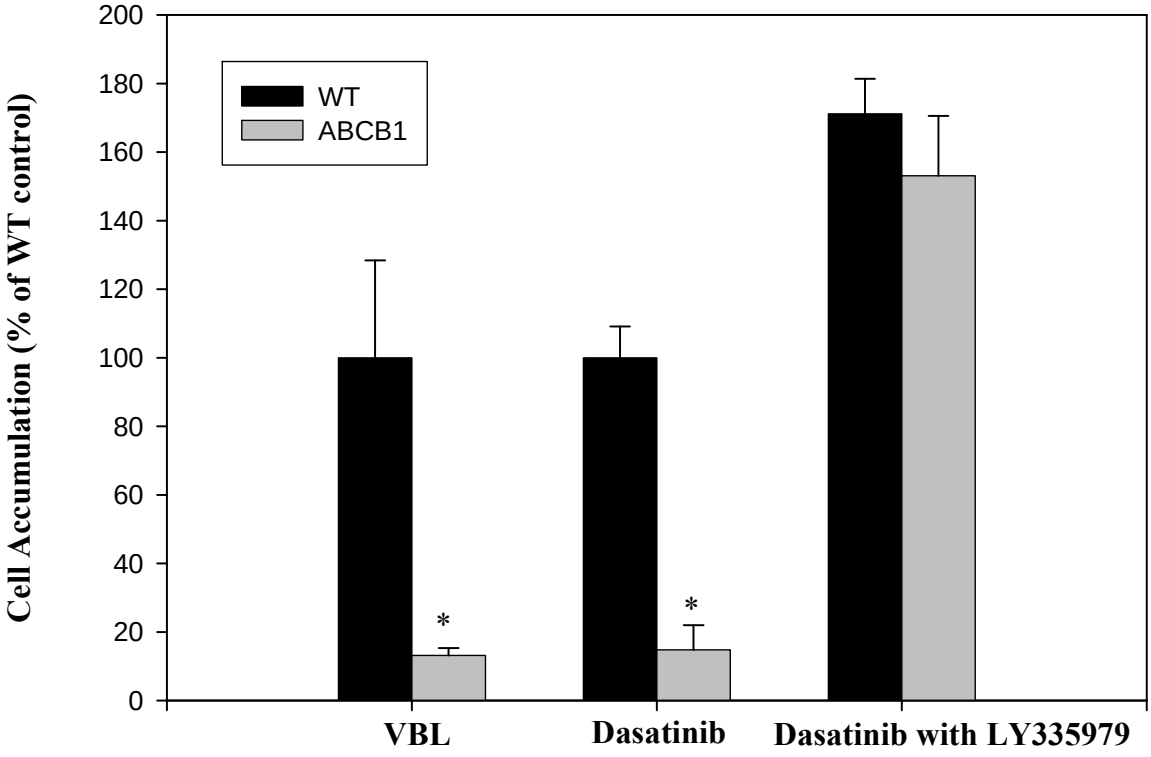

Figure 4.1. Accumulation of [^{3}H] vinblastine (VBL), [^{14}C] dasatinib and [^{14}C] dasatinib with LY335979 (1 μM) in wild-type (black bar) and ABCB1-transfected (gray bar) MDCKII cells.

Results are presented as mean ±S.D. (as percentage of wild-type control), *n* =4 to 12. VBL and Dasatinib accumulation in ABCB1-transfected cells were significantly lower than in the wild-type cells (*, $p < 0.01$).

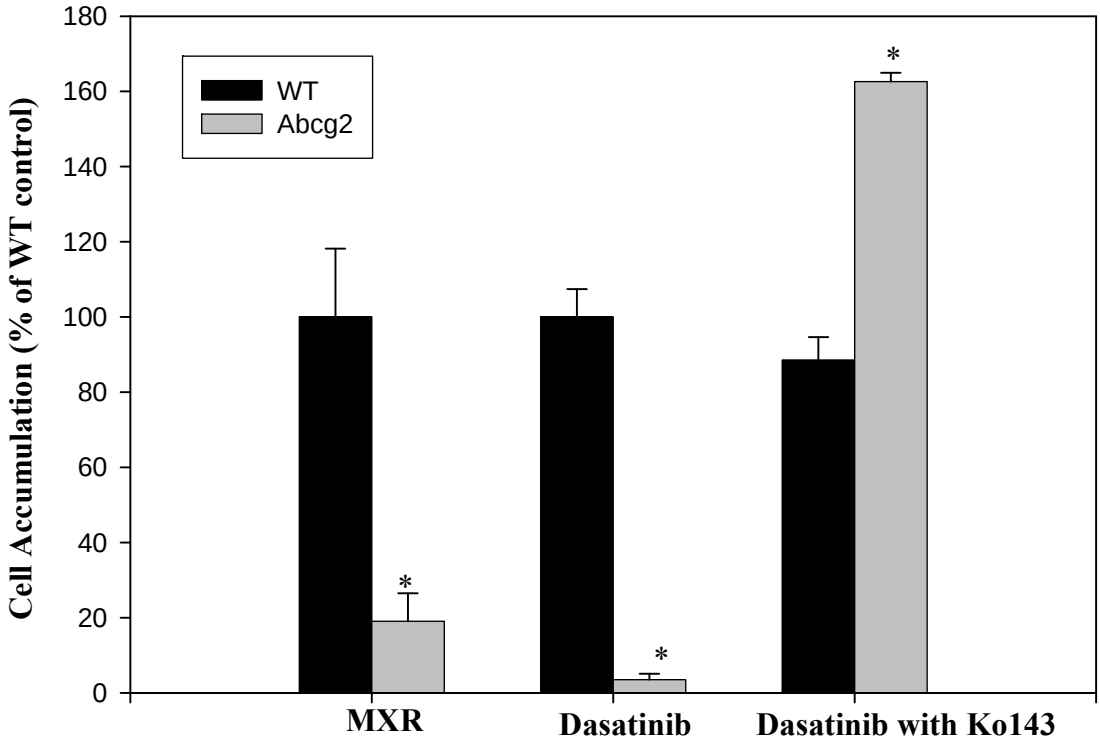

Figure 4.2. Accumulation of [^{3}H] mitoxantrone (MXR), [^{14}C] dasatinib and [^{14}C] dasatinib with Ko143 (200 nM) in wild-type (black bar) and Abcg2-transfected (gray bar) MDCKII cells.

Results are expressed as mean ±S.D. (as percentage of wild-type control), n =6 to 12. MXR and Dasatinib had significantly lower accumulation in Abcg2-transfected cells compared with wild-type control group (*, $p < 0.01$).

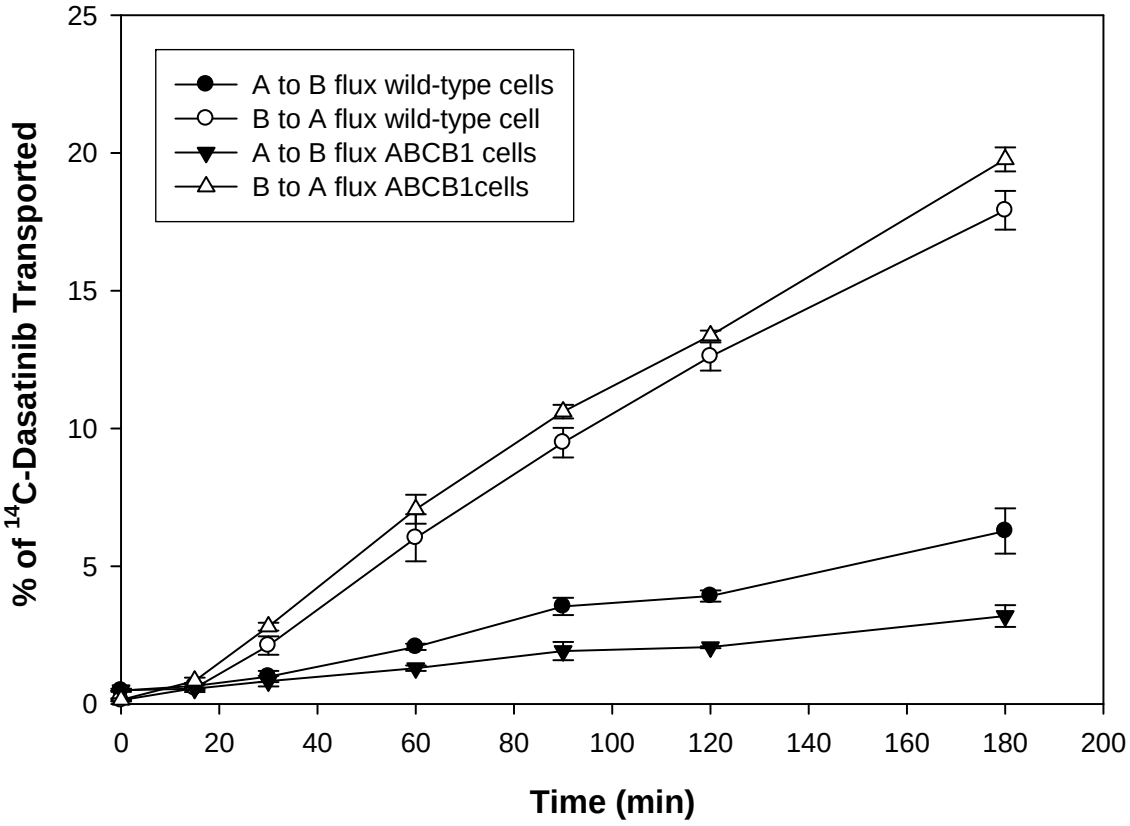

Figure 4.3. Directional flux of [^{14}C] dasatinib across the MDCKII monolayers in wild-type (●, A-to-B direction; ○, B-to-A direction) and ABCB1-transfected cells (▼, A-to-B direction; △, B-to-A direction).

Results are expressed as mean ±S.D., n=9. The difference between the B-to-A flux and A-to-B flux of dasatinib in ABCB1 transfected cells was greater than that in wild-type cells.

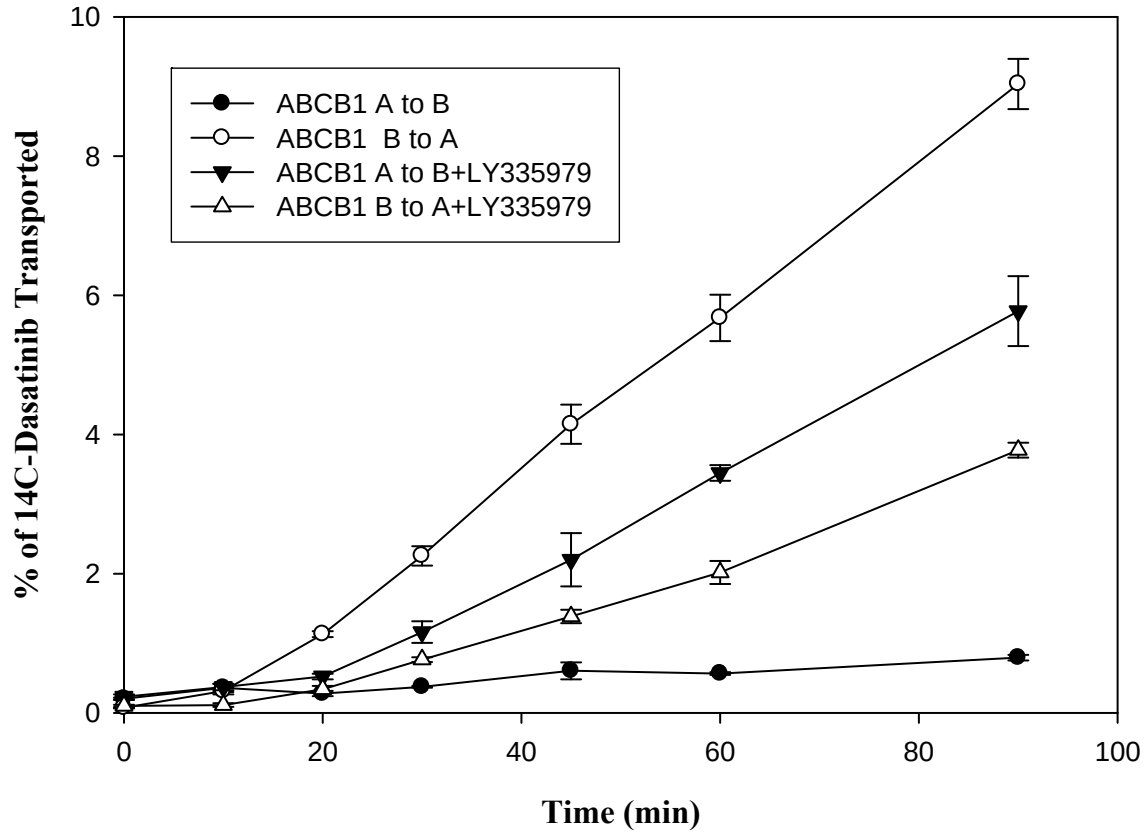

Figure 4.4. Directional flux of [^{14}C] dasatinib across the ABCB1-transfected MDCKII cell monolayers with (▼, A-to-B direction; △, B-to-A direction) and without LY335979 (1 μM) (●, A-to-B direction; ○, B-to-A direction).

Results are expressed as mean ±S.D., n=9. The difference between the B-to-A flux and A-to-B flux of dasatinib in ABCB1 transfected cells was decreased by ABCB1 selective inhibitor LY335979.

Table 4-1. Effective permeability of ^{14}C-dasatinib in WT and ABCB1-transfected MDCKII cells with and without the presence of LY335979 (1 μM) (n=9).

	WT cells w/o inhibitor (cm/s)	ABCB1ls w/o inhibitor (cm/s)	ABCB1s with LY335979(cm/s)
A-to-B	1.85E-06±4.35E-07	7.61E-07±2.83E-07	3.79E-06±3.72E-07
B-to-A	1.18E-05±7.91E-07	1.19E-05±7.46E-07	4.53E-06±1.02E-07
Efflux ratio	6.37	15.61	1.20

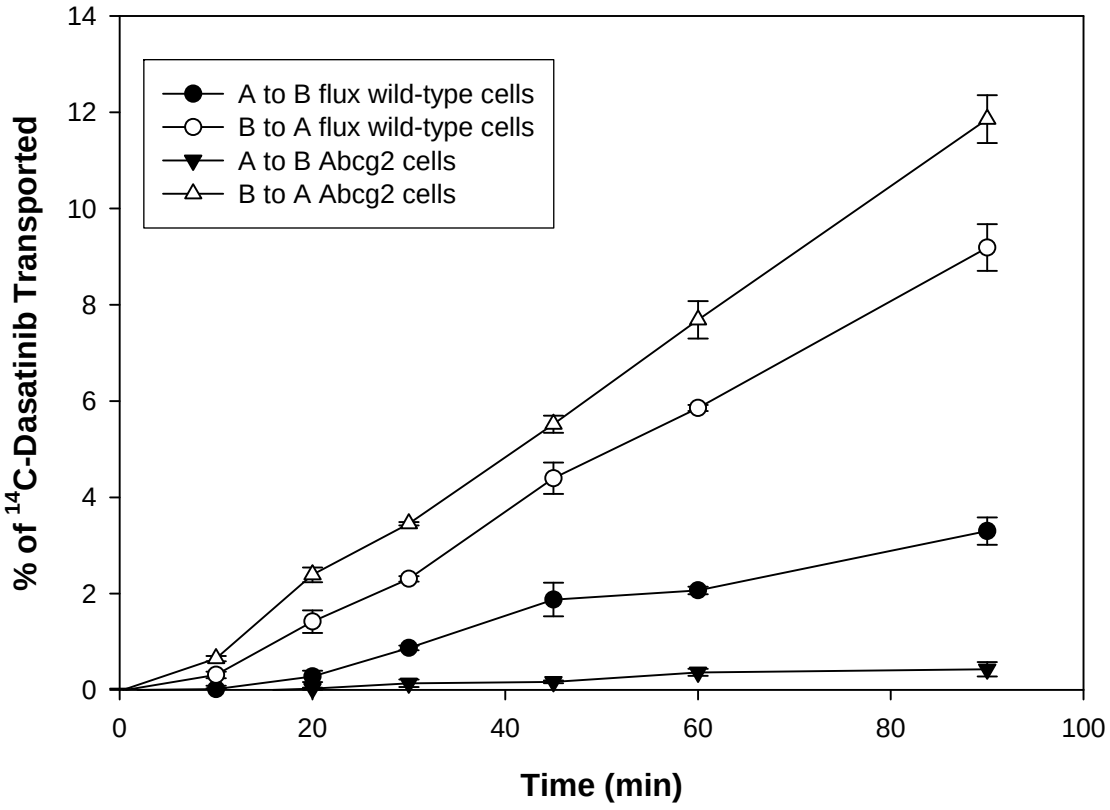

Figure 4.5. Directional flux of [^{14}C] dasatinib across the MDCKII monolayers in wild-type (●, A-to-B direction; ○ B-to-A direction) and Abcg2-transfected cells (▼, A-to-B direction; △, B-to-A direction).

Results are expressed as mean ±S.D., n=9. The difference between the B-to-A flux and A-to-B flux of dasatinib in Abcg2 transfected cells was greater than that in wild-type cells.

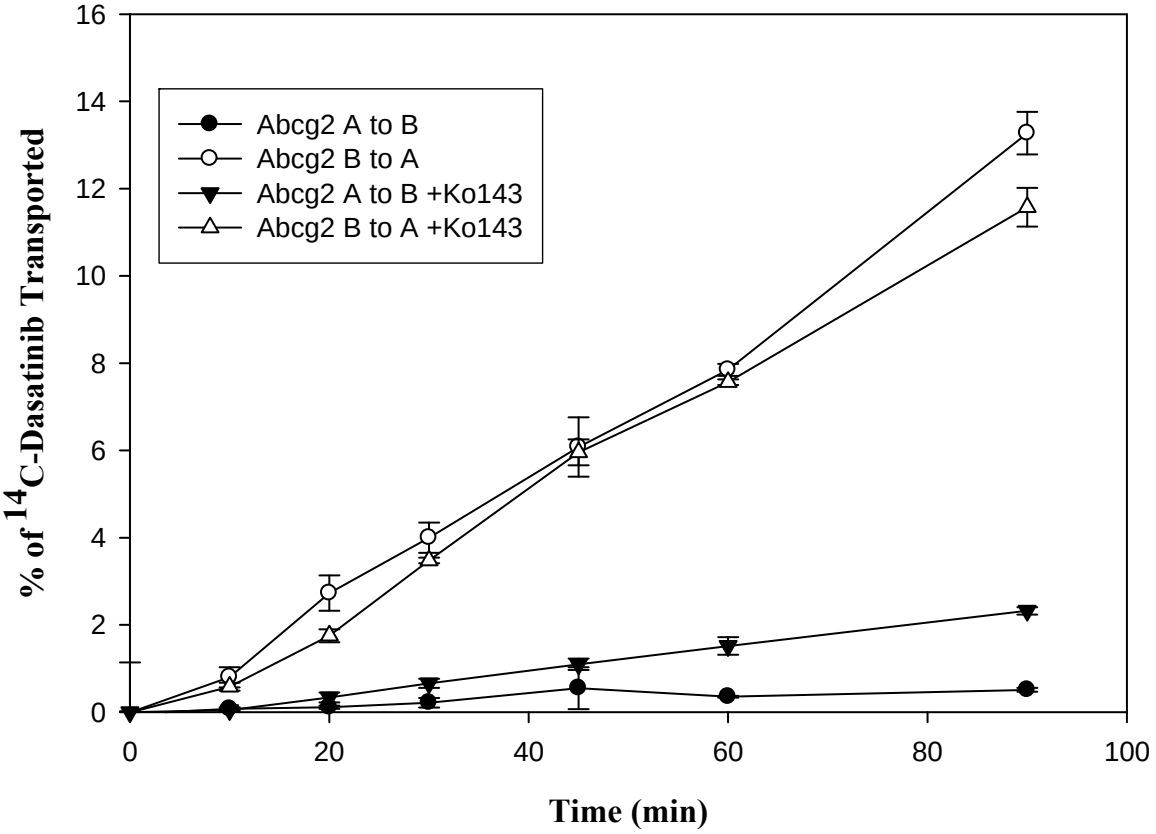

Figure 4.6. Directional flux of [^{14}C] dasatinib across the Abcg2-transfected MDCKII cell monolayers with (▼, A-to-B direction; △, B-to-A direction) and without Ko143 (200 nM) (●, A-to-B direction; ○ B-to-A direction).

Results are expressed as mean ±S.D., n=9. The difference between the B-to-A flux and A-to-B flux of dasatinib in Abcg2 transfected cells was decreased by Abcg2 specific inhibitor Ko143.

Table 4-2. Effective permeability of ^{14}C-dasatinib in Abcg2-transfected and WT MDCKII cells with and without the presence of Ko143 (200nM) (n=9).

	WT cells w/o inhibitor (cm/s)	Abcg2 cells w/o inhibitor (cm/s)	Abcg2 cells with Ko143(cm/s)
A-to-B	2.47E-06±5.61E-07	3.74E-07±1.08E-07	1.66E-06±9.50E-08
B-to-A	1.13E-05±1.44E-06	1.70E-05±1.15E-06	1.52E-05±5.61E-07
Efflux ratio	4.55	45.45	9.17

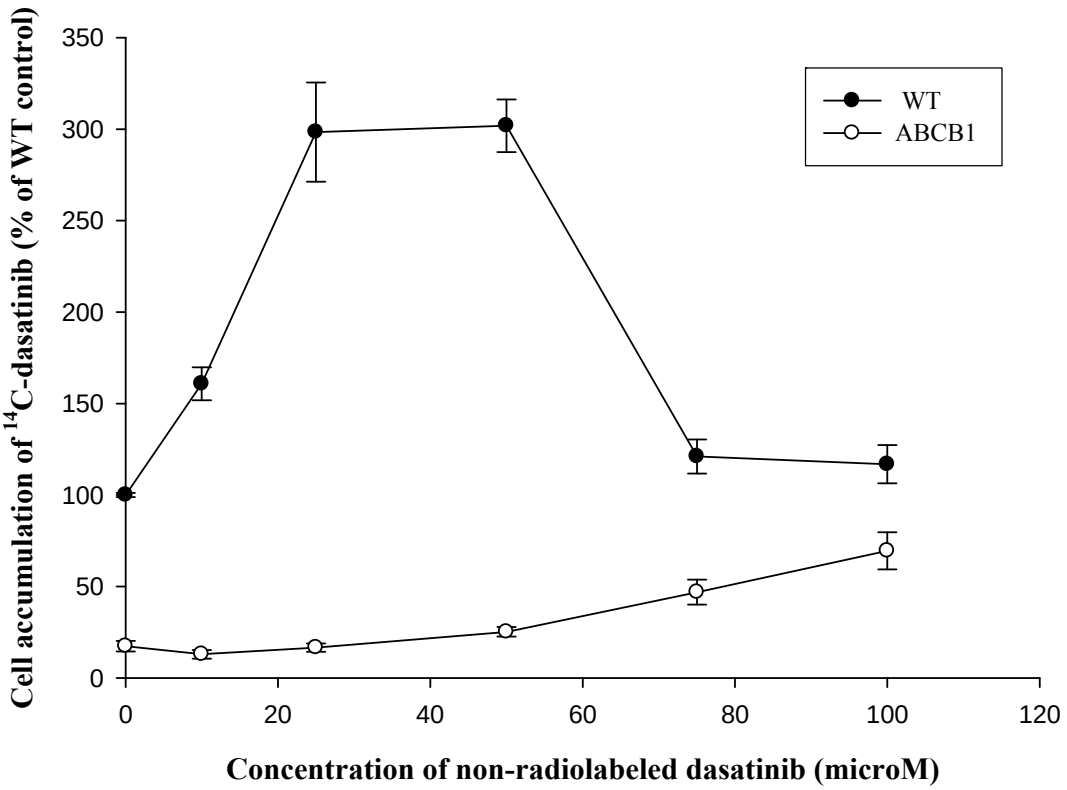

Figure 4.7. Plot of effect of increasing concentration of non-radiolabeled dasatinib (0, 10, 25, 50, 75, 100 μM) on ^{14}C-dasatinib cellular accumulation in WT and ABCB1 transfected MDCKII cells.

Results are expressed as mean ±S.D. (as percentage of wild-type control), *n* =4.

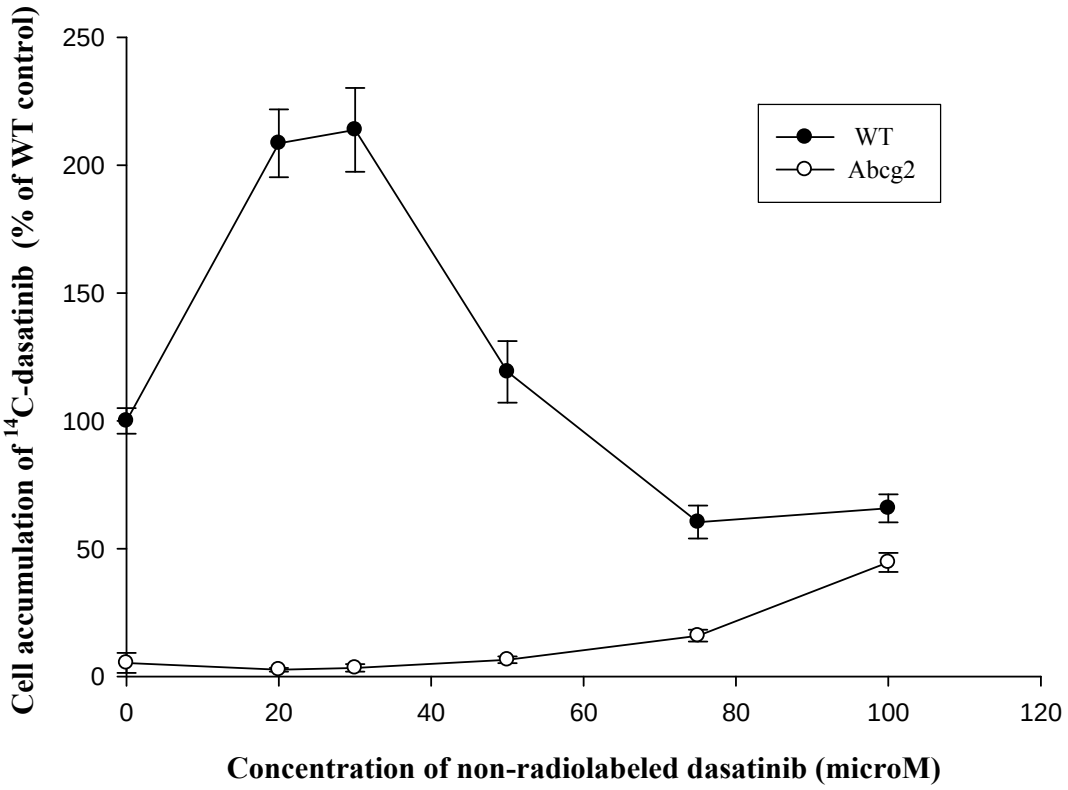

Figure 4.8. Plot of effect of increasing non-radiolabeled dasatinib concentration (0, 20, 30, 50, 75, 100 μM) on ^{14}C-dasatinib cellular accumulation in WT and Abcg2 transfected MDCKII cells.

Results are expressed as mean ±S.D. (as percentage of wild-type control), *n* =4.

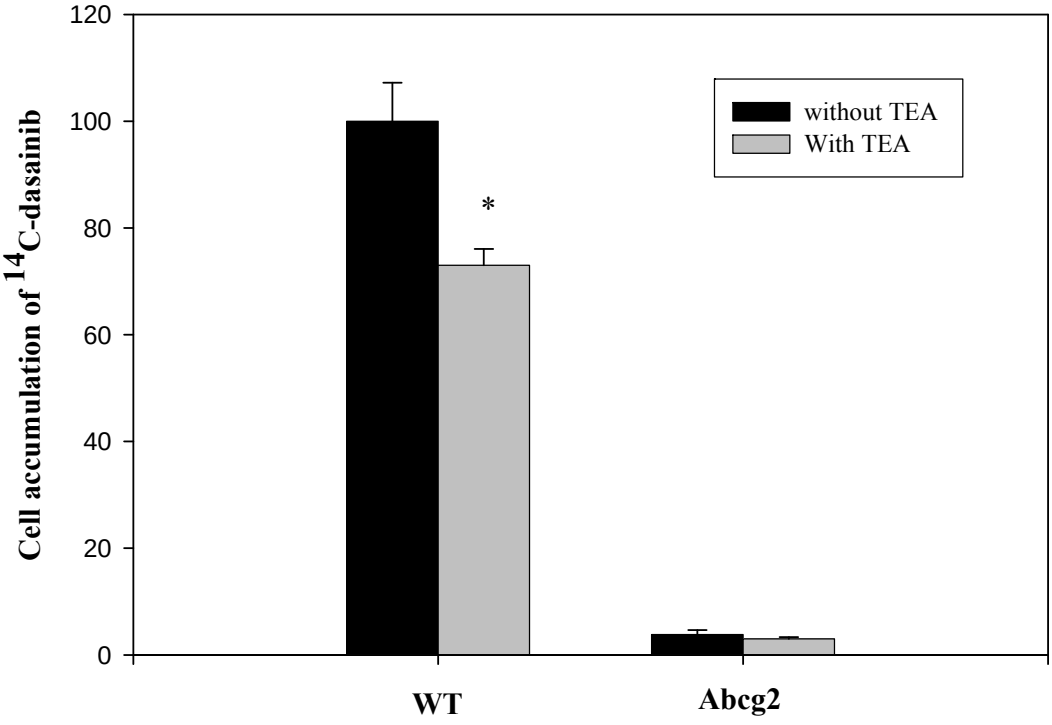

Figure 4.9. Accumulation of ^{14}C-dasatinib in WT and Abcg2 transfected MDCKII cells with (gray bars) and without (black bars) 2 mM TEA.

Results are expressed as mean ±S.D. (as percentage of wild-type control), *n* =6 (*, p <0.01).

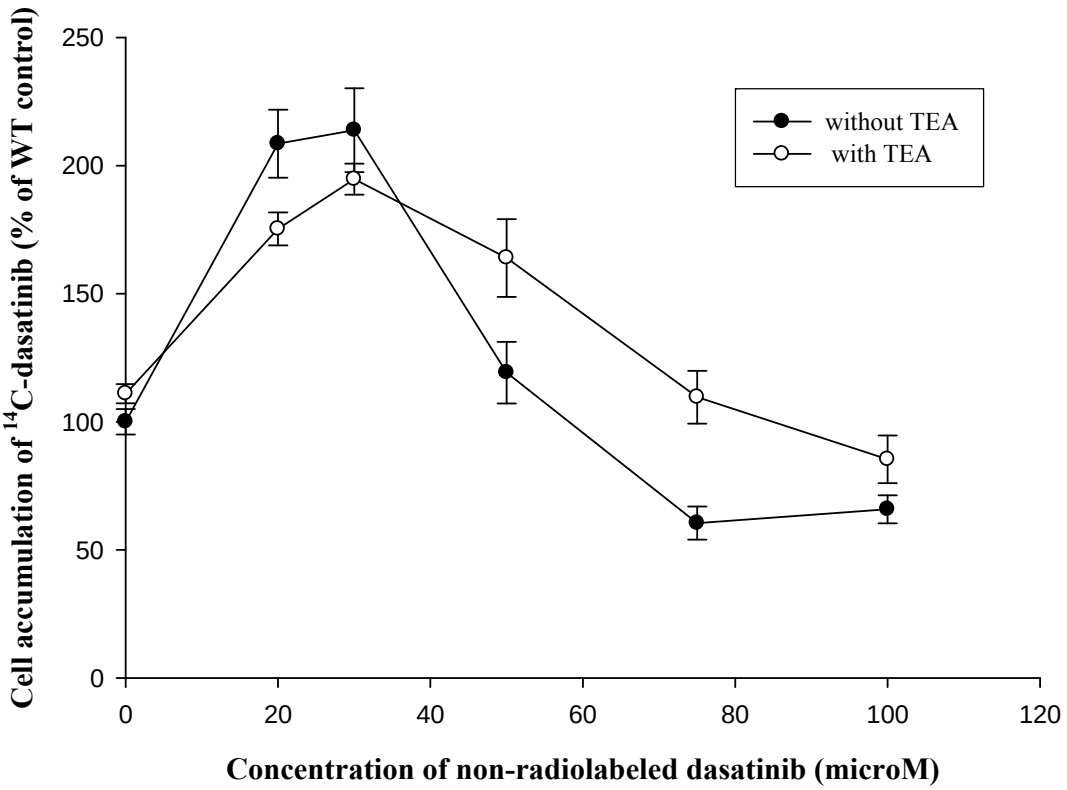

Figure 4.10. Plot of effect of 2 mM TEA on dose dependence of ^{14}C-dasatinib on increasing non-radiolabeled dasatinib concentration (0, 20, 30, 50, 75, 100 μM) in wild type MDCKII cells.

Results are expressed as mean ±S.D. (as percentage of wild-type control), *n* =4.

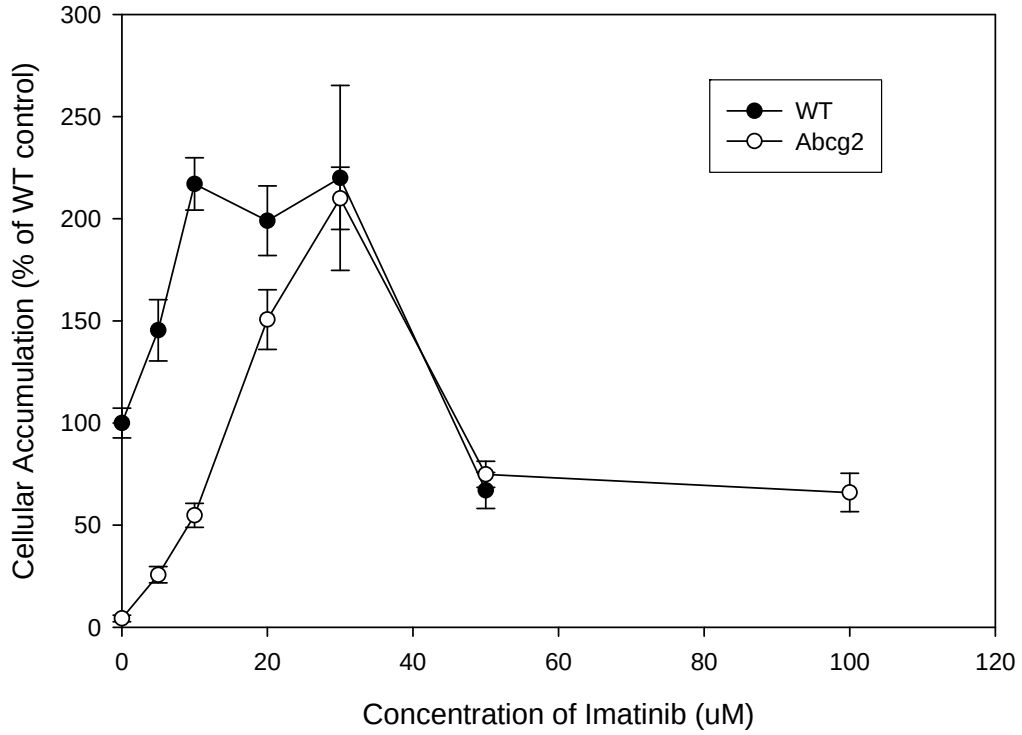

Figure 4.11. Plot of effect of increasing non-radiolabeled imatinib concentration (0, 5, 10, 20, 30, 50, 100 μM) on ^{14}C-dasatinib cellular accumulations in WT and Abcg2 transfected MDCKII cells.

Results are expressed as mean ±S.D. (as percentage of wild-type control), *n* =4.

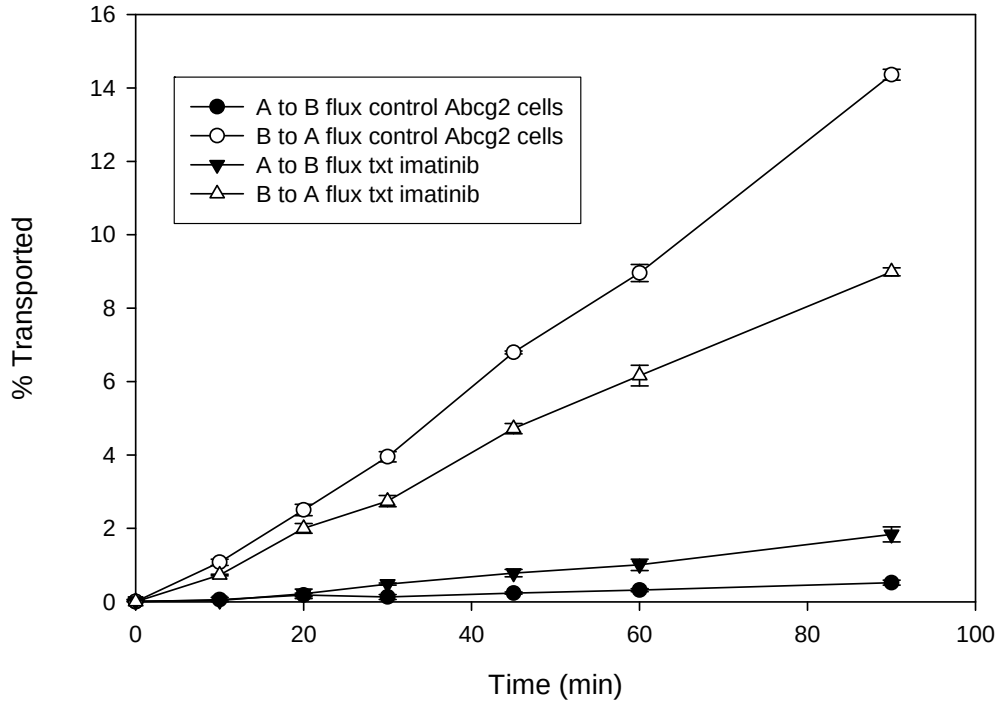

Figure 4.12. Directional flux of [^{14}C] dasatinib across the Abcg2-transfected MDCKII cell monolayers with (▼, A-to-B direction; △, B-to-A direction) and without imatinib (20 μM) (●, A-to-B direction; ○ B-to-A direction).

Results are expressed as mean ±S.D., n=9. The difference between the B-to-A flux and A-to-B flux of dasatinib in Abcg2 transfected cells was decreased by imatinib.

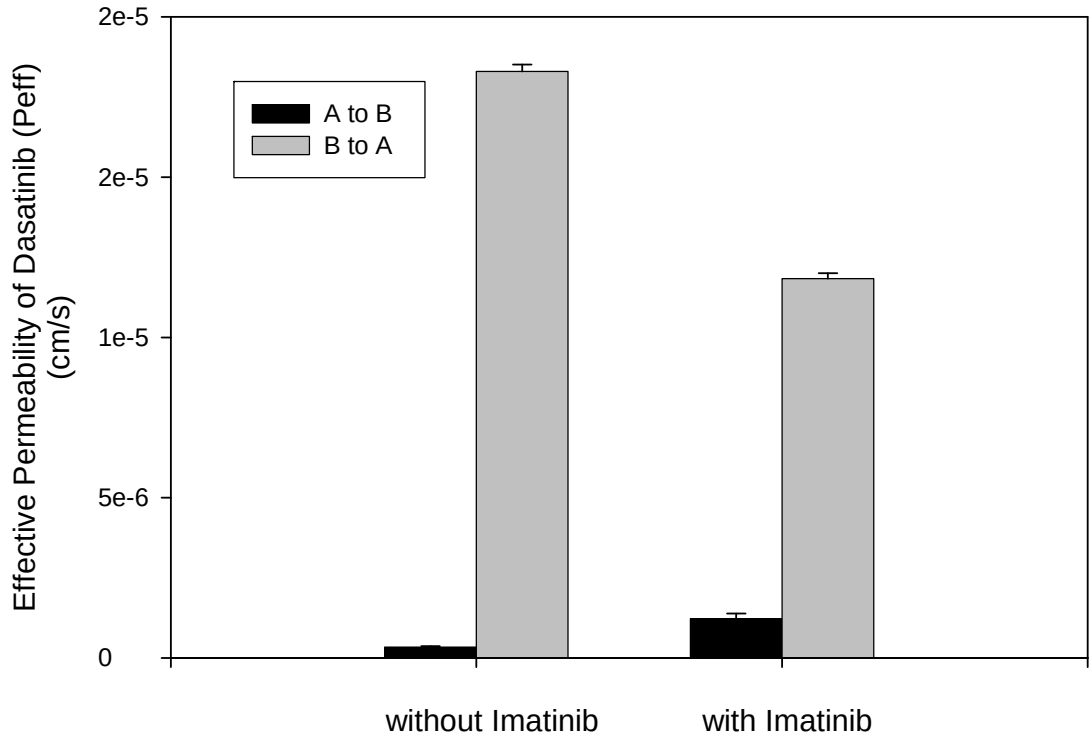

Figure 4.13. The A-to-B direction effective permeability (black bar) and B-to-A direction effective permeability (gray bar) of dasatinib (cm/s) across the Abcg2-transfected MDCKII cell monolayers with and without imatinib (20 μM).

Results are expressed as mean ±S.D., n=6.

CHAPTER 5

IN VIVO EFFECT OF EFFLUX TRANSPORTERS ON THE CNS DELIVERY OF DASATINIB

5.1 Abstract and introduction

5.1.1 Abstract

The objective of this study was to examine the effects of the active efflux transporters, ABCB1 and Abcg2 on the CNS delivery of dasatinib. Wild type and knock-out (Abcb1 knokout, Abcg2 knockout or triple knockout) FVB mice received 5 mg/kg dasatinib as a single bolus via tail vein injection or 10 mg/kg dasatinib via oral gavage with and without the coadministration of inhibitors (25 mg/kg LY335979, 10 mg/kg Ko143 or 10 mg/kg GF120918). Plasma and brain were sampled at various times postdose. The concentration of dasatinib in plasma and brain was determined by LC/MS/MS. The genetic deletion or pharmacological inhibition of Abcb1 or Abcb1 and Abcg2 but not Abcg2 alone was able to increase dasatinib brain penetration. These results indicated that ABCB1 and ABCG2 play a role in the CNS delivery of dasatinib, limiting dasatinib CNS penetration. The use of potent inhibitors for both ABCB1 and ABCG2 should be able to improve dasatinib CNS delivery.

5.1.2 Introduction

Malignant brain tumors are one of the most lethal forms of cancer and are extremely difficult to treat. They remain refractory to conventional treatment approaches, including radiotherapy and cytotoxic chemotherapy (Newton, 2003). Dasatinib is a second generation tyrosine kinase inhibitor that has high potency against Bcr-Abl and is active against various imatinib-resistant Bcr-Abl mutant cell lines, and, as such, can overcome the imatinib-resistance in CML patients (Shah, 2007). In addition to Bcr-Abl, dasatinib also inhibits SRC tyrosine kinase. It is a SRC/BCR-ABL kinase inhibitor

(Nam et al., 2005). Src family is the largest family of nonreceptor tyrosine kinases (Fizazi, 2007; Finn, 2008). Src family kinases (SFKs) are responsible for signal transduction during many cellular activities, including differentiation, adhesion, migration, division, motility, angiogenesis and survival (Summy and Gallick, 2003; Fizazi, 2007). Recent studies revealed that SFKs are involved in signal transduction from many receptor tyrosine kinases, such as PDGFR, EGFR and stem cell factor receptor (Alvarez et al., 2006). A number of studies have shown that SFKs are up regulated in multiple types of human tumors and are typically associated with advanced malignancies and/or metastatic spread (Playford et al., 2004; Park et al., 2008). Recent studies reported that SFKs participate in induction of glioblastoma multiforme (GBM) invasion and glioma migration (Park et al., 2006; Dey et al., 2008; Kleber et al., 2008). Taking all these into account, dasatinib may be very promising in the treatment of brain tumors, both primary and secondary.

However, there are several issues regarding the CNS delivery of chemotherapy agents, such as the anatomical barriers in the CNS, drug efflux transporters in these barriers, and the relative resistance of tumors to chemotherapy. The efflux transport systems are increasingly recognized as important determinants of drug distribution to, and elimination from, different compartments of the CNS. Recently, studies from another group and our group (this thesis) showed that dasatinib is a substrate of efflux transporters ABCB1 and ABCG2 (Hiwase et al., 2008). However, thus far little information is known about the CNS delivery of dasatinib, including the action of relevant BBB transporters in modulating this delivery. In this study the effect of Abcb1

and Abcg2 on the CNS delivery of dasatinib was studied by direct sampling method in an *in vivo* mouse model.

Researchers have frequently utilized genetic knockout mouse or natural mutant mouse models in understanding the physiological functions of transporters and in evaluating the effect of transporter on pharmacokinetics and pharmacodynamics of drugs nowadays (Xia et al., 2007c). Genetic knockout mice are generated by disruption the endogenous transporter(s) gene in order to investigate the specific targeted transporter(s). These animals have been used to study the functions of Abcb1, Abcg2 and Abcc2 (Xia et al., 2007c).

The objective of this chapter was to examine the influence of Abcb1 and Abccg2 on the targeted delivery of dasatinib to the CNS by using an *in vivo* WT and knockout mouse models.

5.2 Material and methods

5.2.1 Chemicals and animals

5.2.1.1 Chemicals

Dasatinib was kindly provided by Bristol-Myers Squibb Company (Princeton, NJ). LY335979 ((*R*)-4-((1a*R*, 6R, 10bS)-1,2-difluoro-1, 1a, 6,10b-tetrahydrodibenzo-(*a*,*e*)cyclopropa(*c*)cycloheptan-6-yl)-α-((5-quinoloyloxy)methyl)-1-piperazineethanol, trihydrochloride) was a gift from Eli Lilly and Co. (Indianapolis, IN). GF120918 (N-[4-[2-(6, 7-Dimethoxy-3, 4-dihydro-1H-isoquinolin-2-yl) ethyl]-5-methoxy-9-oxo-10H-

acridine-4-carboxamide) was generously given by GlaxoSmithKline (Research Triangle, NC). Ko143 was kindly provided by Dr. Alfred Schinkel (Netherlands Cancer Institute, Amsterdam, The Netherlands). All other chemicals used were HPLC or reagent grade.

5.2.1.2 Animals

Wild-type FVB mice, Abcb1 knockout [Mdr1a/b (-/-)] FVB mice, Abcg2 knockout FVB mice and triple knockout [Bcrp-Mdr1a/b (-/-)] FVB mice were purchased from Taconic Farms, Inc. (Germantown, NY). All mice were male and between 8 to 10 weeks old. Animals were maintained under temperature-controlled conditions with a 12-h light/dark cycle and unlimited access to food and water. All studies were approved by the Institutional Animal Care and Use Committee of the University of Minnesota

5.2.2 CNS distribution of i.v. administered dasatinib in WT and knockout FVB mice

Wild-type and triple knockout [Bcrp-Mdr1a/b (-/-)] FVB mice received a dasatinib solution (propylene glycol: water = 1:1, pH 4.6) at a 5 mg/kg dose via tail vein injection. At various time points (5, 20, 60, 120, 180 min postdose), mice (n=4) were euthanized. Blood was immediately harvested via cardiac puncture and collected in tubes preloaded with K_2EDTA (BD, Franklin Lakes, NJ). Then whole brain was harvested within 2 min and rinsed with ice-cold saline to remove extraneous blood. At the end of the experiment, plasma was separated from blood by centrifugation at 3000

rpm for 10 min at 4°C. All plasma and whole brain samples were stored at -80°C until analysis by LC-MS/MS.

Wild-type, Abcb1a/b knockout [Mdr1a/b (-/-)] and Abcg2 Knockout [Bcrp1 (-/-)] FVB mice received a dasatinib solution (propylene glycol: water = 1:1, pH 4.6) at a 5 mg/kg dose via tail vein injection. At two different time points (20, 120min) postdose, mice (n=4) were euthanized. Blood and whole brain were immediately harvested and treated as described previously.

5.2.3 CNS distribution of i.v. administered dasatinib in WT mice with and without coadministration of inhibitors

32 wild-type FVB mice were randomly assigned to 4 groups. Group 1 received 5 mg/kg dasatinib via tail vein injection. Group 2 received 25 mg/kg LY335979 (20% ethanol) via tail vein injection 30 min before the injection of 5 mg/kg dasatinib. Group 3 had a tail vein injection of 10 mg/kg Ko143 (DMSO: TWEEN80: propylene glycol: saline = 5.75: 3.94: 24.675: 65.645) 30 min before the injection of 5 mg/kg dasatinib. Group 4 had an injection of 10 mg/kg GF120918 (DMSO: TWEEN80: propylene glycol: saline = 6.6: 3.95:24.67:64.67) via tail vein and another injection of 5mg/kg dasatinib 30min later. For each group, 4 mice were euthanized at 20 min after dosing of dasatinib and the remaining 4 were euthanized at 120 min postdose. Plasma and whole brain were harvested and treated as described previously in section 5.2.2.

5.2.4 CNS distribution of oral administered dasatinib in WT FVB mice

Wild-type FVB mice received 10 mg/kg dasatinib (propylene glycol: water = 1:1, pH 4.6) via oral gavage. At various time points (15, 60, 120, 240, 480 min postdose), mice (n=4) were euthanized. Blood and whole brain were immediately harvested and treated as described previously in section 5.2.2.

5.2.5 CNS distribution of oral administered dasatinib in WT and knockout FVB mice

24 wild-type FVB mice were randomly assigned to 6 groups. Group 1 received 10 mg/kg dasatinib (propylene glycol: water = 1:1, pH 4.6) via oral gavage. Group 2 received 25 mg/kg LY335979 (20% ethanol) via tail vein injection 30 min before receiving 10 mg/kg dasatinib via oral gavage. Group 3 had a tail vein injection of 10 mg/kg Ko143 (DMSO: TWEEN80: propylene glycol: saline = 5.75: 3.94: 24.675: 65.645) 30 min before the oral dosing of 10 mg/kg dasatinib. Group 4 had an injection of 10mg/kg GF120918 (DMSO: TWEEN80: propylene glycol: saline = 6.6: 3.95:24.67:64.67) via tail vein and then an oral dosing of 10 mg/kg dasatinib 30 min later. Group 5 received a blank vehicle for LY335979 (20% ethanol) via tail vein injection 30 min before receiving 10 mg/kg dasatinib via oral gavage. Group 6 had a tail vein injection of another vehicle control (DMSO: TWEEN80: propylene glycol: saline = 6.6: 3.95:24.67:64.67) 30 min before the oral dosing of 10 mg/kg dasatinib. For each group, mice were euthanized at 120 min after dosing of dasatinib. Plasma and whole brain were harvested and treated as described previously.

Abcb1a/b knockout [Mdr1a/b (-/-)], Abcg2 knockout [Bcrp1 (-/-)] FVB mice and triple knockout [Bcrp-Mdr1a/b (-/-)] FVB mice received a dasatinib solution (propylene glycol: water = 1:1, pH 4.6) at a 10 mg/kg dose via oral gavage. At 120 min postdose, mice (n=4) were euthanized. Blood and whole brain were immediately harvested and treated as described previously.

5.2.6 Determination of Dasatinib Concentrations in Plasma and Brain using LC-MS/MS

Mouse plasma and brain samples were analyzed by LC-MS/MS. Sample preparation included addition of 3 volumes of acetonitrile containing internal standard (IS) d6-dasatinib to the plasma samples. Whole brain samples were first homogenized in water with a volume ratio of 1:3 followed by the addition of acetonitrile containing IS. After centrifugation to remove precipitated proteins, 10 µL of the clear supernatant was analyzed by LC/MS/MS. Chromatographic separation was obtained using an Atlantis® dC18 column (2.1 mm x 50 mm) packed with a 3µM stationary phase (Waters Corporation, Milford, MA). The mobile phase was composed of 10 mM ammonium acetate with 0.1% formic acid (A) and acetonitrile (B). A gradient elution method was used with the initial mobile phase consisting of 90% A and 10% B. After sample injection, the mobile phase was held at the initial condition for 1 min and then changed to 10% solvent A and 90% solvent B over 1 min and held at that composition for an additional 0.8 minutes. The mobile phase was then returned to initial conditions and the column was re-equilibrated for one minute. The total analysis time was 4 minutes. The

HPLC was interfaced to a Micromass Quattro LC triple quadrupole mass spectrometer (Waters, Milford, MA, USA) equipped with electrospray ionization interface. The desolvation temperature was 350°C and the source temperature was 120°C. Data acquisition employed selected reaction monitoring (SRM). Positively charged ion representing the $[MH]^+$ for dasatinib and the internal standard (IS) were selected in MS1 and dissociated with argon at a pressure of 2.5×10^{-3} Torr to form specific product ions which were subsequently monitored by MS2. All dwell times were 100 ms. The SRM transitions monitored were m/z 488 $\rightarrow$ 401 for dasatinib, m/z 496 $\rightarrow$ 409 for the internal standard. The cone voltage was optimized at 35 V for both dasatinib and IS, while the collision energy was 35 eV. The retention time for dasatinib and IS was 2.05 and 2.04 min, respectively. The lower limit of quantification was 1 ng/mL.

5.2.7 Statistical analysis

Statistical analysis was conducted using SigmaStat, version 3.1(Systat Software, Inc., Point Richmond, CA). Statistical comparisons between two groups were made by using two-sample t-test at $p < 0.05$ significance level. If groups failed the normality test, then the nonparametric alternative of two-sample *t* test, the Mann-Whitney rank sum test, was used. Groups more than 2 were compared by one-way analysis of variance with the Holm-Sidak post-hoc test for multiple comparisons at a significance level of $p < 0.05$. When groups failed the normality test, the Kruskal-Wallis one way analysis of variance on ranks was used.

5.3 Results

5.3.1 CNS distribution of i.v. administered dasatinib in WT and triple-knockout FVB mice

The concentrations of dasatinib in plasma and brain after an intravenous bolus dose in wild-type and triple knockout FVB mice were determined by LC-MS/MS. The plasma concentration time profiles of dasatinib in wild-type and triple knockout mice are shown in Figure. 5. 1A. There was no significant difference in the plasma concentrations between the wild-type mice and the triple knockout mice, while the brain concentrations in triple-knockout mice were much greater than that in wild-type mice as shown in Figure 5. 1B. The brain concentration was lower than 12% of the plasma concentration in wild-type mice at all the 5 time points we measured. When the ratios of brain concentration over plasma concentration, which represent the brain penetration of dasatinib were compared between wild-type mice and triple knockout mice, the brain penetration of dasatinib in triple knockout mice was significantly greater than the brain penetration in wild-type mice at the 5 different time points (Figure 5. 1C).

5.3.2 CNS distribution of Dasatinib in Wild-type FVB Mice with and without Coadministration of Pharmacological Inhibitors, Abcb1a/b knockout and Abcg2 knockout FVB mice

The brain concentrations of dasatinib were measured in wild-type mice that received an i.v. bolus dose with and without coadministration of LY335979, Ko143 or GF120918.

The results are shown in Figure. 5.2. The inhibition of Abcb1 by using LY335979 significantly increased brain dasatinib concentrations in wild-type mice. However the inhibition of Abcg2 by using Ko143 was not able to increase the brain concentrations of dasatinib in wild-type mice. When both Abcb1 and Abcg2 were inhibited by a dual inhibitor GF120918, the brain dasatinib concentrations in wild-type mice increased the most. The similar phenomenon was observed with genetic deletion of efflux transporters (Figure 5.3). Brain dasatinib concentrations increased significantly in Abcb1 knockout mice compare with those in wild-type mice. Brain dasatinib concentrations in Abcg2 knockout mice did not increase at all. The highest increase of brain dasatinib concentrations was observed in triple knockout mice that carry the disruption of Abcb1a, Abcb1b and Abcg2 genes**.**

5.3.3 CNS distribution of oral administered dasatinib in WT, triple-knockout, Abcb1 and Abcg1 knockout FVB mice

The brain and plasma concentration-time profiles of dasatinib were determined in wild-type FVB mice that received 10 mg/kg dasatinib orally (Figure 5.4). Both plasma and brain concentrations reached their maximum concentration (Cmax) at 2 hr postdose. Then the effect of pharmacological inhibition of efflux transporters on the brain-to-plasma ratio of dasatinib in wild-type FVB mice at 2 hr postdose was examined (Figure 5.5). The effect of genetic deletion of efflux transporters on the brain distribution of dasatinib in FVB mice at 2 hr post dose was also determined (Figure 5.6). The

genetically deletion or pharmacologically inhibition of both Abcb1 and Abcg2 resulted in significant increase of dasatinib CNS penetration.

The effect of blank vehicle for inhibitors on the brain-to-plasma ratio of dasatinib in wild-type FVB mice was studied. As shown in figure 5.7, there was no significant difference among the B/P ratios in the three groups. The coadministration of blank vehicle for LY335979 or for Ko143 and GF120918 did not change the brain distribution of dasatinib in WT mice.

5.4 Discussion

In vivo CNS distribution of dasatinib in wild-type and efflux transporter(s) knockout mice was examined to further understand the role of efflux transporters in the CNS distribution of dasatinib. In this study, we revealed that the CNS delivery of dasatinib in wild-type FVB mice after i.v. injection was low. The ratios of brain concentration over plasma concentration were less than 0.12 over the time period we studied. Porkka and colleagues showed that on average dasatinib brain concentrations were 5.5% of dasatinib plasma concentration in mice during the absorption phase after oral dosing. In the same study, they also reported that the CSF concentrations of dasatinib in patients at 3 hours after oral dosing were either undetectable or very low (Porkka et al., 2008). The results from both preclinical and clinical reseach all indicated that dasatinib brain penetration is low. Nevertheless, antitumor effect of dasatinib in CNS CML in both preclinical and clinical studies has been observed.(Porkka et al., 2008) In this case, it is very likely due to the advantage of high potency of dasatinib. Dasatinib is approximate

300 fold more potent than imatinib against Bcr-Abl TK, with IC50 in low nanomolar range (O'Hare et al., 2005). Therefore, though the brain dasatinib concentration was low, it was still able to reach the therapeutically effective concentration. However, so far there is no evidence that if this low concentration of dasatinib is enough for the treatment of other diseases, such as glioma.

Transporter gene knockout mouse models are now widely used as useful tools to study the effect of transporters on the pharmacokinetics of drugs (Xia et al., 2007b). In this study, we used 3 transporter gene knockout mouse models: Abcb1a/b knockout [Mdr1a/b (-/-)], Abcg2 knockout [Bcrp1 (-/-)] and triple knockout [Bcrp-Mdr1a/b (-/-)] FVB mice. The difference in dasatinib brain concentrations between wild-type and triple knockout mice was significant while there was no significant difference in dasatinib plasma concentration-time profiles. The ratios of brain concentration over plasma concentration in triple knockout mice were about 10 fold greater when compared with the ratios in wild-type mice (figure 5.1 C). Hence the genetic deletion of both Abcb1 and Abcg2 resulted in significantly enhanced CNS delivery of dasatinib in mice. The role of a single transporter was also examined in our study. Significantly increased dasatinib brain concentrations were observed in Abcb1a/b knockout mice but not Abcg2 knockout mice (figure 5.3).

These results were further confirmed by pharmacological inhibition experiments. Dasatinib brain concentration increased significantly in wild-type mice when the selective Abcb1 inhibitor LY335979 was coadministered, while the selective and potent

Abcg2 inhibitor Ko143 was not able to change dasatinib brain distribution (figure 5.2). The biggest increase in dasatinib brain concentration was observed when mice were treated with dual Abcb1 and Abcg2 inhibitor GF120918.

When only Abcb1 was genetically deleted or pharmacologically inhibited, we observed enhanced CNS delivery of dasatinib. However, enhanced CNS delivery of dasatinib was not observed in our study when only Abcg2 was genetically deleted or pharmacologically inhibited. These results strongly suggested that Abcb1 and Abcg2 play a significant role in the CNS delivery of dasatinib. When the efflux transporters work alone, Abcb1 plays a more important role than Abcg2.

Bihorel et al. reported similar phenomenon with imatinib. In their studies, gene deletion or pharmacological inhibition of Abcb1 did enhance imatinib brain uptake in mice and there was no difference between wild-type and Abcg2 knockout mice. The greatest brain penetration of imatinib was seen in mice with both Abcb1 and Abcg2 blocked (Bihorel et al., 2007a; Bihorel et al., 2007b). Since both dasatinib and imatinib are substrates of Abcb1 and Abcg2, it is very likely that for similar compounds, Abcb1 plays a more important role than Abcg2. When Abcg2 was genetically deleted or pharmacologically inhibited, Abcb1 is able to compensate the effect of Abcg2. Furthermore, when the two transporters work together, there is augmenting effect (i.e., the genetic deletion or pharmacological inhibition of both Abcb1 and Abcg2 has significantly greater effect on dasatinib CNS delivery compared to the genetic deletion or pharmacological inhibition of Abcb1 only). Another compound, topotecan, which is

also a substrate of both Abcb1 and Abcg2, exhibited similar phenomenon in a study reported by deVries and group (DeVries et al., 2008).

Big variations were observed in dasatinib plasma concentrations in mice. Since propylene glycol, which was used to dissolve dasatinib, can cause haemolysis after i.v. injection (Ko et al., 2008), we suspected that haemolysis could be one cause of the variation. Dasatinib was given orally to avoid the haemolysis effect of propylene glycol. However, the variation of dasatinib plasma concentrations in mice that received oral administration was still significant (data not shown). This could be due to other sources of variation that are introduced by oral administration such as absorption and metabolism. In oral studies, we again observed increased dasatinib brain penetration in Abcb1a/b knockout mice and triple knockout mice, but not in Abcg2 knockout mice. Similarly, pharmacological inhibition of Abcb1 or Abcb1 and Abcg2 increased dasatinib brain penetration in WT FVB mice but not the inhibition of Abcg2. These results confirmed that Abcb1 plays a more important role than Abcg2 in the CNS delivery of dasatinib.

The blank vehicles of inhibitors had no significant effect on the brain penetration of dasatinib (figure 5.7). Therefore the change of dasatinib brain concentrations and brain penetration with the coadministration was purely due to the inhibition of specific efflux transporter(s) by the inhibitors.

5.5 Conclusion

In summary, the CNS delivery of dasatinib in mice is low. The genetic deletion or pharmacological inhibition of Abcb1 or Abcb1 and Abcg2 was able to increase dasatinib brain penetration when dasatinib was administrated via i.v. injection or oral. In conclusion, both ABCB1 and ABCG2 play a role in the CNS delivery of dasatinib, limiting dasatinib CNS penetration. The use of potent inhibitors for both ABCB1 and ABCG2 should be able to improve dasatinib CNS delivery. This finding may have direct implications in the treatment of primary and metastatic brain tumors and important implications in dasatinib ADME, and in drug-drug interactions.

5.6 Acknowledgement

We would like to thank Bristol-Myers Squibb Company for kindly providing us dasatinib. We thank Dr. Schinkle from Netherlands Cancer Institute for generously providing us Ko143. We thank Eli Lilly and Co. for kindly providing us LY335979. We thank GlaxoSmithKline for generously providing us GF120918.

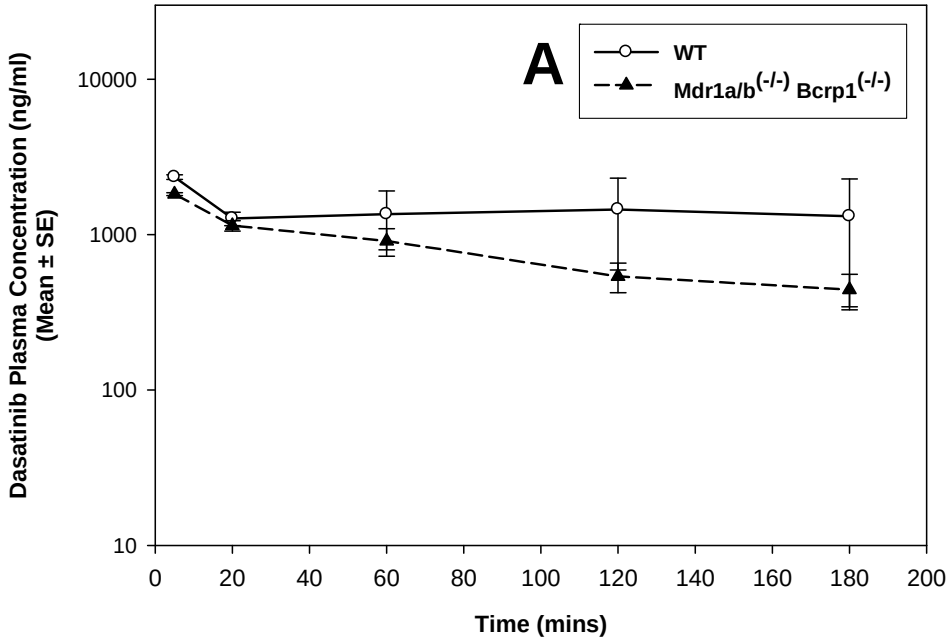
A
WT
Mdr1a/b(-/-) Bcrp1(-/-)
Dasatinib Plasma Concentration (ng/ml)
(Mean ± SE)
10000
1000
100
10
0
20
40
60
80
100
120
140
160
180
200
Time (mins)

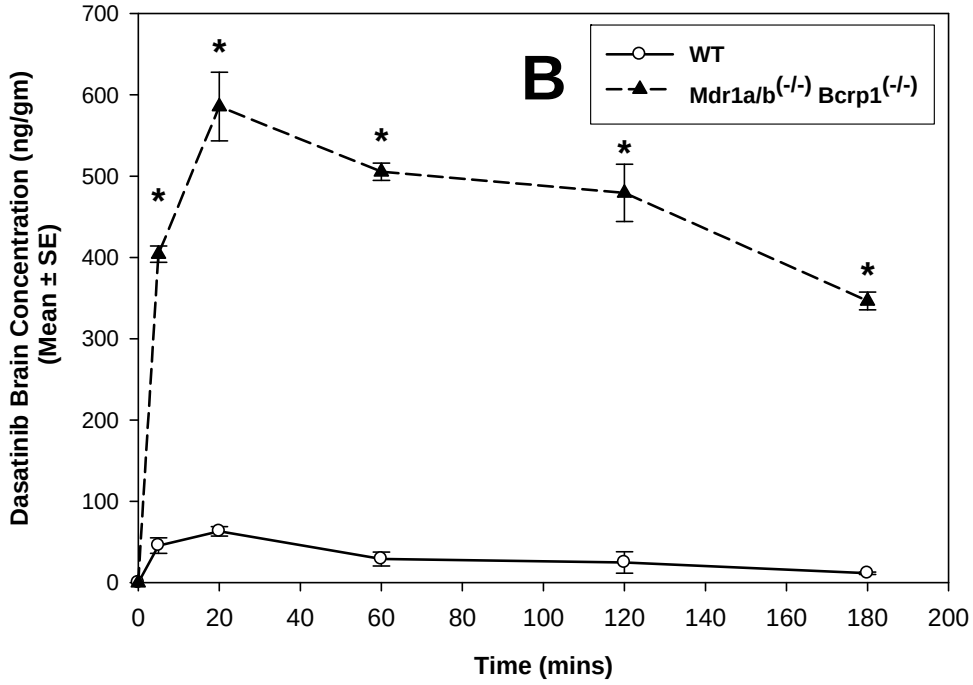
B
WT
Mdr1a/b(-/-) Bcrp1(-/-)
Dasatinib Brain Concentration (ng/gm)
(Mean ± SE)
700
600
500
400
300
200
100
0
*
*
*
*
0
20
40
60
80
100
120
140
160
180
200
Time (mins)

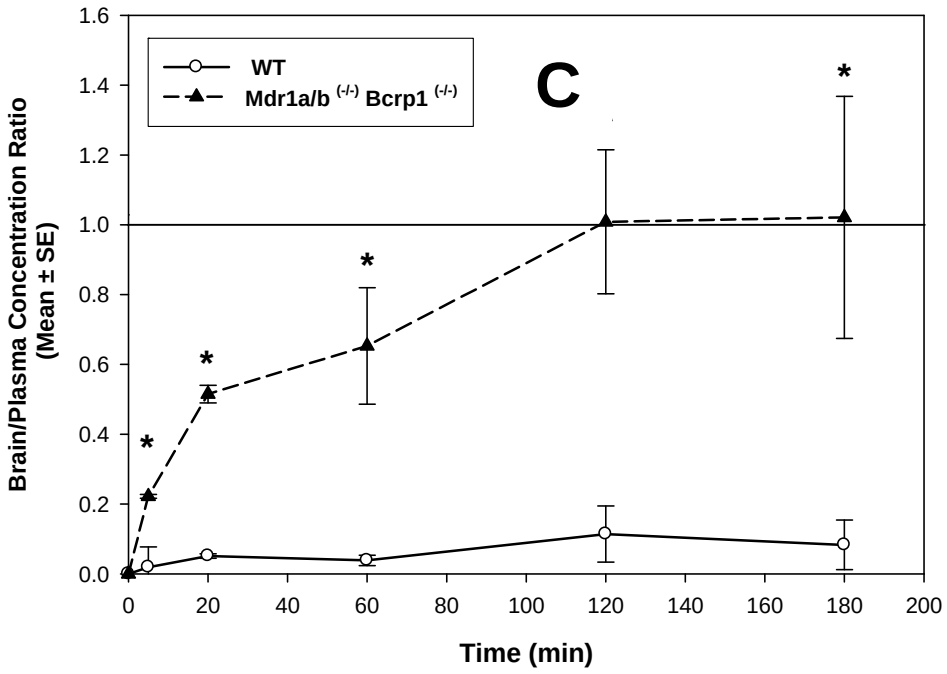

Figure 5.1. Brain distribution of dasatinib in wild-type and triple knockout [Bcrp-Mdr1a/b (-/-)] FVB mice.

The wild-type and triple knockout mice received 5 mg/kg dasatinib via tail vein injection. Plasma and whole brain tissue were collected at different time points (5, 20, 60, 120, 180 min postdose, n=4 at each time point) and analyzed for dasatinib using LC-MS/MS. (A) plasma concentration of dasatinib versus time in wild-type and triple knockout FVB mice. (B) brain concentration of dasatinib versus time in wild-type and triple knockout FVB mice. (C) The brain-to-plasma ratio of dasatinib in wild-type and triple-knockout FVB mice (* $p<0.01$, n=4). Results are presented as mean ± S.E.

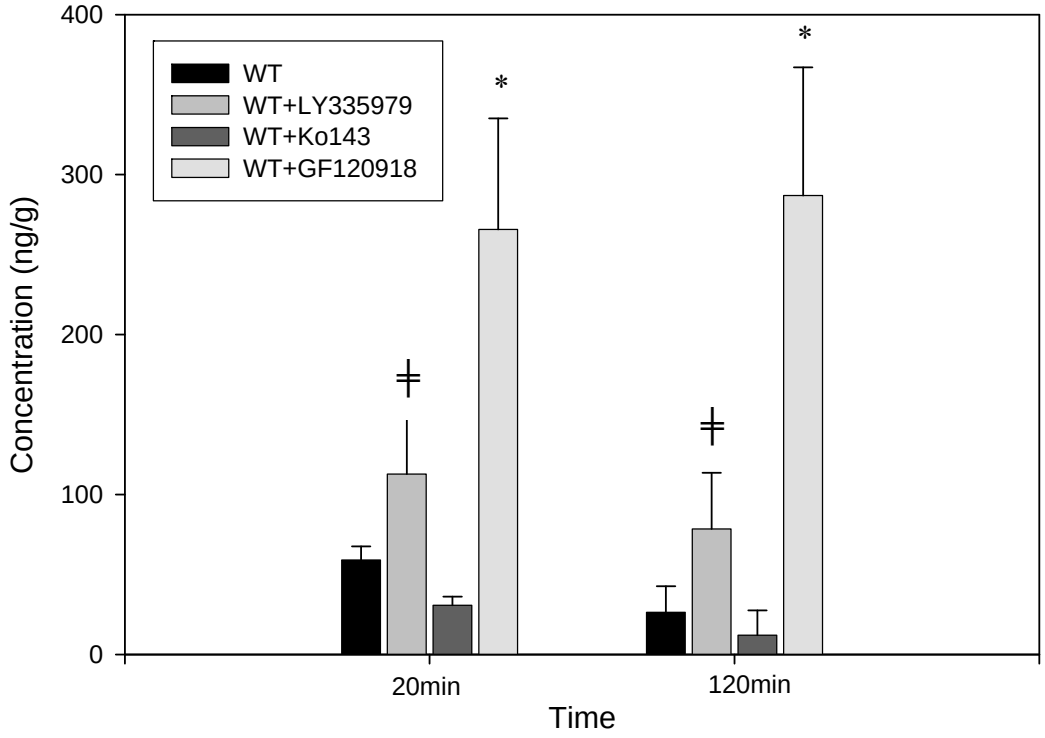

Figure 5.2. Effect of pharmacological inhibition of efflux transporters on the brain distribution of dasatinib in wild-type FVB mice.

The wild-type mice received 5 mg/kg dasatinib via tail vein injection. When inhibitor (25 mg/kg LY335979, 10 mg/kg Ko143 or 10 mg/kg GF10918) was applied, inhibitor solution was given via tail vein injection 30 min before the injection of dasatinib. Whole brain tissue was collected at 2 time points (20, 120 min postdose, n=4 at each time point) and analyzed for dasatinib using LC-MS/MS. The values are presented as mean ± S.D. (*, $p < 0.01$ as ANOVA, ⧺, $p < 0.05$ as two sample t-test).

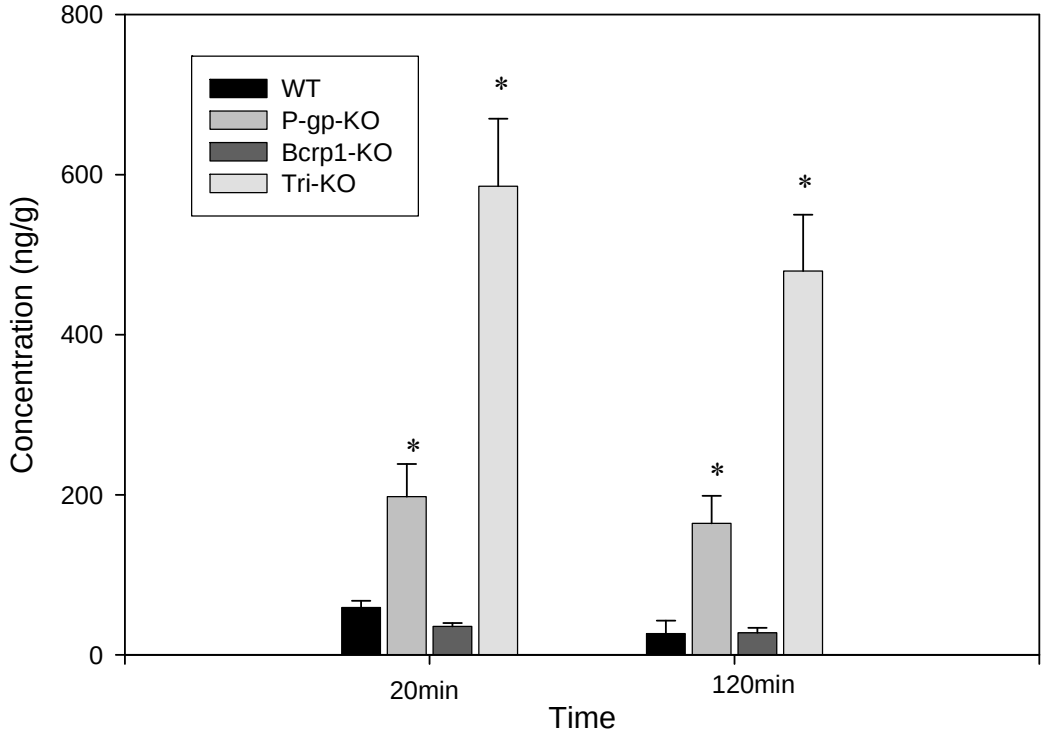

Figure 5.3. Effect of genetic deletion of efflux transporters on the brain distribution of dasatinib in FVB mice.

Wild-type mice, Abcb1a/b knockout and Abcg2 Knockout FVB mice received 5 mg/kg dasatinib via tail vein injection. Whole brain tissue was collected at 2 time points (20, 120 min postdose, n=4 at each time point) and analyzed for dasatinib using LC-MS/MS. The values are presented as mean ± S.D. (*, $p < 0.01$).

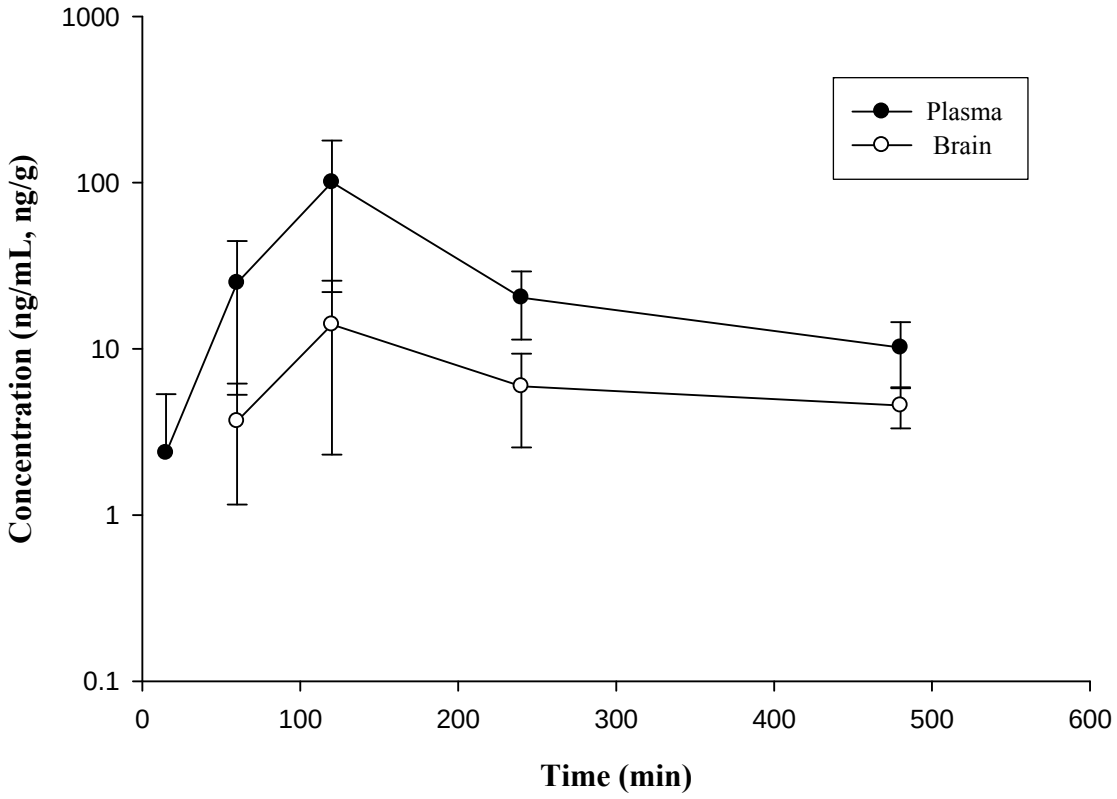

Figure 5.4. Plasma and brain distribution of dasatinib in wild-type FVB mice. Mice received 10 mg/kg dasatinib orally.

Plasma and whole brain tissue were collected at different time points (15, 60, 120, 240, 480 min postdose, n=4 at each time point) and analyzed for dasatinib using LC-MS/MS. Results are presented as mean ± S.D.

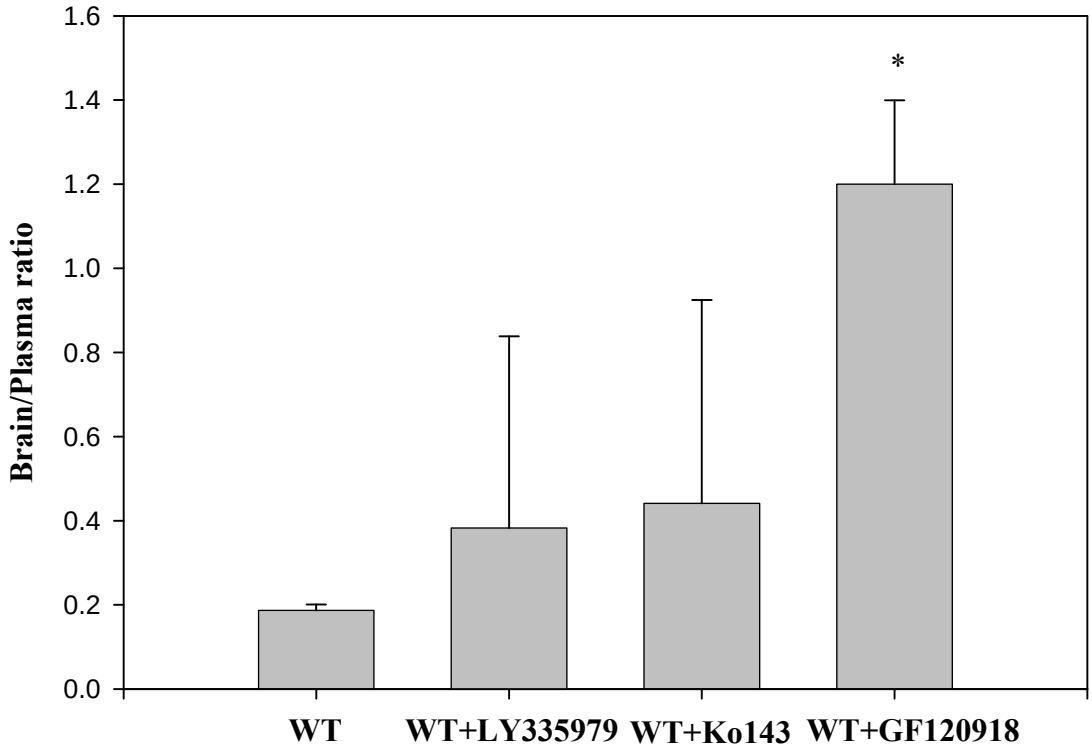

Figure 5.5. Effect of pharmacological inhibition of efflux transporters on the brain-to-plasma ratio of dasatinib in wild-type FVB mice.

The wild-type mice received 10 mg/kg dasatinib orally. When inhibitor (25 mg/kg LY335979, 10 mg/kg Ko143 or 10 mg/kg GF10918) was applied, inhibitor solution was given via tail vein injection 30 min before the dosing of dasatinib. Plasma and whole brain tissue were collected at 120min postdose (n=4) and analyzed for dasatinib using LC-MS/MS. The values are presented as mean ± S.D. (*, $p < 0.01$).

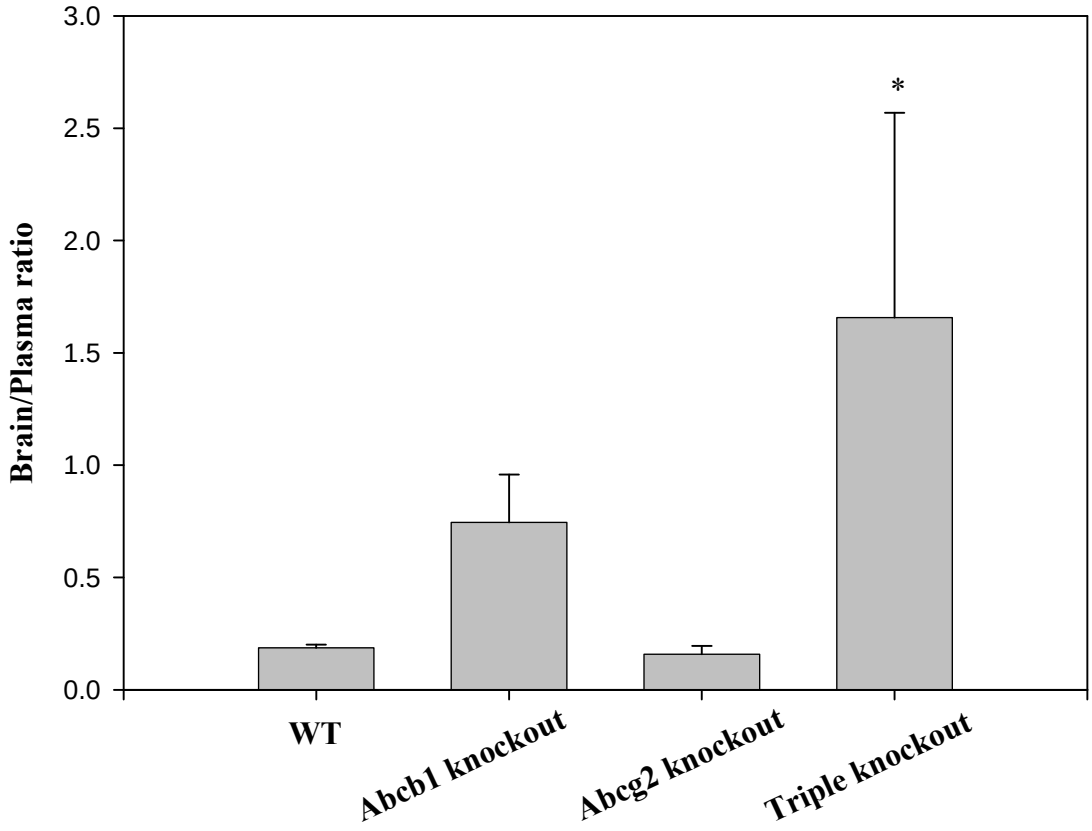

Figure 5.6. Effect of genetic deletion of efflux transporters on the brain-to-plasma ratio of dasatinib in FVB mice.

Wild-type mice, Abcb1a/b knockout and Abcg2 Knockout FVB mice received 10 mg/kg dasatinib via oral gavage. Plasma and whole brain tissue were collected at 120 min postdose (n=4) and analyzed for dasatinib using LC-MS/MS. The values are presented as mean ± S.D. (*, $p < 0.01$).

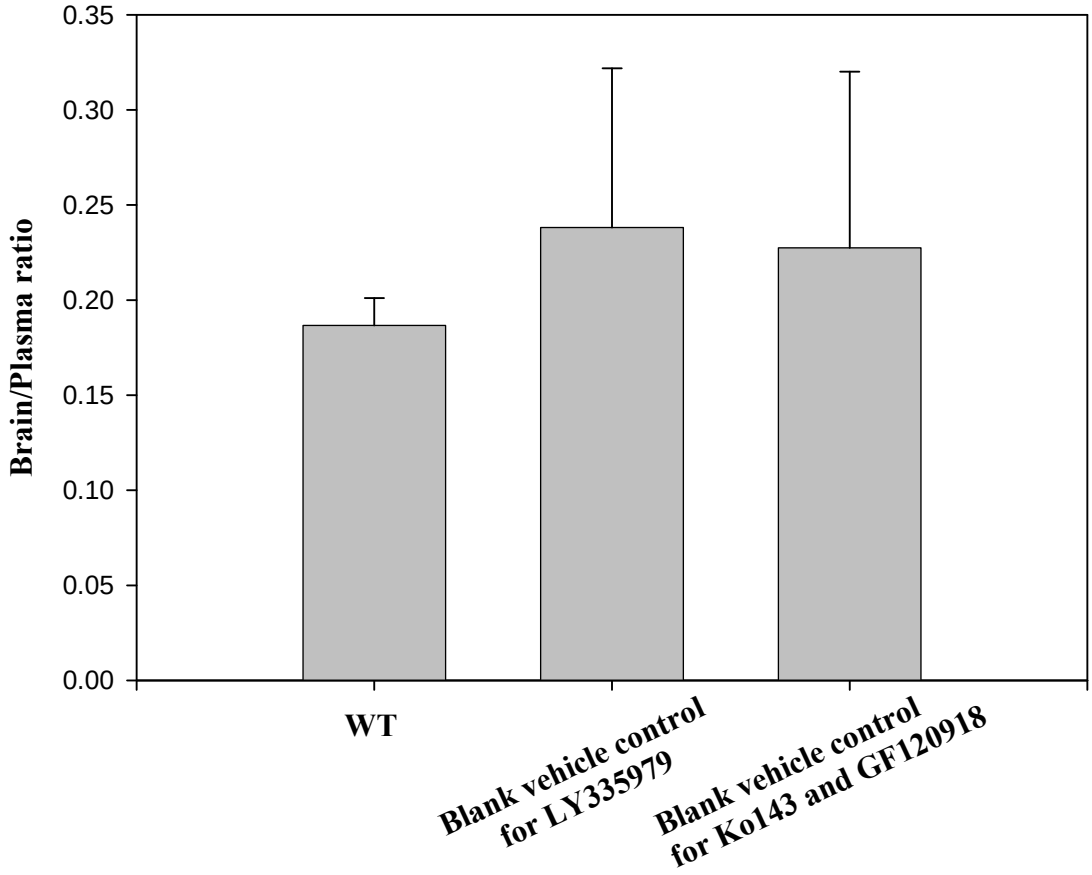

Figure 5.7. Effect of blank vehicle for inhibitors on the brain-to-plasma ratio of dasatinib in wild-type FVB mice.

The wild-type mice received 10 mg/kg dasatinib via oral gavage. When blank vehicle was applied, it was given via tail vein injection 30 min before the dosing of dasatinib. Plasma and whole brain tissue were collected at 120 min postdose (n=4) and analyzed for dasatinib using LC-MS/MS. The values are presented as mean ± S.D.

CHAPTER 6

RECAPITULATION

The rationally designed molecularly targeted tyrosine kinase inhibitors (TKIs) have been shown to clinically inhibit the action of pathogenic tyrosine kinases (TKs). This was one of the most exciting developments in cancer treatment in the past decade. Imatinib (Gleevec, STI571) is a successful example as a first-generation TKI. Imatinib is a small molecule TKI approved as the first line treatment for chronic myelogenous leukemia (CML). However, CNS relapses have been observed in CML patients even though they have shown a complete hematological response to imatinib. An inadequate concentration of imatinib in the CNS makes it a sanctuary for chronic myelogenous leukemia. Dasatinib is a second-generation TKIs that was developed to overcome the molecular resistance to imatinib and is considered as a promising therapyin the treatment of brain tumor. However, little information is known about the CNS delivery of dasatinib. CNS delivery has always been an issue for chemotherapy. Efflux transporter systems in the BBB are an important factor besides the tight junctions that restricts the entry of xenobiotics and toxic metabolites from systemic blood to CNS. Efflux transporters may play a role in limiting the CNS delivery of imatinib and dasatinib, and the inhibition of efflux transporters could potentially result in enhanced CNS delivery of imatinib and dasatinib. The overall aim of the present work was to assess the influence of various drug efflux transporters, such as ABCB1 and ABCG2, on the specific delivery of TKIs to CNS and the possibility of improving CNS delivery of imatinib and dasatinib by effective pharmacological inhibition.

We first studied the interaction between imatinib and Abcg2 by using *in vitro* cell models (chapter 2). The kinetics of cellular accumulation and permeability of imatinib

were studied in MDCKII epithelial cell monolayers, both parental (wild-type) and Abcg2-transfected. The intracellular accumulation of imatinib in the parental cells was significantly greater than that in the Abcg-2 transfected cells. A dual inhibitor of Abcb1 and Abcg2, GF120918, abolished this difference in the intracellular accumulation. The efflux ratio of imatinib in Abcg2-transfected MDCKII cells was 63.03 while the efflux ratio in wild-type cells was 1.77. This difference in directional flux permeability was reduced by Abcg2 inhibiter GF120918 and abolished by a specific Abcg2 inhibiter Ko143. The estimated Km value for the interaction between imatinib and Abcg2 was 3.89 ± 0.44 μM. These *in vitro* data indicated that imatinib is an Abcg2 substrate and the inhibition of Abcg2 will dramatically affect the *in vitro* intracellular accumulation of imatinib in MDCKII cells and the transport of imatinib across MDCKII monolayers. Previous studies from other groups and our group showed that imatinib is a substrate of the efflux transporter Abcb1. In this study, we further demonstrated that LY335979 and GF120918 significantly increased imatinib accumulation in mouse glioma cells by inhibiting Abcb1.

Based on the information gathered from *in vitro* study that imatinib is a substrate of ABCB1 and Abcg2, the effect of these two efflux transporters on the CNS delivery of imatinib was further studied by using an *in vivo* mouse model (chapter 3). The brain penetration of imatinib was low in wild-type FVB mice that received 12.5 mg/kg imatinib as a single bolus via tail vein injection. Increased dosage of imatinib (50 mg/kg) improved its CNS delivery by partially saturating Abcb1 and Abcg2 at BBB. Coadministration of GF120918 was able to increase imatinib CNS delivery by

inhibiting the two efflux transporters at BBB. In summary, ABCB1and ABCG2 together play an important role in limiting the CNS delivery of imatinib. Saturation or inhibition of ABCB1 and ABCG2 could effectively improve CNS delivery of imatinib.

Dasatinib, a promising second generation TKI, was the focus of the second half of this thesis. First, the *in vitro* interaction between dasatinib and ABCB1 and Abcg2 was studied (chapter 4). The cellular accumulation of dasatinib in the wild-type MDCKII cells was significantly lower than that in ABCB1-transfected or Abcg2 transfected MDCKII cells. The ABCB1 specific inhibitor LY 335979 abolished the difference between wild-type and ABCB1-transfected cells and ABCG2 specific inhibitor Ko143 abolished the difference in Abcg2 cells. The efflux ratio of dasatinib in ABCB1-transfected cells was greater than the efflux ratio in wild-type cells and was decreased by LY335979. In Abcg2-transfected cells, the efflux ratio of dasatinib was greater than that in wild-type cells and was decreased by Ko143. These *in vitro* data strongly suggested that dasatinib is a substrate of both ABCB1 and Abcg2. The inhibition of ABCB1 or Abcg2 significantly influences the *in vitro* intracellular accumulation of dasatinib in MDCKII cells and the transport of dasatinib across MDCKII monolayers. We also discovered that OCT-1 might not play a role in the influx of dasatinib. Imatinib and dasatinib interacts with each other and this transporter-mediated drug-drug interaction is important information for the future combination treatment for CML.

Since *in vitro* studies showed that dasatinib is a substrate of ABCB1 and Abcg2, *in vivo* studies were carried out to access the possible influence of these two efflux transporters

on the CNS delivery of dasatinib (chapter 5). The CNS delivery of dasatinib was low in FVB wild-type mice. When Abcb1 and Abcg2 were genetically deleted in triple knockout mice or were pharmacologically inhibited by GF120918 in WT mice, the CNS delivery of dasatinib increased significantly compare to the control WT mice. In Abcb1 knockout mice and WT mice coadministered with LY335979, an increase of dasatinib CNS delivery was also observed. However, the genetic deletion of Abcg2 in Abcg2 knockout mice or the pharmacological inhibition of Abcg2 in WT mice by Ko143 was not able to increase the CNS delivery of dasatinib. Therefore, ABCB1 and ABCG2 play a role in the CNS delivery of dasatinib, limiting dasatinib CNS delivery. ABCB1 plays a more important role than ABCG2 in effecting the CNS delivery of dasatinib. The use of potent inhibitors for both ABCB1 and ABCG2 is able to improve dasatinib CNS delivery.

In conclusion, the overall important findings of the present work are briefly outlined as follows. (1) *In vitro* studies demonstrated that imatinib is a substrate of Abcg2. *In vivo* studies further explored that ABCB1and ABCG2 together play an important role in limiting the CNS delivery of imatinib. Saturation or inhibition of ABCB1 and ABCG2 could effectively improve CNS delivery of imatinib. (2) In *vitro* evidence indicated that dasatinib is a substrate of both ABCB1 and Abcg2. *In vivo* results revealed that the CNS delivery of dasatinib was low. ABCB1 and ABCG2 could be a factor limiting the CNS delivery of dasatinib, with ABCB1 having more influence than ABCG2. Dasatinib CNS delivery can be improved by the use of potent inhibitors for both ABCB1 and ABCG2. These findings significantly contribute to the research being conducted in this

field and are very useful in providing insight into current and new clinical strategies to more effectively use the TKIs for CNS disease treatment and prevention.

Future work in this field would be *in vivo* study to show proof of concept of the role of the drug efflux transporters ABCB1 and ABCG2 in the CNS delivery of imatinib and dasatinib. The specific inhibition of ABCB1 and/or ABCG2 and the resulting changes in the efficacy of imatinib and dasatinib will be studied in *in vitro* tumor models and in the setting of intracerebral brain tumor mouse models. The completion of this study will provide pharmacodynamic information about the contribution of ABCB1 and ABCG2 in influencing the targeted delivery of imatinib and dasatinib to CNS.

BIBLIOGRAPHY

References for Chapter 1

Abruzzese E, Cantonetti M, Morino L, Orlandi G, Tendas A, Del Principe MI, Masi M, Amadori S, Orlandi A, Anemona L and Campione E (2003) CNS and cutaneous involvement in patients with chronic myeloid leukemia treated with imatinib in hematologic complete remission: two case reports. *Journal of Clinical Oncology* 21:4256-4258.

Ali S (2007) Role of c-kit/SCF in cause and treatment of gastrointestinal stromal tumors (GIST). *Gene* 401:38-45.

Allen JD, van Loevezijn A, Lakhai JM, van der Valk M, van Tellingen O, Reid G, Schellens JH, Koomen GJ and Schinkel AH (2002) Potent and specific inhibition of the breast cancer resistance protein multidrug transporter in vitro and in mouse intestine by a novel analogue of fumitremorgin C. *Mol Cancer Ther* 1:417-425.

Alvarez RH, Kantarjian HM and Cortes JE (2006) The role of Src in solid and hematologic malignancies: development of new-generation Src inhibitors. *Cancer* 107:1918-1929.

Bach F, Sorensen JB, Adrian L, Larsen H, Langer SW, Nelausen KM and Engelholm SA (1996) Brain relapses in chemotherapy-treated small cell lung cancer: a retrospective review of two time-dose regimens of therapeutic brain irradiation. *Lung Cancer* 15:171-181.

Bardelmeijer HA, Beijnen JH, Brouwer KR, Rosing H, Nooijen WJ, Schellens JH and van Tellingen O (2000) Increased oral bioavailability of paclitaxel by GF120918 in mice through selective modulation of P-glycoprotein. *Clin Cancer Res* 6:4416-4421.

Baselga J (2006) Targeting tyrosine kinases in cancer: the second wave. *Science* 312:1175-1178.

Baselga J and Hammond LA (2002) HER-targeted tyrosine-kinase inhibitors. *Oncology* 63 Suppl 1:6-16.

Beaulieu E, Demeule M, Ghitescu L and Beliveau R (1997) P-glycoprotein is strongly expressed in the luminal membranes of the endothelium of blood vessels in the brain. *Biochemical Journal* 326:539-544.

Begley DJ (2004a) ABC transporters and the blood-brain barrier. *Curr Pharm Des* 10:1295-1312.

Biswas G, Bhagwat R, Khurana R, Menon H, Prasad N and Parikh PM (2006) Brain metastasis--evidence based management. *Journal of Cancer Research & Therapeutics* 2:5-13.

Blanke CD, Eisenberg BL and Heinrich MC (2001) Gastrointestinal stromal tumors. *Current Treatment Options in Oncology* 2:485-491.

Blume-Jensen P and Hunter T (2001) Oncogenic kinase signalling. *Nature* 411:355-365.

Cooray HC, Blackmore CG, Maskell L and Barrand MA (2002) Localisation of breast cancer resistance protein in microvessel endothelium of human brain. *Neuroreport* 13:2059-2063.

Cordon-Cardo C, O'Brien JP, Casals D, Rittman-Grauer L, Biedler JL, Melamed MR and Bertino JR (1989) Multidrug-resistance gene (P-glycoprotein) is expressed by endothelial cells at blood-brain barrier sites. *Proceedings of the National Academy of Sciences of the United States of America* 86:695-698.

Dantzig AH, Law KL, Cao J and Starling JJ (2001) Reversal of multidrug resistance by the P-glycoprotein modulator, LY335979, from the bench to the clinic. *Curr Med Chem* 8:39-50.

Dantzig AH, Shepard RL, Cao J, Law KL, Ehlhardt WJ, Baughman TM, Bumol TF and Starling JJ (1996) Reversal of P-glycoprotein-mediated multidrug resistance by a potent cyclopropyldibenzosuberane modulator, LY335979. *Cancer Res* 56:4171-4179.

Dantzig AH, Shepard RL, Law KL, Tabas L, Pratt S, Gillespie JS, Binkley SN, Kuhfeld MT, Starling JJ and Wrighton SA (1999) Selectivity of the multidrug resistance modulator, LY335979, for P-glycoprotein and effect on cytochrome P-450 activities. *J Pharmacol Exp Ther* 290:854-862.

de Bruin M, Miyake K, Litman T, Robey R and Bates SE (1999) Reversal of resistance by GF120918 in cell lines expressing the ABC half-transporter, MXR. *Cancer Lett* 146:117-126.

Deininger MW and Druker BJ (2003) Specific targeted therapy of chronic myelogenous leukemia with imatinib. *Pharmacological Reviews* 55:401-423.

Doyle LA and Ross DD (2003) Multidrug resistance mediated by the breast cancer resistance protein BCRP (ABCG2). *Oncogene* 22:7340-7358.

Druker BJ (2003) David A. Karnofsky Award lecture. Imatinib as a paradigm of targeted therapies. *Journal of Clinical Oncology* 21:239s-245s.

Edling CE and Hallberg B (2007) c-Kit--a hematopoietic cell essential receptor tyrosine kinase. *Int J Biochem Cell Biol* 39:1995-1998.

Edwards JE, Brouwer KR and McNamara PJ (2002) GF120918, a P-glycoprotein modulator, increases the concentration of unbound amprenavir in the central nervous system in rats. *Antimicrob Agents Chemother* 46:2284-2286.

Efferth T, Ramirez T, Gebhart E and Halatsch ME (2004) Combination treatment of glioblastoma multiforme cell lines with the anti-malarial artesunate and the epidermal growth factor receptor tyrosine kinase inhibitor OSI-774. *Biochemical Pharmacology* 67:1689-1700.

Evers R, Kool M, Smith AJ, van Deemter L, de Haas M and Borst P (2000) Inhibitory effect of the reversal agents V-104, GF120918 and Pluronic L61 on MDR1 Pgp-, MRP1- and MRP2-mediated transport. *Br J Cancer* 83:366-374.

Fenner MH and Possinger K (2002) Chemotherapy for breast cancer brain metastases. *Onkologie* 25:474-479.

Finn RS (2008) Targeting Src in breast cancer. *Ann Oncol* 19:1379-1386.

Fizazi K (2007) The role of Src in prostate cancer. *Ann Oncol* 18:1765-1773.

Fraering PC, Ye W, LaVoie MJ, Ostaszewski BL, Selkoe DJ, Wolfe MS, (2005) gamma-Secretase substrate selectivity can be modulated directly via interaction with a nucleotide-binding site. *Journal of Biological Chemistry* 280:41987-41996.

Fricker G and Miller DS (2004) Modulation of drug transporters at the blood-brain barrier. *Pharmacology* 70:169-176.

Gaya A, Rees J, Greenstein A and Stebbing J (2002) The use of temozolomide in recurrent malignant gliomas. *Cancer Treatment Reviews* 28:115-120.

Germann UA, Ford PJ, Shlyakhter D, Mason VS and Harding MW (1997) Chemosensitization and drug accumulation effects of VX-710, verapamil, cyclosporin A, MS-209 and GF120918 in multidrug resistant HL60/ADR cells expressing the multidrug resistance-associated protein MRP. *Anticancer Drugs* 8:141-155.

Golden PL and Pollack GM (2003) Blood-brain barrier efflux transport. *Journal of Pharmaceutical Sciences* 92:1739-1753.

Heimberger AB, Learn CA, Archer GE, McLendon RE, Chewning TA, Tuck FL, Pracyk JB, Friedman AH, Friedman HS, Bigner DD and Sampson JH (2002) Brain tumors in mice are susceptible to blockade of epidermal growth factor receptor (EGFR) with the oral, specific, EGFR-tyrosine kinase inhibitor ZD1839 (Iressa). *Clinical Cancer Research* 8:3496-3502.

Heldin CH and Westermark B (1999) Mechanism of action and in vivo role of platelet-derived growth factor. *Physiol Rev* 79:1283-1316.

Hennessy M and Spiers JP (2007) A primer on the mechanics of P-glycoprotein the multidrug transporter. *Pharmacological Research* 55:1-15.

Hernandez-Boluda JC, Cervantes F, Hernandez-Boluda JC and Cervantes F (2002) Imatinib mesylate (Gleevec, Glivec): a new therapy for chronic myeloid leukemia and other malignancies. *Drugs of Today* 38:601-613.

Hyafil F, Vergely C, Du Vignaud P and Grand-Perret T (1993) In vitro and in vivo reversal of multidrug resistance by GF120918, an acridonecarboxamide derivative. *Cancer Res* 53:4595-4602.

Irby RB and Yeatman TJ (2000) Role of Src expression and activation in human cancer. *Oncogene* 19:5636-5642.

Joensuu H, Roberts PJ, Sarlomo-Rikala M, Andersson LC, Tervahartiala P, Tuveson D, Silberman S, Capdeville R, Dimitrijevic S, Druker B and Demetri GD (2001)

Effect of the tyrosine kinase inhibitor STI571 in a patient with a metastatic gastrointestinal stromal tumor. *New England Journal of Medicine* 344:1052-1056.

Johansson Swartling F (2008) Identifying candidate genes involved in brain tumor formation. *Upsala Journal of Medical Sciences* 113:1-38.

Juliano RL and Ling V (1976) A surface glycoprotein modulating drug permeability in Chinese hamster ovary cell mutants. *Biochim Biophys Acta* 455:152-162.

Kilic T, Alberta JA, Zdunek PR, Acar M, Iannarelli P, O'Reilly T, Buchdunger E, Black PM and Stiles CD (2000) Intracranial inhibition of platelet-derived growth factor-mediated glioblastoma cell growth by an orally active kinase inhibitor of the 2-phenylaminopyrimidine class. *Cancer Research* 60:5143-5150.

Kantarjian HM, Talpaz M, Giles F, O'Brien S, Cortes J, (2006) New insights into the pathophysiology of chronic myeloid leukemia and imatinib resistance. *Annals of Internal Medicine* **145**:913-923.

Kuppens IE, Witteveen EO, Jewell RC, Radema SA, Paul EM, Mangum SG, Beijnen JH, Voest EE and Schellens JH (2007) A phase I, randomized, open-label, parallel-cohort, dose-finding study of elacridar (GF120918) and oral topotecan in cancer patients. *Clin Cancer Res* 13:3276-3285.

Lesniak MS and Brem H (2004) Targeted therapy for brain tumours. *Nature Reviews* Drug Discovery. 3:499-508.

Lin NU, Bellon JR and Winer EP (2004) CNS metastases in breast cancer. *Journal of Clinical Oncology* 22:3608-3617.

Lombardo LJ, Lee FY, Chen P, et al. (2004) Discovery of N-(2-chloro-6-methyl-phenyl)-2-(6-(4-(2-hydroxyethyl)- piperazin-1-yl)-2-methylpyrimidin-4-ylamino)thiazole-5-carboxamide (BMS-354825), a dual Src/Abl kinase inhibitor with potent antitumor activity in preclinical assays. *Journal of Medicinal Chemistry* 47:6658-6661.

Loscher W and Potschka H (2005) Drug resistance in brain diseases and the role of drug efflux transporters. *Nature Reviews Neuroscience* 6:591-602.

Lydon NB, Druker BJ, (2004) Lessons learned from the development of imatinib. *Leukemia Research* 28 Suppl 1:S29-38.

Malingre MM, Beijnen JH, Rosing H, Koopman FJ, Jewell RC, Paul EM, Ten Bokkel Huinink WW and Schellens JH (2001) Co-administration of GF120918 significantly increases the systemic exposure to oral paclitaxel in cancer patients. *Br J Cancer* 84:42-47.

Mauro MJ and Druker BJ (2001) STI571: targeting BCR-ABL as therapy for CML. *Oncologist* 6:233-238.

Miettinen M, Lasota J, Miettinen M and Lasota J (2005) KIT (CD117): a review on expression in normal and neoplastic tissues, and mutations and their clinicopathologic correlation. *Applied Immunohistochemistry & Molecular Morphology* 13:205-220.

Miller G (2002) Drug targeting. Breaking down barriers. *Science* 297:1116-1118.

Morschhauser F, Zinzani PL, Burgess M, Sloots L, Bouafia F and Dumontet C (2007) Phase I/II trial of a P-glycoprotein inhibitor, Zosuquidar.3HCl trihydrochloride (LY335979), given orally in combination with the CHOP regimen in patients with non-Hodgkin's lymphoma. *Leuk Lymphoma* 48:708-715.

Motl S, Zhuang Y, Waters CM, Stewart CF, (2006) Pharmacokinetic considerations in the treatment of CNS tumours. *Clinical Pharmacokinetics* 45:871-903.

National Cancer Institute Fact Sheet 7.49 (2006)
(http://www.cancer.gov/cancertopics/factsheet/Therapy/targeted, accessed March 24, 2009)

Netzer WJ, Dou F, Cai D, Veach D, Jean S, Li Y, Bornmann WG, Clarkson B, Xu H, Greengard P, (2003) Gleevec inhibits beta-amyloid production but not Notch cleavage. *Proceedings of the National Academy of Sciences of the United States of America* 100:12444-12449.

Nikolova Z, Peng B, Hubert M, Sieberling M, Keller U, Ho YY, Schran H and Capdeville R (2004) Bioequivalence, safety, and tolerability of imatinib tablets compared with capsules. *Cancer Chemotherapy & Pharmacology* 53:433-438.

Ostman A and Heldin CH (2001) Involvement of platelet-derived growth factor in disease: development of specific antagonists. *Adv Cancer Res* 80:1-38.

Pardridge WM, Oldendorf WH, Cancilla P and Frank HJ (1986) Blood-brain barrier: interface between internal medicine and the brain. *Annals of Internal Medicine* 105:82-95.

Park SI, Zhang J, Phillips KA, Araujo JC, Najjar AM, Volgin AY, Gelovani JG, Kim SJ, Wang Z and Gallick GE (2008) Targeting SRC family kinases inhibits growth and lymph node metastases of prostate cancer in an orthotopic nude mouse model. *Cancer Res* 68:3323-3333.

Peng B, Dutreix C, Mehring G, Hayes MJ, Ben-Am M, Seiberling M, Pokorny R, Capdeville R and Lloyd P (2004) Absolute bioavailability of imatinib (Glivec) orally versus intravenous infusion. *Journal of Clinical Pharmacology* 44:158-162.

Pfeifer H, Wassmann B, Hofmann WK, Komor M, Scheuring U, Bruck P, Binckebanck A, Schleyer E, Gokbuget N, Wolff T, Lubbert M, Leimer L, Gschaidmeier H, Hoelzer D and Ottmann OG (2003) Risk and prognosis of central nervous system leukemia in patients with Philadelphia chromosome-positive acute leukemias treated with imatinib mesylate. *Clinical Cancer Research* 9:4674-4681.

Planting AS, Sonneveld P, van der Gaast A, Sparreboom A, van der Burg ME, Luyten GP, de Leeuw K, de Boer-Dennert M, Wissel PS, Jewell RC, Paul EM, Purvis NB, Jr. and Verweij J (2005) A phase I and pharmacologic study of the MDR converter GF120918 in combination with doxorubicin in patients with advanced solid tumors. *Cancer Chemother Pharmacol* 55:91-99.

Playford MP, Schaller MD, (2004) The interplay between Src and integrins in normal and tumor biology. *Oncogene* 23:7928-7946.

Pottgen C, Eberhardt W and Stuschke M (2004) Prophylactic cranial irradiation in lung cancer. *Curr Treat Options Oncol* 5:43-50.

Quintas-Cardama A, Kantarjian H, Jones D, Nicaise C, O'Brien S, Giles F, Talpaz M, Cortes J, (2007) Dasatinib (BMS-354825) is active in Philadelphia

chromosome-positive chronic myelogenous leukemia after imatinib and nilotinib (AMN107) therapy failure. *Blood* 109:497-499.

Raymond E, Brandes AA, Dittrich C, Fumoleau P, Coudert B, Clement PM, Frenay M, Rampling R, Stupp R, Kros JM, Heinrich MC, Gorlia T, Lacombe D, van den Bent MJ, European Organisation for R, Treatment of Cancer Brain Tumor Group S, (2008) Phase II study of imatinib in patients with recurrent gliomas of various histologies: a European Organisation for Research and Treatment of Cancer Brain Tumor Group Study. *Journal of Clinical Oncology* 26:4659-4665.

Rich JN and Bigner DD (2004) Development of novel targeted therapies in the treatment of malignant glioma. *Nature Reviews* Drug Discovery. 3:430-446.

Robey RW, Honjo Y, Morisaki K, Nadjem TA, Runge S, Risbood M, Poruchynsky MS and Bates SE (2003) Mutations at amino-acid 482 in the ABCG2 gene affect substrate and antagonist specificity. *Br J Cancer* 89:1971-1978.

Roussidis AE, Theocharis AD, Tzanakakis GN and Karamanos NK (2007) The importance of c-Kit and PDGF receptors as potential targets for molecular therapy in breast cancer. *Curr Med Chem* 14:735-743.

Rubin EH, de Alwis DP, Pouliquen I, Green L, Marder P, Lin Y, Musanti R, Grospe SL, Smith SL, Toppmeyer DL, Much J, Kane M, Chaudhary A, Jordan C, Burgess M and Slapak CA (2002) A phase I trial of a potent P-glycoprotein inhibitor, Zosuquidar.3HCl trihydrochloride (LY335979), administered orally in combination with doxorubicin in patients with advanced malignancies. *Clin Cancer Res* 8:3710-3717.

Sandler A, Gordon M, De Alwis DP, Pouliquen I, Green L, Marder P, Chaudhary A, Fife K, Battiato L, Sweeney C, Jordan C, Burgess M and Slapak CA (2004) A Phase I trial of a potent P-glycoprotein inhibitor, zosuquidar trihydrochloride (LY335979), administered intravenously in combination with doxorubicin in patients with advanced malignancy. *Clin Cancer Res* 10:3265-3272.

Sarkadi B, Ozvegy-Laczka C, Nemet K and Varadi A (2004) ABCG2 -- a transporter for all seasons. *FEBS Lett* 567:116-120.

Schinkel AH and Jonker JW (2003) Mammalian drug efflux transporters of the ATP binding cassette (ABC) family: an overview. *Adv Drug Deliv Rev* 55:3-29.

Schittenhelm MM, Shiraga S, Schroeder A, Corbin AS, Griffith D, Lee FY, Bokemeyer C, Deininger MW, Druker BJ and Heinrich MC (2006) Dasatinib (BMS-354825), a dual SRC/ABL kinase inhibitor, inhibits the kinase activity of wild-type, juxtamembrane, and activation loop mutant KIT isoforms associated with human malignancies. *Cancer Research* 66:473-481.

Schlessinger J (2000) Cell signaling by receptor tyrosine kinases. *Cell* 103:211-225.

Shah NP (2007) Medical Management of CML. *Hematology Am Soc Hematol Educ Program* 2007:371-375.

Shepard RL, Cao J, Starling JJ and Dantzig AH (2003) Modulation of P-glycoprotein but not MRP1- or BCRP-mediated drug resistance by LY335979. *Int J Cancer* 103:121-125.

Smith QR (1996) Brain perfusion systems for studies of drug uptake and metabolism in the central nervous system. *Pharmaceutical Biotechnology* 8:285-307.

Starling JJ, Shepard RL, Cao J, Law KL, Norman BH, Kroin JS, Ehlhardt WJ, Baughman TM, Winter MA, Bell MG, Shih C, Gruber J, Elmquist WF and Dantzig AH (1997) Pharmacological characterization of LY335979: a potent cyclopropyldibenzosuberane modulator of P-glycoprotein. *Adv Enzyme Regul* 37:335-347.

Su EJ, Fredriksson L, Geyer M, Folestad E, Cale J, Andrae J, Gao Y, Pietras K, Mann K, Yepes M, Strickland DK, Betsholtz C, Eriksson U, Lawrence DA, (2008) Activation of PDGF-CC by tissue plasminogen activator impairs blood-brain barrier integrity during ischemic stroke. *Nature Medicine* 14:731-737.

Summy JM and Gallick GE (2003) Src family kinases in tumor progression and metastasis. *Cancer Metastasis Rev* 22:337-358.

Sun H, Dai H, Shaik N and Elmquist WF (2003) Drug efflux transporters in the CNS. *Advanced Drug Delivery Reviews* 55:83-105.

Takayama N, Sato N, O'Brien SG, Ikeda Y and Okamoto S (2002) Imatinib mesylate has limited activity against the central nervous system involvement of

Philadelphia chromosome-positive acute lymphoblastic leukaemia due to poor penetration into cerebrospinal fluid. *British Journal of Haematology* 119:106-108.

Talpaz M, Shah NP, Kantarjian H, Donato N, Nicoll J, Paquette R, Cortes J, O'Brien S, Nicaise C, Bleickardt E, Blackwood-Chirchir MA, Iyer V, Chen TT, Huang F, Decillis AP, Sawyers CL, (2006) Dasatinib in imatinib-resistant Philadelphia chromosome-positive leukemias. *New England Journal of Medicine* 354:2531-2541.

Taylor EM (2002) The impact of efflux transporters in the brain on the development of drugs for CNS disorders. *Clinical Pharmacokinetics* 41:81-92.

Tremont-Lukats IW and Gilbert MR (2003) Advances in molecular therapies in patients with brain tumors. *Cancer Control* 10:125-137.

Tsuji A, Terasaki T, Takabatake Y, Tenda Y, Tamai I, Yamashima T, Moritani S, Tsuruo T and Yamashita J (1992) P-glycoprotein as the drug efflux pump in primary cultured bovine brain capillary endothelial cells. *Life Sciences* 51:1427-1437.

Vlahovic G and Crawford J (2003) Activation of tyrosine kinases in cancer. *Oncologist* 8:531-538.

Wolff NC, Richardson JA, Egorin M and Ilaria RL, Jr. (2003) The CNS is a sanctuary for leukemic cells in mice receiving imatinib mesylate for Bcr/Abl-induced leukemia. *Blood* 101:5010-5013.

Xia CQ, Milton MN, Gan LS, (2007) Evaluation of drug-transporter interactions using in vitro and in vivo models. *Current Drug Metabolism* 8:341-363.

Yarden Y, Kuang WJ, Yang-Feng T, Coussens L, Munemitsu S, Dull TJ, Chen E, Schlessinger J, Francke U and Ullrich A (1987) Human proto-oncogene c-kit: a new cell surface receptor tyrosine kinase for an unidentified ligand. *EMBO Journal* 6:3341-3351.

Young AM, Allen CE and Audus KL (2003) Efflux transporters of the human placenta. *Advanced Drug Delivery Reviews* 55:125-132.

References for Chapter 2

Abruzzese E, Cantonetti M, Morino L, Orlandi G, Tendas A, Del Principe MI, Masi M, Amadori S, Orlandi A, Anemona L and Campione E (2003) CNS and cutaneous involvement in patients with chronic myeloid leukemia treated with imatinib in hematologic complete remission: two case reports. *Journal of Clinical Oncology* **21**:4256-4258.

Agarwal S, Jain R, Pal D, Mitra AK, (2007) Functional characterization of peptide transporters in MDCKII-MDR1 cell line as a model for oral absorption studies. *International Journal of Pharmaceutics* **332**:147-152.

Allen JD, van Loevezijn A, Lakhai JM, van der Valk M, van Tellingen O, Reid G, Schellens JH, Koomen GJ, Schinkel AH, (2002) Potent and specific inhibition of the breast cancer resistance protein multidrug transporter in vitro and in mouse intestine by a novel analogue of fumitremorgin C. *Molecular Cancer Therapeutics* **1**:417-425.

Blanke CD, Eisenberg BL and Heinrich MC (2001) Gastrointestinal stromal tumors. *Current Treatment Options in Oncology* **2**:485-491.

Bornhauser M, Jenke A, Freiberg-Richter J, Radke J, Schuler US, Mohr B, Ehninger G and Schleyer E (2004) CNS blast crisis of chronic myelogenous leukemia in a patient with a major cytogenetic response in bone marrow associated with low levels of imatinib mesylate and its N-desmethylated metabolite in cerebral spinal fluid. *Annals of Hematology* **83**:401-402.

Breedveld P, Zelcer N, Pluim D, Sonmezer O, Tibben MM, Beijnen JH, Schinkel AH, van Tellingen O, Borst P and Schellens JH (2004) Mechanism of the pharmacokinetic interaction between methotrexate and benzimidazoles: potential role for breast cancer resistance protein in clinical drug-drug interactions. *Cancer Res* **64**:5804-5811.

Bujassoum S, Rifkind J and Lipton JH (2004) Isolated central nervous system relapse in lymphoid blast crisis chronic myeloid leukemia and acute lymphoblastic leukemia in patients on imatinib therapy. *Leukemia & Lymphoma* **45**:401-403.

Burger H, van Tol H, Boersma AW, Brok M, Wiemer EA, Stoter G and Nooter K (2004) Imatinib mesylate (STI571) is a substrate for the breast cancer resistance protein (BCRP)/ABCG2 drug pump. *Blood* **104**:2940-2942.

Chen L, Wang JM, Xu XP, Gao L, Fei XH, Lou JW and Huang ZX (2003) [The reverse effect on drug-resistance against tyrosine kinase inhibitor STI571 in mdr1 and bcr-abl positive leukemic cells]. *Zhongguo Shi Yan Xue Ye Xue Za Zhi* **11**:600-603.

Cooray HC, Blackmore CG, Maskell L and Barrand MA (2002a) Localisation of breast cancer resistance protein in microvessel endothelium of human brain. *Neuroreport* **13**:2059-2063.

Cordon-Cardo C, O'Brien JP, Casals D, Rittman-Grauer L, Biedler JL, Melamed MR and Bertino JR (1989) Multidrug-resistance gene (P-glycoprotein) is expressed by endothelial cells at blood-brain barrier sites. *Proceedings of the National Academy of Sciences of the United States of America* **86**:695-698.

Dai H, Marbach P, Lemaire M, Hayes M and Elmquist WF (2003) Distribution of STI-571 to the brain is limited by P-glycoprotein-mediated efflux. *Journal of Pharmacology & Experimental Therapeutics* **304**:1085-1092.

Deininger MW and Druker BJ (2003) Specific targeted therapy of chronic myelogenous leukemia with imatinib. *Pharmacological Reviews* **55**:401-423.

Doyle LA, Ross DD, (2003) Multidrug resistance mediated by the breast cancer resistance protein BCRP (ABCG2). *Oncogene* **22**:7340-7358.

Doyle LA, Yang W, Abruzzo LV, Krogmann T, Gao Y, Rishi AK and Ross DD (1998) A multidrug resistance transporter from human MCF-7 breast cancer cells.[erratum appears in Proc Natl Acad Sci U S A 1999 Mar 2;96(5):2569]. *Proceedings of the National Academy of Sciences of the United States of America* **95**:15665-15670.

Druker BJ (2003) David A. Karnofsky Award lecture. Imatinib as a paradigm of targeted therapies. *Journal of Clinical Oncology* **21**:239s-245s.

Friche E, Jensen PB and Nissen NI (1992) Comparison of cyclosporin A and SDZ PSC833 as multidrug-resistance modulators in a daunorubicin-resistant Ehrlich ascites tumor. *Cancer Chemotherapy & Pharmacology* **30**:235-237.

Golden PL and Pollack GM (2003) Blood-brain barrier efflux transport. *J Pharm Sci* **92**:1739-1753.

Houghton PJ, Germain GS, Harwood FC, Schuetz JD, Stewart CF, Buchdunger E and Traxler P (2004a) Imatinib mesylate is a potent inhibitor of the ABCG2 (BCRP) transporter and reverses resistance to topotecan and SN-38 in vitro. *Cancer Res* **64**:2333-2337.

Jonker JW, Smit JW, Brinkhuis RF, Maliepaard M, Beijnen JH, Schellens JH and Schinkel AH (2000) Role of breast cancer resistance protein in the bioavailability and fetal penetration of topotecan. *Journal of the National Cancer Institute* **92**:1651-1656.

Kilic T, Alberta JA, Zdunek PR, Acar M, Iannarelli P, O'Reilly T, Buchdunger E, Black PM and Stiles CD (2000) Intracranial inhibition of platelet-derived growth factor-mediated glioblastoma cell growth by an orally active kinase inhibitor of the 2-phenylaminopyrimidine class. *Cancer Research* **60**:5143-5150.

Leis JF, Stepan DE, Curtin PT, Ford JM, Peng B, Schubach S, Druker BJ and Maziarz RT (2004) Central nervous system failure in patients with chronic myelogenous leukemia lymphoid blast crisis and Philadelphia chromosome positive acute lymphoblastic leukemia treated with imatinib (STI-571). *Leukemia & Lymphoma* **45**:695-698.

Marchetti S, Oostendorp RL, Pluim D, van Eijndhoven M, van Tellingen O, Schinkel AH, Versace R, Beijnen JH, Mazzanti R, Schellens JH, (2007) In vitro transport of gimatecan (7-t-butoxyiminomethylcamptothecin) by breast cancer resistance protein, P-glycoprotein, and multidrug resistance protein 2. *Molecular Cancer Therapeutics* **6**:3307-3313.

Merino V, Jimenez-Torres NV and Merino-Sanjuan M (2004) Relevance of multidrug resistance proteins on the clinical efficacy of cancer therapy. *Current Drug Delivery* **1**:203-212.

Muenster U, Grieshop B, Ickenroth K, Gnoth MJ, (2008) Characterization of substrates and inhibitors for the in vitro assessment of Bcrp mediated drug-drug interactions. *Pharmaceutical Research* **25**:2320-2326.

Neville K, Parise RA, Thompson P, Aleksic A, Egorin MJ, Balis FM, McGuffey L, McCully C, Berg SL and Blaney SM (2004) Plasma and cerebrospinal fluid pharmacokinetics of imatinib after administration to nonhuman primates. *Clinical Cancer Research* **10**:2525-2529.

Nies AT (2007) The role of membrane transporters in drug delivery to brain tumors. *Cancer Letters* **254**:11-29.

Ozvegy-Laczka C, Hegedus T, Varady G, Ujhelly O, Schuetz JD, Varadi A, Keri G, Orfi L, Nemet K and Sarkadi B (2004) High-affinity interaction of tyrosine kinase inhibitors with the ABCG2 multidrug transporter. *Mol Pharmacol* **65**:1485-1495.

Pan G, Elmquist WF, (2007) Mitoxantrone permeability in MDCKII cells is influenced by active influx transport. *Molecular Pharmaceutics* **4**:475-483.

Pavek P, Merino G, Wagenaar E, Bolscher E, Novotna M, Jonker JW and Schinkel AH (2005) Human Breast Cancer Resistance Protein: Interactions with Steroid Drugs, Hormones, the Dietary Carcinogen 2-Amino-1-methyl-6-phenylimidazo(4,5-b)pyridine, and Transport of Cimetidine. *J Pharmacol Exp Ther* **312**:144-152.

Pfeifer H, Wassmann B, Hofmann WK, Komor M, Scheuring U, Bruck P, Binckebanck A, Schleyer E, Gokbuget N, Wolff T, Lubbert M, Leimer L, Gschaidmeier H, Hoelzer D and Ottmann OG (2003) Risk and prognosis of central nervous system leukemia in patients with Philadelphia chromosome-positive acute leukemias treated with imatinib mesylate. *Clinical Cancer Research* **9**:4674-4681.

Rabindran SK, Ross DD, Doyle LA, Yang W and Greenberger LM (2000) Fumitremorgin C reverses multidrug resistance in cells transfected with the breast cancer resistance protein. *Cancer Research* **60**:47-50.

Rajappa S, Uppin SG, Raghunadharao D, Rao IS and Surath A (2004) Isolated central nervous system blast crisis in chronic myeloid leukemia. *Hematological Oncology* **22**:179-181.

Schinkel AH, Jonker JW, (2003) Mammalian drug efflux transporters of the ATP binding cassette (ABC) family: an overview. *Advanced Drug Delivery Reviews* **55**:3-29.

Sun H, Dai H, Shaik N and Elmquist WF (2003) Drug efflux transporters in the CNS. *Advanced Drug Delivery Reviews* **55**:83-105.

Takayama N, Sato N, O'Brien SG, Ikeda Y and Okamoto S (2002) Imatinib mesylate has limited activity against the central nervous system involvement of Philadelphia chromosome-positive acute lymphoblastic leukaemia due to poor penetration into cerebrospinal fluid. *British Journal of Haematology* **119**:106-108.

Wang Q, Rager JD, Weinstein K, Kardos PS, Dobson GL, Li J, Hidalgo IJ, (2005) Evaluation of the MDR-MDCK cell line as a permeability screen for the blood-brain barrier. *International Journal of Pharmaceutics* **288**:349-359.

Xia CQ, Liu N, Miwa GT, Gan LS, (2007a) Interactions of cyclosporin a with breast cancer resistance protein. *Drug Metabolism & Disposition* **35**:576-582.

Xia CQ, Milton MN, Gan LS, (2007b) Evaluation of drug-transporter interactions using in vitro and in vivo models. *Current Drug Metabolism* **8**:341-363.

References for Chapter 3

Abruzzese E, Cantonetti M, Morino L, Orlandi G, Tendas A, Del Principe MI, Masi M, Amadori S, Orlandi A, Anemona L and Campione E (2003) CNS and cutaneous involvement in patients with chronic myeloid leukemia treated with imatinib in hematologic complete remission: two case reports. *Journal of Clinical Oncology* 21:4256-4258.

Bihorel S, Camenisch G, Lemaire M and Scherrmann JM (2007) Modulation of the brain distribution of imatinib and its metabolites in mice by valspodar, zosuquidar and elacridar. *Pharm Res* 24:1720-1728.

Bornhauser M, Jenke A, Freiberg-Richter J, Radke J, Schuler US, Mohr B, Ehninger G and Schleyer E (2004) CNS blast crisis of chronic myelogenous leukemia in a patient with a major cytogenetic response in bone marrow associated with low levels of imatinib mesylate and its N-desmethylated metabolite in cerebral spinal fluid. *Annals of Hematology* 83:401-402.

Breedveld P, Pluim D, Cipriani G, Wielinga P, van Tellingen O, Schinkel AH and Schellens JH (2005) The effect of Bcrp1 (Abcg2) on the in vivo pharmacokinetics and brain penetration of imatinib mesylate (Gleevec): implications for the use of breast cancer resistance protein and P-glycoprotein inhibitors to enable the brain penetration of imatinib in patients. *Cancer Res* 65:2577-2582.

Bujassoum S, Rifkind J and Lipton JH (2004) Isolated central nervous system relapse in lymphoid blast crisis chronic myeloid leukemia and acute lymphoblastic leukemia in patients on imatinib therapy. *Leukemia & Lymphoma* 45:401-403.

Burger H, van Tol H, Boersma AW, Brok M, Wiemer EA, Stoter G and Nooter K (2004) Imatinib mesylate (STI571) is a substrate for the breast cancer resistance protein (BCRP)/ABCG2 drug pump. *Blood* 104:2940-2942.

Dai H, Marbach P, Lemaire M, Hayes M and Elmquist WF (2003) Distribution of STI-571 to the brain is limited by P-glycoprotein-mediated efflux. *Journal of Pharmacology & Experimental Therapeutics* 304:1085-1092.

Druker BJ (2003) David A. Karnofsky Award lecture. Imatinib as a paradigm of targeted therapies. *Journal of Clinical Oncology* 21:239s-245s.

Gambacorti-Passerini C, Zucchetti M, Russo D, Frapolli R, Verga M, Bungaro S, Tornaghi L, Rossi F, Pioltelli P, Pogliani E, Alberti D, Corneo G, D'Incalci M, (2003) Alpha1 acid glycoprotein binds to imatinib (STI571) and substantially alters its pharmacokinetics in chronic myeloid leukemia patients. *Clinical Cancer Research* 9:625-632.

Golden PL and Pollack GM (2003) Blood-brain barrier efflux transport. *J Pharm Sci* 92:1739-1753.

Kilic T, Alberta JA, Zdunek PR, Acar M, Iannarelli P, O'Reilly T, Buchdunger E, Black PM and Stiles CD (2000) Intracranial inhibition of platelet-derived growth factor-mediated glioblastoma cell growth by an orally active kinase inhibitor of the 2-phenylaminopyrimidine class. *Cancer Research* 60:5143-5150.

Kretz O, Weiss HM, Schumacher MM, Gross G, (2004) In vitro blood distribution and plasma protein binding of the tyrosine kinase inhibitor imatinib and its active metabolite, CGP74588, in rat, mouse, dog, monkey, healthy humans and patients with acute lymphatic leukaemia. *British Journal of Clinical Pharmacology* 58:212-216.

Leis JF, Stepan DE, Curtin PT, Ford JM, Peng B, Schubach S, Druker BJ and Maziarz RT (2004) Central nervous system failure in patients with chronic myelogenous leukemia lymphoid blast crisis and Philadelphia chromosome positive acute lymphoblastic leukemia treated with imatinib (STI-571). *Leukemia & Lymphoma* 45:695-698.

Mahon FX, Belloc F, Lagarde V, Chollet C, Moreau-Gaudry F, Reiffers J, Goldman JM, Melo JV, (2003) MDR1 gene overexpression confers resistance to imatinib mesylate in leukemia cell line models.[see comment]. *Blood* 101:2368-2373.

Motl S, Zhuang Y, Waters CM, Stewart CF, (2006) Pharmacokinetic considerations in the treatment of CNS tumours. *Clinical Pharmacokinetics* 45:871-903.

Neville K, Parise RA, Thompson P, Aleksic A, Egorin MJ, Balis FM, McGuffey L, McCully C, Berg SL and Blaney SM (2004) Plasma and cerebrospinal fluid

pharmacokinetics of imatinib after administration to nonhuman primates. *Clinical Cancer Research* 10:2525-2529.

Ozvegy-Laczka C, Hegedus T, Varady G, Ujhelly O, Schuetz JD, Varadi A, Keri G, Orfi L, Nemet K and Sarkadi B (2004) High-affinity interaction of tyrosine kinase inhibitors with the ABCG2 multidrug transporter. *Mol Pharmacol* 65:1485-1495.

Pfeifer H, Wassmann B, Hofmann WK, Komor M, Scheuring U, Bruck P, Binckebanck A, Schleyer E, Gokbuget N, Wolff T, Lubbert M, Leimer L, Gschaidmeier H, Hoelzer D and Ottmann OG (2003) Risk and prognosis of central nervous system leukemia in patients with Philadelphia chromosome-positive acute leukemias treated with imatinib mesylate. *Clinical Cancer Research* 9:4674-4681.

Rajappa S, Uppin SG, Raghunadharao D, Rao IS and Surath A (2004) Isolated central nervous system blast crisis in chronic myeloid leukemia. *Hematological Oncology* 22:179-181.

Raymond E, Brandes AA, Dittrich C, et al (2008) Phase II study of imatinib in patients with recurrent gliomas of various histologies: a European Organisation for Research and Treatment of Cancer Brain Tumor Group Study. *Journal of Clinical Oncology* 26:4659-4665.

Schinkel AH, Smit JJ, van Tellingen O, Beijnen JH, Wagenaar E, van Deemter L, Mol CA, van der Valk MA, Robanus-Maandag EC, te Riele HP and et al. (1994) Disruption of the mouse mdr1a P-glycoprotein gene leads to a deficiency in the blood-brain barrier and to increased sensitivity to drugs. *Cell* 77:491-502.

Takayama N, Sato N, O'Brien SG, Ikeda Y and Okamoto S (2002) Imatinib mesylate has limited activity against the central nervous system involvement of Philadelphia chromosome-positive acute lymphoblastic leukaemia due to poor penetration into cerebrospinal fluid. *British Journal of Haematology* 119:106-108.

Toffoli G, Corona G, Gigante M and Boiocchi M (1996) Inhibition of Pgp activity and cell cycle-dependent chemosensitivity to doxorubicin in the multidrug-resistant

LoVo human colon cancer cell line. *European Journal of Cancer* 32A:1591-1597.

References for Chapter 4

Abruzzese E, Cantonetti M, Morino L, Orlandi G, Tendas A, Del Principe MI, Masi M, Amadori S, Orlandi A, Anemona L and Campione E (2003) CNS and cutaneous involvement in patients with chronic myeloid leukemia treated with imatinib in hematologic complete remission: two case reports. *Journal of Clinical Oncology* **21**:4256-4258.

Baccarani M, Saglio G, Goldman J, Hochhaus A, Simonsson B, Appelbaum F, Apperley J, Cervantes F, Cortes J, Deininger M, Gratwohl A, Guilhot F, Horowitz M, Hughes T, Kantarjian H, Larson R, Niederwieser D, Silver R, Hehlmann R, European L (2006) Evolving concepts in the management of chronic myeloid leukemia: recommendations from an expert panel on behalf of the European LeukemiaNet. *Blood* **108**:1809-1820.

Baselga J (2006) Targeting tyrosine kinases in cancer: the second wave. *Science* **312**:1175-1178.

Bihorel S, Camenisch G, Lemaire M and Scherrmann JM (2007) Modulation of the brain distribution of imatinib and its metabolites in mice by valspodar, zosuquidar and elacridar. *Pharm Res* **24**:1720-1728.

Bornhauser M, Jenke A, Freiberg-Richter J, Radke J, Schuler US, Mohr B, Ehninger G and Schleyer E (2004) CNS blast crisis of chronic myelogenous leukemia in a patient with a major cytogenetic response in bone marrow associated with low levels of imatinib mesylate and its N-desmethylated metabolite in cerebral spinal fluid. *Annals of Hematology* **83**:401-402.

Breedveld P, Pluim D, Cipriani G, Wielinga P, van Tellingen O, Schinkel AH and Schellens JH (2005) The effect of Bcrp1 (Abcg2) on the in vivo pharmacokinetics and brain penetration of imatinib mesylate (Gleevec): implications for the use of breast cancer resistance protein and P-glycoprotein inhibitors to enable the brain penetration of imatinib in patients. *Cancer Res* **65**:2577-2582.

Bujassoum S, Rifkind J and Lipton JH (2004) Isolated central nervous system relapse in lymphoid blast crisis chronic myeloid leukemia and acute lymphoblastic leukemia in patients on imatinib therapy. *Leukemia & Lymphoma* **45**:401-403.

Dai H, Marbach P, Lemaire M, Hayes M and Elmquist WF (2003) Distribution of STI-571 to the brain is limited by P-glycoprotein-mediated efflux. *Journal of Pharmacology & Experimental Therapeutics* **304**:1085-1092.

Druker BJ (2003) David A. Karnofsky Award lecture. Imatinib as a paradigm of targeted therapies. *Journal of Clinical Oncology* **21**:239s-245s.

Druker BJ, Guilhot F, O'Brien SG, Gathmann I, Kantarjian H, Gattermann N, Deininger MW, Silver RT, Goldman JM, Stone RM, Cervantes F, Hochhaus A, Powell BL, Gabrilove JL, Rousselot P, Reiffers J, Cornelissen JJ, Hughes T, Agis H, Fischer T, Verhoef G, Shepherd J, Saglio G, Gratwohl A, Nielsen JL, Radich JP, Simonsson B, Taylor K, Baccarani M, So C, Letvak L, Larson RA, Investigators I, (2006) Five-year follow-up of patients receiving imatinib for chronic myeloid leukemia. *New England Journal of Medicine* **355**:2408-2417.

Giannoudis A, Davies A, Lucas CM, Harris RJ, Pirmohamed M and Clark RE (2008) Effective dasatinib uptake may occur without human organic Cation Transporter 1 (hOCT1): implications for the treatment of imatinib resistant chronic myeloid leukaemia. *Blood*.

Giles FJ, DeAngelo DJ, Baccarani M, Deininger M, Guilhot F, Hughes T, Mauro M, Radich J, Ottmann O, Cortes J, (2008) Optimizing outcomes for patients with advanced disease in chronic myelogenous leukemia. *Seminars in Oncology* **35**:S1-17; quiz S18-20.

Goh LB, Spears KJ, Yao D, Ayrton A, Morgan P, Roland Wolf C, Friedberg T, (2002) Endogenous drug transporters in in vitro and in vivo models for the prediction of drug disposition in man. *Biochemical Pharmacology* **64**:1569-1578.

Gora-Tybor J, Robak T, (2008) Targeted drugs in chronic myeloid leukemia. *Current Medicinal Chemistry* **15**:3036-3051.

Hiwase DK, Saunders V, Hewett D, Frede A, Zrim S, Dang P, Eadie L, To LB, Melo J, Kumar S, Hughes TP and White DL (2008) Dasatinib cellular uptake and efflux

in chronic myeloid leukemia cells: therapeutic implications. *Clin Cancer Res* **14**:3881-3888.

Jabbour E, Cortes JE, Ghanem H, O'Brien S, Kantarjian HM, (2008) Targeted therapy in chronic myeloid leukemia. *Expert Review of Anticancer Therapy* **8**:99-110.

Jonker JW, Schinkel AH, (2004) Pharmacological and physiological functions of the polyspecific organic cation transporters: OCT1, 2, and 3 (SLC22A1-3). *Journal of Pharmacology & Experimental Therapeutics* **308**:2-9.

Kantarjian HM, Talpaz M, Giles F, O'Brien S, Cortes J (2006) New insights into the pathophysiology of chronic myeloid leukemia and imatinib resistance. *Annals of Internal Medicine* **145**:913-923.

Koepsell H, Lips K, Volk C, (2007) Polyspecific organic cation transporters: structure, function, physiological roles, and biopharmaceutical implications. *Pharmaceutical Research* **24**:1227-1251.

Lee F, Fandi A, Voi M, (2008) Overcoming kinase resistance in chronic myeloid leukemia. *International Journal of Biochemistry & Cell Biology* **40**:334-343.

Leis JF, Stepan DE, Curtin PT, Ford JM, Peng B, Schubach S, Druker BJ and Maziarz RT (2004) Central nervous system failure in patients with chronic myelogenous leukemia lymphoid blast crisis and Philadelphia chromosome positive acute lymphoblastic leukemia treated with imatinib (STI-571). *Leukemia & Lymphoma* **45**:695-698.

Neville K, Parise RA, Thompson P, Aleksic A, Egorin MJ, Balis FM, McGuffey L, McCully C, Berg SL and Blaney SM (2004) Plasma and cerebrospinal fluid pharmacokinetics of imatinib after administration to nonhuman primates. *Clinical Cancer Research* **10**:2525-2529.

Pfeifer H, Wassmann B, Hofmann WK, Komor M, Scheuring U, Bruck P, Binckebanck A, Schleyer E, Gokbuget N, Wolff T, Lubbert M, Leimer L, Gschaidmeier H, Hoelzer D and Ottmann OG (2003) Risk and prognosis of central nervous system leukemia in patients with Philadelphia chromosome-positive acute leukemias treated with imatinib mesylate. *Clinical Cancer Research* **9**:4674-4681.

Rajappa S, Uppin SG, Raghunadharao D, Rao IS and Surath A (2004) Isolated central nervous system blast crisis in chronic myeloid leukemia. *Hematological Oncology* **22**:179-181.

Schittenhelm MM, Shiraga S, Schroeder A, Corbin AS, Griffith D, Lee FY, Bokemeyer C, Deininger MW, Druker BJ and Heinrich MC (2006) Dasatinib (BMS-354825), a dual SRC/ABL kinase inhibitor, inhibits the kinase activity of wild-type, juxtamembrane, and activation loop mutant KIT isoforms associated with human malignancies. *Cancer Research* **66**:473-481.

Shah NP (2007) Medical Management of CML. *Hematology Am Soc Hematol Educ Program* **2007**:371-375.

Shah NP, Skaggs BJ, Branford S, Hughes TP, Nicoll JM, Paquette RL, Sawyers CL, (2007) Sequential ABL kinase inhibitor therapy selects for compound drug-resistant BCR-ABL mutations with altered oncogenic potency. *Journal of Clinical Investigation* **117**:2562-2569.

Takayama N, Sato N, O'Brien SG, Ikeda Y and Okamoto S (2002) Imatinib mesylate has limited activity against the central nervous system involvement of Philadelphia chromosome-positive acute lymphoblastic leukaemia due to poor penetration into cerebrospinal fluid. *British Journal of Haematology* **119**:106-108.

Thomas J, Wang L, Clark RE, Pirmohamed M, (2004) Active transport of imatinib into and out of cells: implications for drug resistance.[see comment]. *Blood* **104**:3739-3745.

White DL, Saunders VA, Dang P, Engler J, Zannettino ACW, Cambareri AC, Quinn SR, Manley PW and Hughes T (2006) OCT-1-mediated influx is a key determinant of the intracellular uptake of imatinib but not nilotinib (AMN107): reduced OCT-1 activity is the cause of low in vitro sesitivity to imatinib. *Blood* **108**:697-704.

Wright SH (2005) Role of organic cation transporters in the renal handling of therapeutic agents and xenobiotics. *Toxicology & Applied Pharmacology* **204**:309-319.

References for Chapter 5

Abruzzese E, Cantonetti M, Morino L, Orlandi G, Tendas A, Del Principe MI, Masi M, Amadori S, Orlandi A, Anemona L and Campione E (2003) CNS and cutaneous involvement in patients with chronic myeloid leukemia treated with imatinib in hematologic complete remission: two case reports. *Journal of Clinical Oncology* **21**:4256-4258.

Agarwal S, Jain R, Pal D, Mitra AK, (2007) Functional characterization of peptide transporters in MDCKII-MDR1 cell line as a model for oral absorption studies. *International Journal of Pharmaceutics* **332**:147-152.

Ali S (2007) Role of c-kit/SCF in cause and treatment of gastrointestinal stromal tumors (GIST). *Gene* **401**:38-45.

Allen JD, van Loevezijn A, Lakhai JM, van der Valk M, van Tellingen O, Reid G, Schellens JH, Koomen GJ and Schinkel AH (2002a) Potent and specific inhibition of the breast cancer resistance protein multidrug transporter in vitro and in mouse intestine by a novel analogue of fumitremorgin C. *Mol Cancer Ther* **1**:417-425.

Alvarez RH, Kantarjian HM and Cortes JE (2006) The role of Src in solid and hematologic malignancies: development of new-generation Src inhibitors. *Cancer* **107**:1918-1929.

Baccarani M, Saglio G, Goldman J, Hochhaus A, Simonsson B, Appelbaum F, Apperley J, Cervantes F, Cortes J, Deininger M, Gratwohl A, Guilhot F, Horowitz M, Hughes T, Kantarjian H, Larson R, Niederwieser D, Silver R, Hehlmann R, European L, (2006) Evolving concepts in the management of chronic myeloid leukemia: recommendations from an expert panel on behalf of the European LeukemiaNet. *Blood* **108**:1809-1820.

Bach F, Sorensen JB, Adrian L, Larsen H, Langer SW, Nelausen KM and Engelholm SA (1996) Brain relapses in chemotherapy-treated small cell lung cancer: a retrospective review of two time-dose regimens of therapeutic brain irradiation. *Lung Cancer* **15**:171-181.

Bardelmeijer HA, Beijnen JH, Brouwer KR, Rosing H, Nooijen WJ, Schellens JH and van Tellingen O (2000) Increased oral bioavailability of paclitaxel by GF120918 in mice through selective modulation of P-glycoprotein. *Clin Cancer Res* **6**:4416-4421.

Baselga J (2006) Targeting tyrosine kinases in cancer: the second wave. *Science* **312**:1175-1178.

Baselga J and Hammond LA (2002) HER-targeted tyrosine-kinase inhibitors. *Oncology* **63 Suppl 1**:6-16.

Beaulieu E, Demeule M, Ghitescu L and Beliveau R (1997) P-glycoprotein is strongly expressed in the luminal membranes of the endothelium of blood vessels in the brain. *Biochemical Journal* **326**:539-544.

Begley DJ (2004a) ABC transporters and the blood-brain barrier. *Curr Pharm Des* **10**:1295-1312.

Bihorel S, Camenisch G, Lemaire M and Scherrmann JM (2007a) Influence of breast cancer resistance protein (Abcg2) and p-glycoprotein (Abcb1a) on the transport of imatinib mesylate (Gleevec) across the mouse blood-brain barrier. *J Neurochem* **102**:1749-1757.

Bihorel S, Camenisch G, Lemaire M and Scherrmann JM (2007b) Modulation of the brain distribution of imatinib and its metabolites in mice by valspodar, zosuquidar and elacridar. *Pharm Res* **24**:1720-1728.

Biswas G, Bhagwat R, Khurana R, Menon H, Prasad N and Parikh PM (2006) Brain metastasis--evidence based management. *Journal of Cancer Research & Therapeutics* **2**:5-13.

Blanke CD, Eisenberg BL and Heinrich MC (2001) Gastrointestinal stromal tumors. *Current Treatment Options in Oncology* **2**:485-491.

Blume-Jensen P and Hunter T (2001) Oncogenic kinase signalling. *Nature* **411**:355-365.

Bornhauser M, Jenke A, Freiberg-Richter J, Radke J, Schuler US, Mohr B, Ehninger G and Schleyer E (2004) CNS blast crisis of chronic myelogenous leukemia in a patient with a major cytogenetic response in bone marrow associated with low

levels of imatinib mesylate and its N-desmethylated metabolite in cerebral spinal fluid. *Annals of Hematology* **83**:401-402.

Breedveld P, Pluim D, Cipriani G, Wielinga P, van Tellingen O, Schinkel AH and Schellens JH (2005) The effect of Bcrp1 (Abcg2) on the in vivo pharmacokinetics and brain penetration of imatinib mesylate (Gleevec): implications for the use of breast cancer resistance protein and P-glycoprotein inhibitors to enable the brain penetration of imatinib in patients. *Cancer Res* **65**:2577-2582.

Breedveld P, Zelcer N, Pluim D, Sonmezer O, Tibben MM, Beijnen JH, Schinkel AH, van Tellingen O, Borst P and Schellens JH (2004) Mechanism of the pharmacokinetic interaction between methotrexate and benzimidazoles: potential role for breast cancer resistance protein in clinical drug-drug interactions. *Cancer Res* **64**:5804-5811.

Bujassoum S, Rifkind J and Lipton JH (2004) Isolated central nervous system relapse in lymphoid blast crisis chronic myeloid leukemia and acute lymphoblastic leukemia in patients on imatinib therapy. *Leukemia & Lymphoma* **45**:401-403.

Burger H, van Tol H, Boersma AW, Brok M, Wiemer EA, Stoter G and Nooter K (2004) Imatinib mesylate (STI571) is a substrate for the breast cancer resistance protein (BCRP)/ABCG2 drug pump. *Blood* **104**:2940-2942.

Chen L, Wang JM, Xu XP, Gao L, Fei XH, Lou JW and Huang ZX (2003) [The reverse effect on drug-resistance against tyrosine kinase inhibitor STI571 in mdr1 and bcr-abl positive leukemic cells]. *Zhongguo Shi Yan Xue Ye Xue Za Zhi* **11**:600-603.

Cooray HC, Blackmore CG, Maskell L and Barrand MA (2002a) Localisation of breast cancer resistance protein in microvessel endothelium of human brain. *Neuroreport* **13**:2059-2063.

Cordon-Cardo C, O'Brien JP, Casals D, Rittman-Grauer L, Biedler JL, Melamed MR and Bertino JR (1989) Multidrug-resistance gene (P-glycoprotein) is expressed by endothelial cells at blood-brain barrier sites. *Proceedings of the National Academy of Sciences of the United States of America* **86**:695-698.

Dai H, Marbach P, Lemaire M, Hayes M and Elmquist WF (2003) Distribution of STI-571 to the brain is limited by P-glycoprotein-mediated efflux. *Journal of Pharmacology & Experimental Therapeutics* **304**:1085-1092.

Dantzig AH, Law KL, Cao J and Starling JJ (2001) Reversal of multidrug resistance by the P-glycoprotein modulator, LY335979, from the bench to the clinic. *Curr Med Chem* **8**:39-50.

Dantzig AH, Shepard RL, Cao J, Law KL, Ehlhardt WJ, Baughman TM, Bumol TF and Starling JJ (1996) Reversal of P-glycoprotein-mediated multidrug resistance by a potent cyclopropyldibenzosuberane modulator, LY335979. *Cancer Res* **56**:4171-4179.

Dantzig AH, Shepard RL, Law KL, Tabas L, Pratt S, Gillespie JS, Binkley SN, Kuhfeld MT, Starling JJ and Wrighton SA (1999) Selectivity of the multidrug resistance modulator, LY335979, for P-glycoprotein and effect on cytochrome P-450 activities. *J Pharmacol Exp Ther* **290**:854-862.

de Bruin M, Miyake K, Litman T, Robey R and Bates SE (1999) Reversal of resistance by GF120918 in cell lines expressing the ABC half-transporter, MXR. *Cancer Lett* **146**:117-126.

Deininger MW and Druker BJ (2003) Specific targeted therapy of chronic myelogenous leukemia with imatinib. *Pharmacological Reviews* **55**:401-423.

DeVries NA, Gassman EE, Kallemeyn NA, Shivanna KH, Magnotta VA and Grosland NM (2008) Validation of phalanx bone three-dimensional surface segmentation from computed tomography images using laser scanning. *Skeletal Radiol* **37**:35-42.

Dey N, Crosswell HE, De P, Parsons R, Peng Q, Su JD, Durden DL, (2008) The protein phosphatase activity of PTEN regulates SRC family kinases and controls glioma migration. *Cancer Research* **68**:1862-1871.

Doyle LA and Ross DD (2003) Multidrug resistance mediated by the breast cancer resistance protein BCRP (ABCG2). *Oncogene* **22**:7340-7358.

Doyle LA, Yang W, Abruzzo LV, Krogmann T, Gao Y, Rishi AK and Ross DD (1998) A multidrug resistance transporter from human MCF-7 breast cancer

cells.[erratum appears in Proc Natl Acad Sci U S A 1999 Mar 2;96(5):2569]. *Proceedings of the National Academy of Sciences of the United States of America* **95**:15665-15670.

Druker BJ (2003) David A. Karnofsky Award lecture. Imatinib as a paradigm of targeted therapies. *Journal of Clinical Oncology* **21**:239s-245s.

Druker BJ, Guilhot F, O'Brien SG, Gathmann I, Kantarjian H, Gattermann N, Deininger MW, Silver RT, Goldman JM, Stone RM, Cervantes F, Hochhaus A, Powell BL, Gabrilove JL, Rousselot P, Reiffers J, Cornelissen JJ, Hughes T, Agis H, Fischer T, Verhoef G, Shepherd J, Saglio G, Gratwohl A, Nielsen JL, Radich JP, Simonsson B, Taylor K, Baccarani M, So C, Letvak L, Larson RA, Investigators I, (2006) Five-year follow-up of patients receiving imatinib for chronic myeloid leukemia.[see comment]. *New England Journal of Medicine* **355**:2408-2417.

Edling CE and Hallberg B (2007) c-Kit--a hematopoietic cell essential receptor tyrosine kinase. *Int J Biochem Cell Biol* **39**:1995-1998.

Edwards JE, Brouwer KR and McNamara PJ (2002) GF120918, a P-glycoprotein modulator, increases the concentration of unbound amprenavir in the central nervous system in rats. *Antimicrob Agents Chemother* **46**:2284-2286.

Efferth T, Ramirez T, Gebhart E and Halatsch ME (2004) Combination treatment of glioblastoma multiforme cell lines with the anti-malarial artesunate and the epidermal growth factor receptor tyrosine kinase inhibitor OSI-774. *Biochemical Pharmacology* **67**:1689-1700.

Evers R, Kool M, Smith AJ, van Deemter L, de Haas M and Borst P (2000) Inhibitory effect of the reversal agents V-104, GF120918 and Pluronic L61 on MDR1 Pgp-, MRP1- and MRP2-mediated transport. *Br J Cancer* **83**:366-374.

Fenner MH and Possinger K (2002) Chemotherapy for breast cancer brain metastases. *Onkologie* **25**:474-479.

Finn RS (2008) Targeting Src in breast cancer. *Ann Oncol* **19**:1379-1386.

Fizazi K (2007) The role of Src in prostate cancer. *Ann Oncol* **18**:1765-1773.

Fraering PC, Ye W, LaVoie MJ, Ostaszewski BL, Selkoe DJ, Wolfe MS, (2005) gamma-Secretase substrate selectivity can be modulated directly via interaction

with a nucleotide-binding site. *Journal of Biological Chemistry* **280**:41987-41996.

Friche E, Jensen PB and Nissen NI (1992) Comparison of cyclosporin A and SDZ PSC833 as multidrug-resistance modulators in a daunorubicin-resistant Ehrlich ascites tumor. *Cancer Chemotherapy & Pharmacology* **30**:235-237.

Fricker G and Miller DS (2004) Modulation of drug transporters at the blood-brain barrier. *Pharmacology* **70**:169-176.

Gambacorti-Passerini C, Zucchetti M, Russo D, Frapolli R, Verga M, Bungaro S, Tornaghi L, Rossi F, Pioltelli P, Pogliani E, Alberti D, Corneo G, D'Incalci M, (2003) Alpha1 acid glycoprotein binds to imatinib (STI571) and substantially alters its pharmacokinetics in chronic myeloid leukemia patients. *Clinical Cancer Research* **9**:625-632.

Gaya A, Rees J, Greenstein A and Stebbing J (2002) The use of temozolomide in recurrent malignant gliomas. *Cancer Treatment Reviews* **28**:115-120.

Germann UA, Ford PJ, Shlyakhter D, Mason VS and Harding MW (1997) Chemosensitization and drug accumulation effects of VX-710, verapamil, cyclosporin A, MS-209 and GF120918 in multidrug resistant HL60/ADR cells expressing the multidrug resistance-associated protein MRP. *Anticancer Drugs* **8**:141-155.

Giannoudis A, Davies A, Lucas CM, Harris RJ, Pirmohamed M and Clark RE (2008) Effective dasatinib uptake may occur without human organic Cation Transporter 1 (hOCT1): implications for the treatment of imatinib resistant chronic myeloid leukaemia. *Blood*.

Giles FJ, DeAngelo DJ, Baccarani M, Deininger M, Guilhot F, Hughes T, Mauro M, Radich J, Ottmann O, Cortes J, (2008) Optimizing outcomes for patients with advanced disease in chronic myelogenous leukemia. *Seminars in Oncology* **35**:S1-17; quiz S18-20.

Goh LB, Spears KJ, Yao D, Ayrton A, Morgan P, Roland Wolf C, Friedberg T, (2002) Endogenous drug transporters in in vitro and in vivo models for the prediction of drug disposition in man. *Biochemical Pharmacology* **64**:1569-1578.

Golden PL and Pollack GM (2003a) Blood-brain barrier efflux transport. *J Pharm Sci* **92**:1739-1753.

Gora-Tybor J, Robak T, Gora-Tybor J and Robak T (2008) Targeted drugs in chronic myeloid leukemia. *Current Medicinal Chemistry* **15**:3036-3051.

Heimberger AB, Learn CA, Archer GE, McLendon RE, Chewning TA, Tuck FL, Pracyk JB, Friedman AH, Friedman HS, Bigner DD and Sampson JH (2002) Brain tumors in mice are susceptible to blockade of epidermal growth factor receptor (EGFR) with the oral, specific, EGFR-tyrosine kinase inhibitor ZD1839 (iressa). *Clinical Cancer Research* **8**:3496-3502.

Heldin CH and Westermark B (1999) Mechanism of action and in vivo role of platelet-derived growth factor. *Physiol Rev* **79**:1283-1316.

Hennessy M and Spiers JP (2007) A primer on the mechanics of P-glycoprotein the multidrug transporter. *Pharmacological Research* **55**:1-15.

Hernandez-Boluda JC, Cervantes F, (2002) Imatinib mesylate (Gleevec, Glivec): a new therapy for chronic myeloid leukemia and other malignancies. *Drugs of Today* **38**:601-613.

Hiwase DK, Saunders V, Hewett D, Frede A, Zrim S, Dang P, Eadie L, To LB, Melo J, Kumar S, Hughes TP and White DL (2008) Dasatinib cellular uptake and efflux in chronic myeloid leukemia cells: therapeutic implications. *Clin Cancer Res* **14**:3881-3888.

Houghton PJ, Germain GS, Harwood FC, Schuetz JD, Stewart CF, Buchdunger E and Traxler P (2004a) Imatinib mesylate is a potent inhibitor of the ABCG2 (BCRP) transporter and reverses resistance to topotecan and SN-38 in vitro. *Cancer Res* **64**:2333-2337.

Hyafil F, Vergely C, Du Vignaud P and Grand-Perret T (1993) In vitro and in vivo reversal of multidrug resistance by GF120918, an acridonecarboxamide derivative. *Cancer Res* **53**:4595-4602.

Irby RB and Yeatman TJ (2000) Role of Src expression and activation in human cancer. *Oncogene* **19**:5636-5642.

Jabbour E, Cortes JE, Ghanem H, O'Brien S, Kantarjian HM, (2008) Targeted therapy in chronic myeloid leukemia. *Expert Review of Anticancer Therapy* **8**:99-110.

Joensuu H, Roberts PJ, Sarlomo-Rikala M, Andersson LC, Tervahartiala P, Tuveson D, Silberman S, Capdeville R, Dimitrijevic S, Druker B and Demetri GD (2001) Effect of the tyrosine kinase inhibitor STI571 in a patient with a metastatic gastrointestinal stromal tumor. *New England Journal of Medicine* **344**:1052-1056.

Johansson Swartling F (2008) Identifying candidate genes involved in brain tumor formation. *Upsala Journal of Medical Sciences* **113**:1-38.

Jonker JW, Schinkel AH, (2004) Pharmacological and physiological functions of the polyspecific organic cation transporters: OCT1, 2, and 3 (SLC22A1-3). *Journal of Pharmacology & Experimental Therapeutics* **308**:2-9.

Jonker JW, Smit JW, Brinkhuis RF, Maliepaard M, Beijnen JH, Schellens JH and Schinkel AH (2000) Role of breast cancer resistance protein in the bioavailability and fetal penetration of topotecan.[see comment]. *Journal of the National Cancer Institute* **92**:1651-1656.

Juliano RL and Ling V (1976) A surface glycoprotein modulating drug permeability in Chinese hamster ovary cell mutants. *Biochim Biophys Acta* **455**:152-162.

Kilic T, Alberta JA, Zdunek PR, Acar M, Iannarelli P, O'Reilly T, Buchdunger E, Black PM and Stiles CD (2000) Intracranial inhibition of platelet-derived growth factor-mediated glioblastoma cell growth by an orally active kinase inhibitor of the 2-phenylaminopyrimidine class. *Cancer Research* **60**:5143-5150.

Kleber S, Sancho-Martinez I, Wiestler B, Beisel A, Gieffers C, Hill O, Thiemann M, Mueller W, Sykora J, Kuhn A, Schreglmann N, Letellier E, Zuliani C, Klussmann S, Teodorczyk M, Grone HJ, Ganten TM, Sultmann H, Tuttenberg J, von Deimling A, Regnier-Vigouroux A, Herold-Mende C, Martin-Villalba A, (2008) Yes and PI3K bind CD95 to signal invasion of glioblastoma. *Cancer Cell* **13**:235-248.

Ko JCH, Thurmon JC, Benson GJ, Tranquilli WJ and Hoffrnann WE (2008) Acute haemolysis associated with etomidate-propylene glycol infusion in dogs. *Veterinary Anaesthesia and Analgesia* **20**:92-94.

Koepsell H, Lips K, Volk C, (2007) Polyspecific organic cation transporters: structure, function, physiological roles, and biopharmaceutical implications. *Pharmaceutical Research* **24**:1227-1251.

Kretz O, Weiss HM, Schumacher MM, Gross G, (2004) In vitro blood distribution and plasma protein binding of the tyrosine kinase inhibitor imatinib and its active metabolite, CGP74588, in rat, mouse, dog, monkey, healthy humans and patients with acute lymphatic leukaemia. *British Journal of Clinical Pharmacology* **58**:212-216.

Kuppens IE, Witteveen EO, Jewell RC, Radema SA, Paul EM, Mangum SG, Beijnen JH, Voest EE and Schellens JH (2007) A phase I, randomized, open-label, parallel-cohort, dose-finding study of elacridar (GF120918) and oral topotecan in cancer patients. *Clin Cancer Res* **13**:3276-3285.

Lee F, Fandi A, Voi M, Lee F, Fandi A and Voi M (2008) Overcoming kinase resistance in chronic myeloid leukemia. *International Journal of Biochemistry & Cell Biology* **40**:334-343.

Leis JF, Stepan DE, Curtin PT, Ford JM, Peng B, Schubach S, Druker BJ and Maziarz RT (2004) Central nervous system failure in patients with chronic myelogenous leukemia lymphoid blast crisis and Philadelphia chromosome positive acute lymphoblastic leukemia treated with imatinib (STI-571). *Leukemia & Lymphoma* **45**:695-698.

Lesniak MS and Brem H (2004) Targeted therapy for brain tumours. *Nature Reviews* **Drug Discovery. 3**:499-508.

Lin NU, Bellon JR and Winer EP (2004) CNS metastases in breast cancer. *Journal of Clinical Oncology* **22**:3608-3617.

Lombardo LJ, Lee FY, Chen P, Norris D, Barrish JC, Behnia K, Castaneda S, Cornelius LA, Das J, Doweyko AM, Fairchild C, Hunt JT, Inigo I, Johnston K, Kamath A, Kan D, Klei H, Marathe P, Pang S, Peterson R, Pitt S, Schieven GL, Schmidt

RJ, Tokarski J, Wen ML, Wityak J, Borzilleri RM, (2004) Discovery of N-(2-chloro-6-methyl- phenyl)-2-(6-(4-(2-hydroxyethyl)- piperazin-1-yl)-2-methylpyrimidin-4- ylamino)thiazole-5-carboxamide (BMS-354825), a dual Src/Abl kinase inhibitor with potent antitumor activity in preclinical assays. *Journal of Medicinal Chemistry* **47**:6658-6661.

Loscher W and Potschka H (2005) Drug resistance in brain diseases and the role of drug efflux transporters. *Nature Reviews Neuroscience* **6**:591-602.

Lydon NB, Druker BJ, (2004) Lessons learned from the development of imatinib. *Leukemia Research* **28 Suppl 1**:S29-38.

Mahon FX, Belloc F, Lagarde V, Chollet C, Moreau-Gaudry F, Reiffers J, Goldman JM, Melo JV, (2003) MDR1 gene overexpression confers resistance to imatinib mesylate in leukemia cell line models.[see comment]. *Blood* **101**:2368-2373.

Malingre MM, Beijnen JH, Rosing H, Koopman FJ, Jewell RC, Paul EM, Ten Bokkel Huinink WW and Schellens JH (2001) Co-administration of GF120918 significantly increases the systemic exposure to oral paclitaxel in cancer patients. *Br J Cancer* **84**:42-47.

Marchetti S, Oostendorp RL, Pluim D, van Eijndhoven M, van Tellingen O, Schinkel AH, Versace R, Beijnen JH, Mazzanti R, Schellens JH, (2007) In vitro transport of gimatecan (7-t-butoxyiminomethylcamptothecin) by breast cancer resistance protein, P-glycoprotein, and multidrug resistance protein 2. *Molecular Cancer Therapeutics* **6**:3307-3313.

Mauro MJ and Druker BJ (2001) STI571: targeting BCR-ABL as therapy for CML.[see comment]. *Oncologist* **6**:233-238.

Merino V, Jimenez-Torres NV and Merino-Sanjuan M (2004) Relevance of multidrug resistance proteins on the clinical efficacy of cancer therapy. *Current Drug Delivery* **1**:203-212.

Miettinen M, Lasota J, (2005) KIT (CD117): a review on expression in normal and neoplastic tissues, and mutations and their clinicopathologic correlation. *Applied Immunohistochemistry & Molecular Morphology* **13**:205-220.

Miller G (2002) Drug targeting. Breaking down barriers. *Science* **297**:1116-1118.

Morschhauser F, Zinzani PL, Burgess M, Sloots L, Bouafia F and Dumontet C (2007) Phase I/II trial of a P-glycoprotein inhibitor, Zosuquidar.3HCl trihydrochloride (LY335979), given orally in combination with the CHOP regimen in patients with non-Hodgkin's lymphoma. *Leuk Lymphoma* **48**:708-715.

Motl S, Zhuang Y, Waters CM, Stewart CF, (2006) Pharmacokinetic considerations in the treatment of CNS tumours. *Clinical Pharmacokinetics* **45**:871-903.

Muenster U, Grieshop B, Ickenroth K, Gnoth MJ, (2008) Characterization of substrates and inhibitors for the in vitro assessment of Bcrp mediated drug-drug interactions. *Pharmaceutical Research* **25**:2320-2326.

Nam S, Kim D, Cheng JQ, Zhang S, Lee JH, Buettner R, Mirosevich J, Lee FY and Jove R (2005) Action of the Src family kinase inhibitor, dasatinib (BMS-354825), on human prostate cancer cells. *Cancer Res* **65**:9185-9189.

Netzer WJ, Dou F, Cai D, Veach D, Jean S, Li Y, Bornmann WG, Clarkson B, Xu H, Greengard P, (2003) Gleevec inhibits beta-amyloid production but not Notch cleavage. *Proceedings of the National Academy of Sciences of the United States of America* **100**:12444-12449.

Neville K, Parise RA, Thompson P, Aleksic A, Egorin MJ, Balis FM, McGuffey L, McCully C, Berg SL and Blaney SM (2004) Plasma and cerebrospinal fluid pharmacokinetics of imatinib after administration to nonhuman primates. *Clinical Cancer Research* **10**:2525-2529.

Newton HB (2003) Molecular neuro-oncology and development of targeted therapeutic strategies for brain tumors. Part 1: Growth factor and Ras signaling pathways. *Expert Rev Anticancer Ther* **3**:595-614.

Nies AT (2007) The role of membrane transporters in drug delivery to brain tumors. *Cancer Letters* **254**:11-29.

Nikolova Z, Peng B, Hubert M, Sieberling M, Keller U, Ho YY, Schran H and Capdeville R (2004) Bioequivalence, safety, and tolerability of imatinib tablets compared with capsules. *Cancer Chemotherapy & Pharmacology* **53**:433-438.

O'Hare T, Walters DK, Stoffregen EP, Jia T, Manley PW, Mestan J, Cowan-Jacob SW, Lee FY, Heinrich MC, Deininger MW and Druker BJ (2005) In vitro activity of

Bcr-Abl inhibitors AMN107 and BMS-354825 against clinically relevant imatinib-resistant Abl kinase domain mutants. *Cancer Res* **65**:4500-4505.

Ostman A and Heldin CH (2001) Involvement of platelet-derived growth factor in disease: development of specific antagonists. *Adv Cancer Res* **80**:1-38.

Ozvegy-Laczka C, Hegedus T, Varady G, Ujhelly O, Schuetz JD, Varadi A, Keri G, Orfi L, Nemet K and Sarkadi B (2004) High-affinity interaction of tyrosine kinase inhibitors with the ABCG2 multidrug transporter. *Mol Pharmacol* **65**:1485-1495.

Pan G, Elmquist WF, (2007) Mitoxantrone permeability in MDCKII cells is influenced by active influx transport. *Molecular Pharmaceutics* **4**:475-483.

Pardridge WM, Oldendorf WH, Cancilla P and Frank HJ (1986) Blood-brain barrier: interface between internal medicine and the brain. *Annals of Internal Medicine* **105**:82-95.

Park CM, Park MJ, Kwak HJ, Lee HC, Kim MS, Lee SH, Park IC, Rhee CH, Hong SI, (2006) Ionizing radiation enhances matrix metalloproteinase-2 secretion and invasion of glioma cells through Src/epidermal growth factor receptor-mediated p38/Akt and phosphatidylinositol 3-kinase/Akt signaling pathways. *Cancer Research* **66**:8511-8519.

Park SI, Zhang J, Phillips KA, Araujo JC, Najjar AM, Volgin AY, Gelovani JG, Kim SJ, Wang Z and Gallick GE (2008) Targeting SRC family kinases inhibits growth and lymph node metastases of prostate cancer in an orthotopic nude mouse model. *Cancer Res* **68**:3323-3333.

Pavek P, Merino G, Wagenaar E, Bolscher E, Novotna M, Jonker JW and Schinkel AH (2005) Human Breast Cancer Resistance Protein: Interactions with Steroid Drugs, Hormones, the Dietary Carcinogen 2-Amino-1-methyl-6-phenylimidazo(4,5-b)pyridine, and Transport of Cimetidine. *J Pharmacol Exp Ther* **312**:144-152.

Peng B, Dutreix C, Mehring G, Hayes MJ, Ben-Am M, Seiberling M, Pokorny R, Capdeville R and Lloyd P (2004) Absolute bioavailability of imatinib (Glivec)

orally versus intravenous infusion. *Journal of Clinical Pharmacology* **44**:158-162.

Pfeifer H, Wassmann B, Hofmann WK, Komor M, Scheuring U, Bruck P, Binckebanck A, Schleyer E, Gokbuget N, Wolff T, Lubbert M, Leimer L, Gschaidmeier H, Hoelzer D and Ottmann OG (2003) Risk and prognosis of central nervous system leukemia in patients with Philadelphia chromosome-positive acute leukemias treated with imatinib mesylate. *Clinical Cancer Research* **9**:4674-4681.

Planting AS, Sonneveld P, van der Gaast A, Sparreboom A, van der Burg ME, Luyten GP, de Leeuw K, de Boer-Dennert M, Wissel PS, Jewell RC, Paul EM, Purvis NB, Jr. and Verweij J (2005) A phase I and pharmacologic study of the MDR converter GF120918 in combination with doxorubicin in patients with advanced solid tumors. *Cancer Chemother Pharmacol* **55**:91-99.

Playford MP, Schaller MD, (2004) The interplay between Src and integrins in normal and tumor biology. *Oncogene* **23**:7928-7946.

Porkka K, Koskenvesa P, Lundan T, Rimpilainen J, Mustjoki S, Smykla R, Wild R, Luo R, Arnan M, Brethon B, Eccersley L, Hjorth-Hansen H, Hoglund M, Klamova H, Knutsen H, Parikh S, Raffoux E, Gruber F, Brito-Babapulle F, Dombret H, Duarte RF, Elonen E, Paquette R, Zwaan CM and Lee FY (2008) Dasatinib crosses the blood-brain barrier and is an efficient therapy for central nervous system Philadelphia chromosome-positive leukemia. *Blood* **112**:1005-1012.

Pottgen C, Eberhardt W and Stuschke M (2004) Prophylactic cranial irradiation in lung cancer. *Curr Treat Options Oncol* **5**:43-50.

Quintas-Cardama A, Kantarjian H, Jones D, Nicaise C, O'Brien S, Giles F, Talpaz M, Cortes J, (2007) Dasatinib (BMS-354825) is active in Philadelphia chromosome-positive chronic myelogenous leukemia after imatinib and nilotinib (AMN107) therapy failure. *Blood* **109**:497-499.

Rabindran SK, Ross DD, Doyle LA, Yang W and Greenberger LM (2000) Fumitremorgin C reverses multidrug resistance in cells transfected with the breast cancer resistance protein. *Cancer Research* **60**:47-50.

Rajappa S, Uppin SG, Raghunadharao D, Rao IS and Surath A (2004) Isolated central nervous system blast crisis in chronic myeloid leukemia. *Hematological Oncology* **22**:179-181.

Raymond E, Brandes AA, Dittrich C, Fumoleau P, Coudert B, Clement PM, Frenay M, Rampling R, Stupp R, Kros JM, Heinrich MC, Gorlia T, Lacombe D, van den Bent MJ, European Organisation for R, Treatment of Cancer Brain Tumor Group S, (2008) Phase II study of imatinib in patients with recurrent gliomas of various histologies: a European Organisation for Research and Treatment of Cancer Brain Tumor Group Study. *Journal of Clinical Oncology* **26**:4659-4665.

Rich JN and Bigner DD (2004) Development of novel targeted therapies in the treatment of malignant glioma. *Nature Reviews* **Drug Discovery. 3**:430-446.

Robey RW, Honjo Y, Morisaki K, Nadjem TA, Runge S, Risbood M, Poruchynsky MS and Bates SE (2003) Mutations at amino-acid 482 in the ABCG2 gene affect substrate and antagonist specificity. *Br J Cancer* **89**:1971-1978.

Roussidis AE, Theocharis AD, Tzanakakis GN and Karamanos NK (2007) The importance of c-Kit and PDGF receptors as potential targets for molecular therapy in breast cancer. *Curr Med Chem* **14**:735-743.

Rubin EH, de Alwis DP, Pouliquen I, Green L, Marder P, Lin Y, Musanti R, Grospe SL, Smith SL, Toppmeyer DL, Much J, Kane M, Chaudhary A, Jordan C, Burgess M and Slapak CA (2002) A phase I trial of a potent P-glycoprotein inhibitor, Zosuquidar.3HCl trihydrochloride (LY335979), administered orally in combination with doxorubicin in patients with advanced malignancies. *Clin Cancer Res* **8**:3710-3717.

Sandler A, Gordon M, De Alwis DP, Pouliquen I, Green L, Marder P, Chaudhary A, Fife K, Battiato L, Sweeney C, Jordan C, Burgess M and Slapak CA (2004) A Phase I trial of a potent P-glycoprotein inhibitor, zosuquidar trihydrochloride (LY335979), administered intravenously in combination with doxorubicin in patients with advanced malignancy. *Clin Cancer Res* **10**:3265-3272.

Sarkadi B, Ozvegy-Laczka C, Nemet K and Varadi A (2004) ABCG2 -- a transporter for all seasons. *FEBS Lett* **567**:116-120.

Schinkel AH and Jonker JW (2003) Mammalian drug efflux transporters of the ATP binding cassette (ABC) family: an overview. *Adv Drug Deliv Rev* **55**:3-29.

Schinkel AH, Jonker JW, (2003) Mammalian drug efflux transporters of the ATP binding cassette (ABC) family: an overview. *Advanced Drug Delivery Reviews* **55**:3-29.

Schinkel AH, Smit JJ, van Tellingen O, Beijnen JH, Wagenaar E, van Deemter L, Mol CA, van der Valk MA, Robanus-Maandag EC, te Riele HP and et al. (1994) Disruption of the mouse mdr1a P-glycoprotein gene leads to a deficiency in the blood-brain barrier and to increased sensitivity to drugs. *Cell* **77**:491-502.

Schittenhelm MM, Shiraga S, Schroeder A, Corbin AS, Griffith D, Lee FY, Bokemeyer C, Deininger MW, Druker BJ and Heinrich MC (2006) Dasatinib (BMS-354825), a dual SRC/ABL kinase inhibitor, inhibits the kinase activity of wild-type, juxtamembrane, and activation loop mutant KIT isoforms associated with human malignancies. *Cancer Research* **66**:473-481.

Schlessinger J (2000) Cell signaling by receptor tyrosine kinases. *Cell* **103**:211-225.

Shah NP (2007) Medical Management of CML. *Hematology Am Soc Hematol Educ Program* **2007**:371-375.

Shah NP, Skaggs BJ, Branford S, Hughes TP, Nicoll JM, Paquette RL, Sawyers CL, (2007) Sequential ABL kinase inhibitor therapy selects for compound drug-resistant BCR-ABL mutations with altered oncogenic potency. *Journal of Clinical Investigation* **117**:2562-2569.

Shepard RL, Cao J, Starling JJ and Dantzig AH (2003) Modulation of P-glycoprotein but not MRP1- or BCRP-mediated drug resistance by LY335979. *Int J Cancer* **103**:121-125.

Smith QR (1996) Brain perfusion systems for studies of drug uptake and metabolism in the central nervous system. *Pharmaceutical Biotechnology* **8**:285-307.

Starling JJ, Shepard RL, Cao J, Law KL, Norman BH, Kroin JS, Ehlhardt WJ, Baughman TM, Winter MA, Bell MG, Shih C, Gruber J, Elmquist WF and Dantzig AH (1997) Pharmacological characterization of LY335979: a potent

cyclopropyldibenzosuberane modulator of P-glycoprotein. *Adv Enzyme Regul* **37**:335-347.

Su EJ, Fredriksson L, Geyer M, Folestad E, Cale J, Andrae J, Gao Y, Pietras K, Mann K, Yepes M, Strickland DK, Betsholtz C, Eriksson U, Lawrence DA, (2008) Activation of PDGF-CC by tissue plasminogen activator impairs blood-brain barrier integrity during ischemic stroke.[see comment]. *Nature Medicine* **14**:731-737.

Summy JM and Gallick GE (2003) Src family kinases in tumor progression and metastasis. *Cancer Metastasis Rev* **22**:337-358.

Sun H, Dai H, Shaik N and Elmquist WF (2003) Drug efflux transporters in the CNS. *Advanced Drug Delivery Reviews* **55**:83-105.

Takayama N, Sato N, O'Brien SG, Ikeda Y and Okamoto S (2002) Imatinib mesylate has limited activity against the central nervous system involvement of Philadelphia chromosome-positive acute lymphoblastic leukaemia due to poor penetration into cerebrospinal fluid. *British Journal of Haematology* **119**:106-108.

Talpaz M, Shah NP, Kantarjian H, Donato N, Nicoll J, Paquette R, Cortes J, O'Brien S, Nicaise C, Bleickardt E, Blackwood-Chirchir MA, Iyer V, Chen TT, Huang F, Decillis AP, Sawyers CL, (2006) Dasatinib in imatinib-resistant Philadelphia chromosome-positive leukemias.[see comment]. *New England Journal of Medicine* **354**:2531-2541.

Taylor EM (2002) The impact of efflux transporters in the brain on the development of drugs for CNS disorders. *Clinical Pharmacokinetics* **41**:81-92.

Thomas J, Wang L, Clark RE, Pirmohamed M, (2004) Active transport of imatinib into and out of cells: implications for drug resistance.[see comment]. *Blood* **104**:3739-3745.

Toffoli G, Corona G, Gigante M and Boiocchi M (1996) Inhibition of Pgp activity and cell cycle-dependent chemosensitivity to doxorubicin in the multidrug-resistant LoVo human colon cancer cell line. *European Journal of Cancer* **32A**:1591-1597.

Tremont-Lukats IW and Gilbert MR (2003) Advances in molecular therapies in patients with brain tumors. *Cancer Control* **10**:125-137.

Tsuji A, Terasaki T, Takabatake Y, Tenda Y, Tamai I, Yamashima T, Moritani S, Tsuruo T and Yamashita J (1992) P-glycoprotein as the drug efflux pump in primary cultured bovine brain capillary endothelial cells. *Life Sciences* **51**:1427-1437.

Vlahovic G and Crawford J (2003) Activation of tyrosine kinases in cancer. *Oncologist* **8**:531-538.

Wang Q, Rager JD, Weinstein K, Kardos PS, Dobson GL, Li J, Hidalgo IJ, (2005) Evaluation of the MDR-MDCK cell line as a permeability screen for the blood-brain barrier. *International Journal of Pharmaceutics* **288**:349-359.

White DL, Saunders VA, Dang P, Engler J, Zannettino ACW, Cambareri AC, Quinn SR, Manley PW and Hughes T (2006) OCT-1-mediated influx is a key determinant of the intacellular uptake of imatinib but not nilotinib (AMN107): reduced OCT-1 activity is the cause of low in vitro sesitivity to imatinib. *Blood* **108**:697-704.

Wolff NC, Richardson JA, Egorin M and Ilaria RL, Jr. (2003) The CNS is a sanctuary for leukemic cells in mice receiving imatinib mesylate for Bcr/Abl-induced leukemia. *Blood* **101**:5010-5013.

Wright SH (2005) Role of organic cation transporters in the renal handling of therapeutic agents and xenobiotics. *Toxicology & Applied Pharmacology* **204**:309-319.

Xia CQ, Liu N, Miwa GT, Gan LS, (2007a) Interactions of cyclosporin a with breast cancer resistance protein. *Drug Metabolism & Disposition* **35**:576-582.

Xia CQ, Milton MN and Gan LS (2007b) Evaluation of drug-transporter interactions using in vitro and in vivo models. *Curr Drug Metab* **8**:341-363.

Yarden Y, Kuang WJ, Yang-Feng T, Coussens L, Munemitsu S, Dull TJ, Chen E, Schlessinger J, Francke U and Ullrich A (1987) Human proto-oncogene c-kit: a new cell surface receptor tyrosine kinase for an unidentified ligand. *EMBO Journal* **6**:3341-3351.

Young AM, Allen CE and Audus KL (2003) Efflux transporters of the human placenta. *Advanced Drug Delivery Reviews* 55:125-132.